


Fall 12-2008

## Preparation of Carboxylic Acid Functionalized Glycopolymers through RAFT and Post-Polymerization Modification for Biomedical Application

Husnu Alp Alidedeoglu  
*University of Southern Mississippi*

Follow this and additional works at: <https://aquila.usm.edu/dissertations>

 Part of the [Materials Chemistry Commons](#), and the [Polymer Chemistry Commons](#)

---

### Recommended Citation

Alidedeoglu, Husnu Alp, "Preparation of Carboxylic Acid Functionalized Glycopolymers through RAFT and Post-Polymerization Modification for Biomedical Application" (2008). *Dissertations*. 1134.  
<https://aquila.usm.edu/dissertations/1134>

This Dissertation is brought to you for free and open access by The Aquila Digital Community. It has been accepted for inclusion in Dissertations by an authorized administrator of The Aquila Digital Community. For more information, please contact [aquilastaff@usm.edu](mailto:aquilastaff@usm.edu).

The University of Southern Mississippi

PREPARATION OF CARBOXYLIC ACID FUNCTIONALIZED GLYCOPOLYMERS  
THROUGH RAFT AND POST-POLYMERIZATION MODIFICATION FOR  
BIOMEDICAL APPLICATION

by

Husnu Alp Alidedeoglu

Abstract of a Dissertation  
Submitted to the Graduate Studies Office  
of The University of Southern Mississippi  
in Partial Fulfillment of the Requirements  
for the Degree of Doctor of Philosophy

December 2008

COPYRIGHT BY  
HUSNU ALP ALIDEDEOGLU  
2008

The University of Southern Mississippi

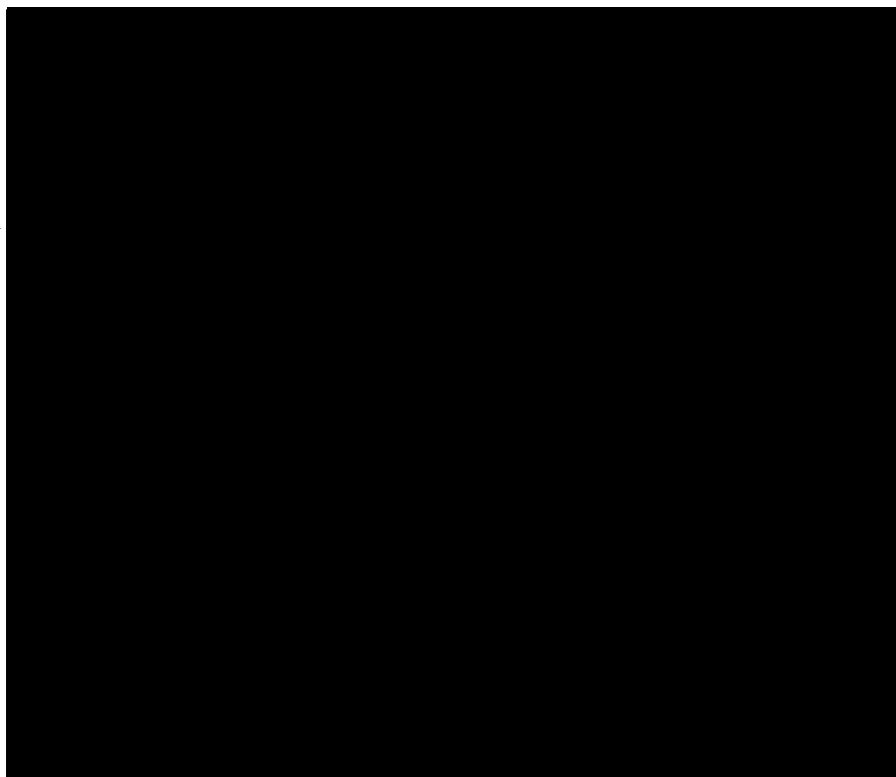
PREPARATION OF CARBOXYLIC ACID FUNCTIONALIZED GLYCOPOLYMERS  
THROUGH RAFT AND POST-POLYMERIZATION MODIFICATION FOR  
BIOMEDICAL APPLICATION

by

Husnu Alp Alidedeoglu

A Dissertation  
Submitted to the Graduate Studies Office  
of The University of Southern Mississippi  
in Partial Fulfillment of the Requirements  
for the Degree of Doctor of Philosophy

Approved:



December 2008

## ABSTRACT

# PREPARATION OF CARBOXYLIC ACID FUNCTIONALIZED GLYCOPOLYMERS THROUGH RAFT AND POST-POLYMERIZATION MODIFICATION FOR BIOMEDICAL APPLICATION

by Husnu Alp Alidedeoglu

December 2008

The primary theme of this dissertation involves the synthesis of well-defined primary amine functionalized polymers, subsequent modification of the polymers to produce novel carboxylic acid functionalized glycopolymers and surface polymerization of these systems utilizing controlled polymerization techniques. Additionally, the synthesis of new water-based allylic copolymer latexes is described.

Carbohydrates are natural polymers which possess unlimited structural variations. They carry a huge density of information, and play major roles in recognition events and complex biological operations. For example, hyaluronic acid (HA), an anionic glycosaminoglycan, provides lubricating and cushioning properties in the extracellular matrix and has been found to be involved in the regulation of many cellular and biological processes. In industry, HA is used in a wide range of biomedical applications, including post surgical adhesion prevention, rheology modification in orthopedics, ophthalmic procedures, tissue engineering, hydrogels and implants. Limitations of current systems include cost, allergy induction and reduced performance capabilities in comparison to native HA. Therefore, it is of interest to prepare synthetic glycopolymer analogues to specifically target performance capabilities for biomedical applications.

Reversible addition–fragmentation chain transfer polymerization (RAFT) is arguably the most versatile living radical polymerization technique in terms of the reaction conditions and monomer selection. Since the introduction of RAFT in 1998, researchers have employed the RAFT process to synthesize a wide range of water soluble (co)polymers with predetermined molecular weights, low polydispersities, and advanced architectures. However the RAFT polymerization of primary amine containing monomers such as 2-(aminoethyl methacrylate) (AEMA) and *N*-(3-aminopropyl methacrylamide) (APMA) directly in water has yet to be reported. Since primary amine groups are amenable to a wide range of post-polymerization chemistries, primary amine functionalized polymers enable developments in the synthesis of controlled architecture glycopolymers. In addition, “click” chemistry can provide us an easy route to modify solid substrates with these polymers due to its simple reaction conditions and high reaction yield properties.

The overall goal of this research is to prepare well-defined synthetic anionic glycosaminoglycan polymers by combining well-defined primary amine functionalized polymers with carboxylic acid functionalized sugars through a one-step reductive amination reaction. To achieve these goals, first, primary amine functionalized polymers were prepared through aqueous RAFT polymerization of AEMA and APMA. Second, D-glucuronic acid sodium salt was attached to reactive polymer precursors *via* reductive amination reactions in alkaline medium. Finally, the surface modification capabilities of primary amine functionalized polymers were investigated using “click” chemistry to create reactive surfaces allowing post-polymerization reactions.

In this thesis, the first chapter concerns the first successful RAFT polymerization of unprotected AEMA directly in water and its successful block copolymerization with *N*-2-hydroxypropylmethacrylamide (HPMA). The controlled “living” polymerization of AEMA was carried out directly in aqueous buffer using 4-cyanopentanoic acid dithiobenzoate (CTP) as the chain transfer agent (CTA), and 2,2'-Azobis(2-imidazolinypropane) dihydrochloride (VA-044) as the initiator at 50 °C. The living character of the polymerization was verified with pseudo first order kinetic plots, a linear increase of the molecular weight with conversion, and low polydispersities (PDI) (<1.2). In addition, well-defined copolymers of poly(2-aminoethyl methacrylate-*b*-*N*-2-hydroxypropylmethacrylamide) (PAEMA-*b*-PHPMA) have been prepared through chain extension of poly(2-aminoethyl methacrylate) (PAEMA) macroCTA with HPMA in water. It is shown that the macroCTA can be extended in a controlled fashion resulting in near monodisperse block copolymers.

The second chapter demonstrates the synthesis of novel carboxylic acid functionalized glycopolymers prepared *via* one step post-polymerization modification of poly(*N*-[3-aminopropyl] methacrylamide) (PAPMA), a water soluble primary amine methacrylamide, in aqueous medium. PAPMA was first polymerized *via* aqueous RAFT polymerization using CTP as CTA, and 4,4'-Azobis(4-cyanovaleric acid) (V-501) as the initiator at 70 °C. The resulting well-defined PAPMA was then conjugated with D-glucuronic acid sodium salt through reductive amination in alkaline medium (pH 8.5) at 45 °C. The successful bioconjugation was proven through proton (<sup>1</sup>H) and carbon (<sup>13</sup>C) Nuclear Magnetic Resonance (NMR) spectroscopy and Matrix Assisted Laser Desorption Ionization Time of Flight (MALDI-TOF) mass spectroscopy analysis, which indicated

near quantitative conversion. A similar bioconjugation reaction was conducted with PAEMA and PAEMA-*b*-PHPMA. For the PAEMA homo and block copolymers, however, poor conversion was obtained, most likely due to degradation reactions of PAEMA in alkaline medium.

The third chapter details the direct preparation of  $\alpha$ -alkynyl-functionalized PAEMA *via* RAFT polymerization. The controlled “living” polymerization of AEMA was carried out directly in dimethylsulfoxide (DMSO) using  $\alpha$ -alkynyl functionalized CTP as CTA, and 2,2'-azobis(2,4-dimethyl-4-methoxyvaleronitrile) (V-70) as the initiator at 45 °C. The resulting polymers display low PDIs (<1.2). In addition, the  $\alpha$ -alkynyl-functionalized PAEMA was attached to an azide functionalized silicon wafer *via* “click” chemistry. Various characterization techniques including ellipsometry, contact angle measurements, attenuated total reflectance-Fourier transform infrared spectroscopy (ATR-IR), and atomic force microscopy (AFM) were used to characterize the polymer modified silicon wafers. It was shown that a non-uniform surface with a thickness of 11.1 nm was obtained.

The last chapter (an additional chapter) details the copolymerization behavior of styrene with *sec*-butenyl acetate, whose copolymerization properties have not been reported. Copolymers were produced *via* semicontinuous emulsion polymerization and characterized via NMR, gel permeation chromatography, differential scanning calorimetry, dynamic light scattering, and atomic force microscopy. A high degree of chain termination due to allylic hydrogen abstraction was observed, as expected, with resultant decreases in molecular weight and in monomer conversion. However, high conversions were achieved, and it was possible to incorporate high percentages of the



allylic acetate comonomer into the polymer chain. Copolymer thermal properties are reported.

## DEDICATION

To my wonderful wife Hande and our son Ege. You both define my life and make it immeasurably enjoyable.

## ACKNOWLEDGEMENTS

I would like to thank Dr. Sarah Elizabeth Morgan, my research advisor, for her guidance, dedication and encouragement throughout my graduate career. She has given me a great education and wonderful opportunities that I would not have gotten anywhere else. I am grateful for having been able to work under her for the past four years. I would also like to thank the members of my graduate committee: Dr. Charles L. McCormick, Dr. Marek Urban, Dr. James W. Rawlins, Dr. Sabine Heinhorst.

I am extremely grateful to the entire Morgan, McCormick and Thames-Rawlins Research Groups both past and present, for their friendship and advice throughout my graduate career, in particular, Dr. Sundipan Dutta, Kevin Davis, Christopher Harris, Adam W. York, Scott Moravek and Rahul Misra. In addition, I would like to acknowledge Dr. William Jarrett, for his help throughout my graduate career.

I am forever grateful to my wife, my parents, and my entire family, all of whom have provided encouragement and support throughout my life. The authors gratefully acknowledge the support of Noetic Technologies, Inc., the RET program of the National Science Foundation under Award Number EEC-0602032, and the MRSEC Program of the National Science Foundation under Award Number DMR 0213883. We would also like to thank the Department of Chemistry and Biochemistry at USM for use of their MS facilities, and acknowledge the National Science Foundation (DBI 0619455) for funds used to acquire the MALDI MS. INTERFACE (NSF IUCRC) support is also acknowledged.

## TABLE OF CONTENTS

ABSTRACT .....	ii
DEDICATION.....	vii
ACKNOWLEDGEMENTS.....	viii
LIST OF ILLUSTRATIONS.....	xi
LIST OF TABLES.....	xiv
TABLE OF SCHEMES.....	xv
CHEMICAL NAMES AND ABBREVIATIONS.....	xvi
CHAPTER	
I.    INTRODUCTION.....	1
Hyaluronic Acid.....	1
Glycopolymers.....	2
Primary Amine Vinyl Monomers .....	4
Reversible Addition-Fragmentation Chain Transfer (RAFT) Polymerization .....	8
"Click" Chemistry.....	17
Motivation for Research .....	21
Prospectus of Research.....	23
II.   RESEARCH GOAL AND OBJECTIVES.....	27
III.  AQUEOUS RAFT POLYMERIZATION OF NON-PROTONATED 2- AMINOETHYL METHACRYLATE TO PRODUCE WELL-DEFINED, PRIMARY AMINE FUNCTIONAL HOMO- AND COPOLYMERS FOR BIOMEDICAL APPLICATIONS.....	31
Introduction.....	31
Experimental.....	35
Results and Discussion .....	39
Conclusions.....	52

IV. BIOCONJUGATION OF D-GLUCURONIC ACID SODIUM SALT TO WELL-DEFINED PRIMARY AMINE CONTAINING HOMO- AND BLOCK COPOLYMERS FOR POTENTIAL BIOMEDICAL APPLICATIONS .....	53
Introduction.....	53
Experimental.....	57
Results and Discussion .....	64
Conclusions.....	80
V. SURFACE MODIFICATION OF $\alpha$ -ALKYNYL-FUNCTIONALIZED POLY(2-AMINOETHYL METHACRYLATE) VIA “CLICK” CHEMISTRY TO PRODUCE PRIMARY AMINE FUNCTIONALIZED SURFACES .....	81
Introduction.....	81
Experimental.....	85
Results and Discussion .....	89
Conclusions.....	100
VI. COPOLYMERIZATION OF <i>SEC</i> -BUTENYL ACETATE WITH STYRENE VIA EMULSION POLYMERIZATION .....	101
Introduction.....	101
Experimental.....	105
Results and Discussion .....	113
Conclusions.....	126
VII. CONCLUSIONS.....	128
RECOMMENDED FUTUREWORK .....	132
APPENDIXES .....	133
Introduction.....	133
Experimental.....	134
Results and Discussion .....	137
Conclusion .....	142
REFERENCES .....	143

## LIST OF ILLUSTRATIONS

### FIGURE

I-1. Hyaluronic Acid.....	1
I-2. Common thiocarbonylthio CTAs utilized in RAFT.....	11
I-3. Examples of water-soluble monomers polymerized by RAFT.....	16
I-4. Chain transfer agents employed in aqueous RAFT polymerizations.....	17
III-1. ASEC traces for the homopolymerization of AEMA at 50 °C showing the RI signal as a function of elution volume. ....	42
III-2. Pseudo-first-order kinetic plot for the homopolymerization of AEMA at 50 °C....	43
III-3. $M_n$ determined by GPC as a function of conversion for the aqueous homopolymerizations of AEMA at 50 °C. ....	44
III-4. ASECs traces for the homopolymerization of AEMA at 70 °C showing refractive index as a function of elution volume.....	45
III-5. Pseudo-first-order kinetic plot for the homopolymerization of AEMA at 70 °C....	47
III-6. $M_n$ determined by GPC as a function of conversion for the aqueous homopolymerization of AEMA at 70 °C.....	47
III-7. ASEC RI traces for diblock copolymers of AEMA and HPMA and the corresponding AEMA homopolymer macroCTA. ....	50
III-8. $^1\text{H}$ NMR spectrum of PAEMA- <i>b</i> -PHPMA. ....	51
IV-1. $^{13}\text{C}$ NMR spectra of A. Bioconjugated APMA with D-glucuronic acid sodium salt; B. D-Glucuronic acid sodium salt; and C. APMA monomer. ....	67
IV-2. $^1\text{H}$ NMR spectra of A. Bioconjugated APMA with D-glucuronic acid sodium salt; B. D-Glucuronic acid sodium salt; and C. APMA monomer. ....	68
IV-3. $^{13}\text{C}$ NMR spectra of A. Bioconjugated PAPMA with D-glucuronic acid sodium salt; B. PAPMA. ....	70
IV-4. $^1\text{H}$ NMR spectra of A. Bioconjugated PAPMA with D-glucuronic acid sodium salt; B. PAPMA. ....	71
IV-5. MALDI TOF mass spectrum of PAPMA.....	72

IV-6. MALDI TOF mass spectrum of bio-conjugated PAPMA with D-glucuronic acid sodium salt. ....	73
IV-7. <sup>13</sup> C NMR spectra of A. Bio-conjugated PAEMA with D-glucuronic acid sodium; B. salt PAEMA. ....	74
IV-8. <sup>1</sup> H NMR spectra of A. Bioconjugated PAEMA with D-glucuronic acid sodium salt; B. PAEMA. ....	75
IV-9. MALDI TOF mass spectra of A. Bio-conjugated PAEMA with D-glucuronic acid sodium salt; B. PAEMA. ....	76
IV-10. <sup>13</sup> C NMR spectra of A. Bioconjugated PAEMA- <i>b</i> -PHPMA with D-glucuronic acid sodium salt; B. PAEMA- <i>b</i> -PHPMA. ....	77
IV-11. <sup>1</sup> H NMR spectra of A. Bioconjugated PAEMA- <i>b</i> -PHPMA with D-glucuronic acid sodium salt; B. PAEMA- <i>b</i> -PHPMA. ....	78
IV-12. MALDI TOF mass spectra of A. PAEMA- <i>b</i> -PHPMA; B. Bioconjugated PAEMA- <i>b</i> -PHPMA with D-glucuronic acid sodium salt. ....	79
V-1. <sup>1</sup> H NMR spectrum of $\alpha$ -alkynyl functionalized PAEMA. ....	90
V-2. ASECS chromatograms for $\alpha$ -alkynyl functionalized poly(AEMA) prepared at 45 °C in DMSO. ....	91
V-3. <sup>1</sup> H NMR spectrum of $\alpha$ -alkynyl functionalized PAEMA. ....	93
V-4. Tapping mode AFM images of A. Neat silicon wafer; B. Bromide functionalized silicon wafer; C. Azide functionalized silicon wafer; D. Poly(AEMA) modified silicon wafer. ....	96
V-5. ATR-FTIR spectra of A. PAEMA modified silicon wafer; B. Neat silicon wafer. .	98
V-6. 3D surface topography of A. Neat silicon wafer; B. Poly(AEMA) modified silicon wafer. ....	98
VI-1. <sup>1</sup> H NMR spectrum of SBA after purification by vacuum distillation. ....	110
VI-2. <sup>13</sup> C NMR spectrum of SBA after purification by vacuum distillation. ....	111
VI-3. <sup>1</sup> H NMR spectra of STY-SBA 6.1%, STY-SBA 12.5% and STY-SBA 25% copolymers showing increase in SBA tertiary allylic proton signal (3.6 ppm) with increasing SBA feed content. ....	118

VI-4. GPC traces of STY 100, STY-SBA 6.1%, STY-SBA 12.5% and STY-SBA 25% copolymers.....	119
VI-5. Dynamic light scattering traces for a) 6.1% SBA and b) 25% SBA.....	121
VI-6. AFM tapping mode height and phase images of spin coated films prepared from A) STY-SBA 6.1%, B) STY-SBA 12.5% and C) STY-SBA 25% latexes.....	123
VI-7. Conversion as a function of time for STY-SBA 6.1%, STY-SBA 12.5% and STY-SBA 25% copolymers performed in batch process. ....	126
Appendix-1. <sup>1</sup> H-NMR of 9-enyl 4-cyano-4-(phenylcarbanthioylthio)-pentanoate. ....	138
Appendix-2. <sup>1</sup> H-NMR of CTP activation. ....	139
Appendix-3. <sup>1</sup> H-NMR of the double bond functionalized asymmetric diazoinitiator....	141



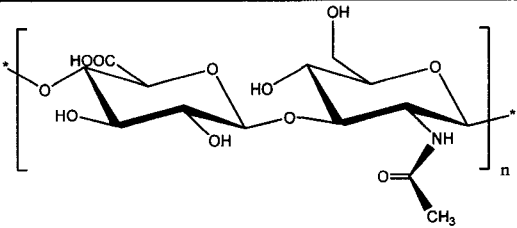
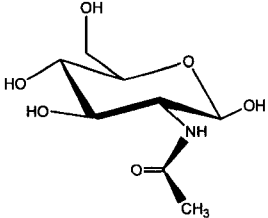
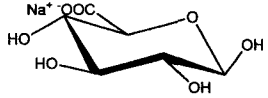
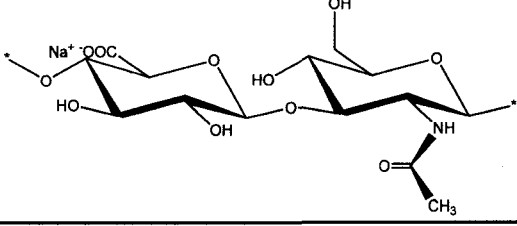
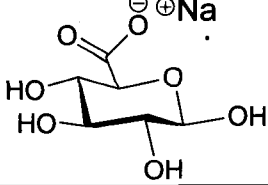
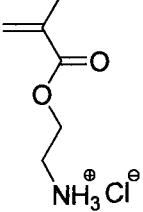
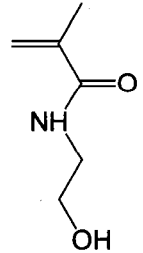
## LIST OF TABLES

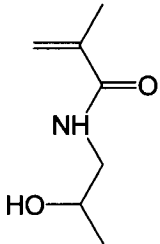
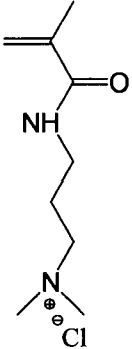
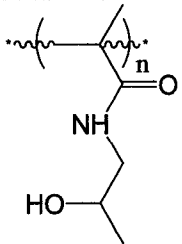
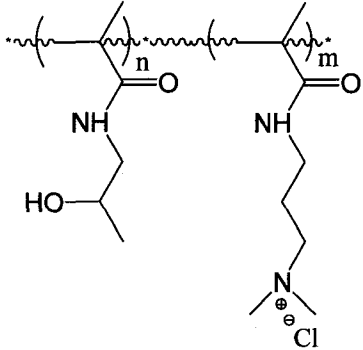
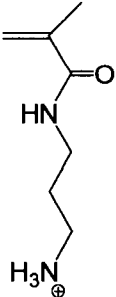
Table	
III-1. Aqueous RAFT polymerization of AEMA at 50 °C. ....	41
III-2. Aqueous RAFT polymerization of AEMA at 70 °C. ....	45
III-3. Conditions for synthesis and physical properties of AEMA MacroCTA at 50 and 70 °C.....	48
III-4. PAEMA- <i>b</i> -PHPMA copolymerization and physical properties.....	49
IV-1. (Co)polymers results. ....	65
V-1. Preparation of $\alpha$ -Alkynyl-Functionalized poly(AEMA) at 45 °C. ....	92
V-2. Preparation of $\alpha$ -Alkynyl-Functionalized poly(AEMA) at 45 °C. ....	93
VI-1. A) Latex Recipe for Semi-Continuous Batch Process (93.9% STY-6.1% SBA); B) Recipe for Batch process (93.9% STY-6.1% SBA). ....	113
VI-2. Retention time of SBA and common commercial monomers characterized through RP-HPLC.....	116
VI-3. Molecular weight, polydispersity index (PDI) and glass transition temperature ( $T_g$ ) for copolymer systems.....	120
VI-4. Number average particle size of latex (via dynamic light scattering (DLS)) and of film (via AFM).....	122
VI-5. Solids, gel content, residual monomer and conversion results for semi-continuous emulsion copolymerization reactions. ....	124

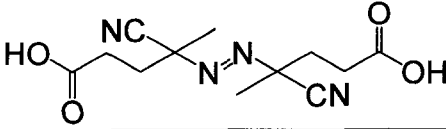
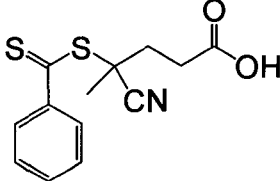
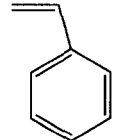
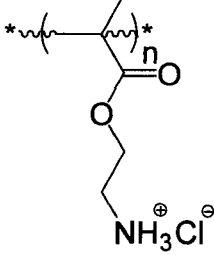
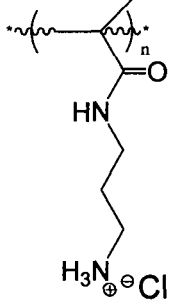
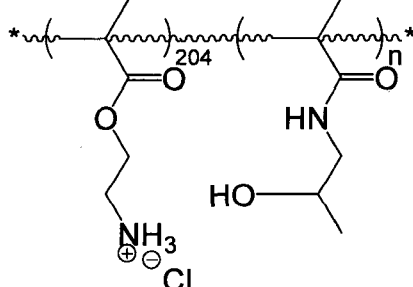
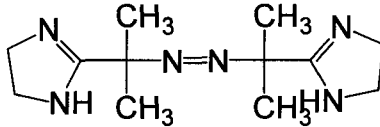
## LIST OF SCHEMES

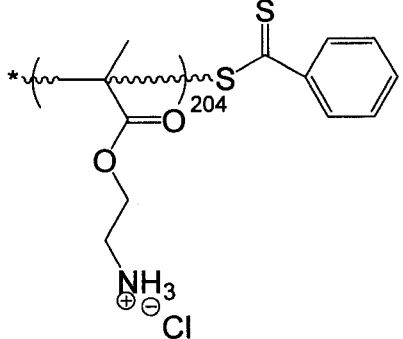
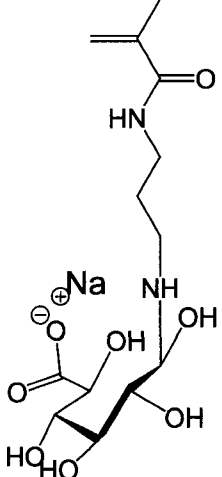
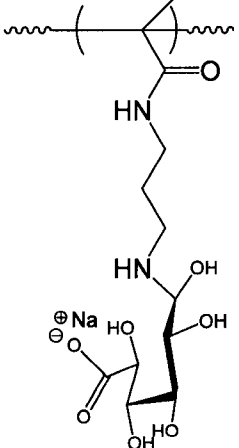
Scheme	
I-1. Accepted RAFT mechanism. <sup>118</sup> .....	10
I-2. Synthesis of AB diblock copolymers <i>via</i> RAFT.....	14
I-3. Regioselective “click” chemistry in the presence of copper catalyst.....	18
III-1. Aqueous RAFT polymerization of AEMA at 50 °C. ....	40
III-2. Block copolmerization of AEMA with HPMA.....	49
IV-1. Model Study for bioconjugation of D-glucuronic acid sodium salt with PAPMA. 66	
IV-2. Bioconjugation of PAPMA with D-glucuronic acid sodium salt.....	69
V-1. Preparation $\alpha$ -alkynyl-functionalized CTP.....	89
V-2. Preparation $\alpha$ -alkynyl-functionalized poly(AEMA) <i>via</i> RAFT polymerization at 45 °C. ....	91
V-3. Synthesis of Azide modified silicon wafer.....	94
V-4. Surface attachment of $\alpha$ -alkynyl-functionalized poly(AEMA) on azide functionalized silicon wafer through click chemistry.....	97
VI-1. SBA Synthesis.....	114
Appendix-1. Synthesis of 9-enyl 4-cyano-4-(phenylcarbanothioylthio)-pentanoate.....	138
Appendix-2. CTP activation. ....	139
Appendix-3. Synthesis of double bond functionalized asymmetric diazoinitiator.....	140

CHEMICAL NAMES AND ABBREVIATIONS

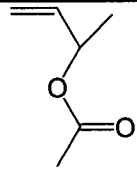
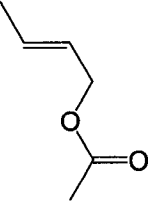
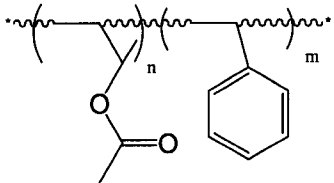
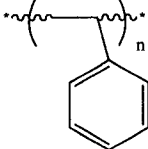
#	Chemical Names	Abbreviations	Structure
1	Hyaluronic acid	HA	 <p>The structure shows a repeating unit of hyaluronic acid in brackets with a subscript 'n'. It consists of two pyranose rings linked by a 1-3 glycosidic bond. The left ring is a β-D-glucopyranose unit with a carboxylic acid group (-COOH) at the C5 position. The right ring is a β-D-glucosamine unit with an acetamido group (-NHCOCH<sub>3</sub>) at the C2 position.</p>
2	<i>N</i> -Acetyl-β-D-glucosamine		 <p>The structure shows a single β-D-glucosamine unit with an acetamido group (-NHCOCH<sub>3</sub>) at the C2 position.</p>
3	β-D-Glucosuronic acid		 <p>The structure shows a single β-D-glucosuronic acid unit with a carboxylic acid group (-COOH) at the C5 position.</p>
4	Hyaluronic acid sodium salt	HA-Na	 <p>The structure shows a repeating unit of hyaluronic acid sodium salt in brackets with a subscript 'n'. It is identical to the repeating unit of hyaluronic acid, but the carboxylic acid group at the C5 position of the left ring is in its sodium salt form (-COO<sup>-</sup>Na<sup>+</sup>).</p>
5	D-Glucuronic acid sodium salt		 <p>The structure shows a single D-glucuronic acid sodium salt unit with a carboxylate group (-COO<sup>-</sup>Na<sup>+</sup>) at the C5 position.</p>
6	2-Aminoethyl methacrylate	AEMA	 <p>The structure shows a methacrylate backbone with an aminoethyl group (-CH<sub>2</sub>CH<sub>2</sub>NH<sub>2</sub>) attached to the ester oxygen. The amino group is shown as a protonated ammonium ion (-NH<sub>3</sub><sup>+</sup>Cl<sup>-</sup>).</p>
7	2-Hydroxyethyl methacrylamide		 <p>The structure shows a methacrylamide backbone with a hydroxyethyl group (-CH<sub>2</sub>CH<sub>2</sub>OH) attached to the amide nitrogen.</p>

#	Chemical Names	Abbreviations	Structure
8	2 <i>N</i> -(2-hydroxypropyl) methacrylamide	HPMA	
9	<i>N</i> -[3-(dimethylamino)propyl] methacrylamide	DMAPMA	
10	Poly(2 <i>N</i> -(2-hydroxypropyl) methacrylamide)	PHPMA	
11	Poly(2 <i>N</i> -(2-hydroxypropyl) methacrylamide- <i>b</i> - <i>N</i> -[3-(dimethylamino)propyl] methacrylamide)	Poly(HPMA- <i>b</i> -DMAPMA)	
12	3-Aminopropyl methacrylamide	APMA	

#	Chemical Names	Abbreviations	Structure
13	4, 4'-Azobis (4-cyanopentanoic acid)	V-501	
14	4-Cyanopentanoic acid	CTP	
15	Styrene	STY	
16	Poly(2-aminoethyl methacrylate)	PAEMA	
17	Poly(3-aminopropyl methacrylamide)	PAPMA	
18	Poly(2-aminoethyl methacrylate-b-2 N-(2-hydroxypropyl) methacrylamide)	PAEMA-b-PHPMA	
19	2,2'-Azobis(2-imidazolinylpropane) dihydrochloride	VA-044	

#	Chemical Names	Abbreviations	Structure
20	Poly(2-Aminoethyl methacrylate) macroCTA	PAEMA macrCTA	
21	Bioconjugated-3-aminopropyl methacrylamide	Bioconjugated APMA	
22	Bioconjugated-poly(3-aminopropyl methacrylamide)	Bioconjugated PAPMA	

#	Chemical Names	Abbreviations	Structure
23	Bioconjugated-poly(2-Aminoethyl methacrylate)	Bioconjugated PAEMA	
24	Bioconjugated-poly(2-Aminoethyl methacrylate-b-2 N-(2-hydroxypropyl) methacrylamide)	Bioconjugated PAEMA-b-PHPMA	
25	$\alpha$ -Alkynyl functionalized 4-cyanopentanoic acid	$\alpha$ -Alkynyl functionalized CTP	
26	$\alpha$ -Alkynyl functionalized poly(2-Aminoethyl methacrylate)	$\alpha$ -Alkynyl functionalized PAEMA	
27	2,2'-Azobis(2,4-dimethyl-4-methoxyvaleronitrile)	V-70	

#	Chemical Names	Abbreviations	Structure
28	sec-Butenyl acetate	SBA	
29	Crotyl acetate		
30	sec-Butenyl acetate-styrene Latex	STY-SBA	
31	Poly(styrene)	poly(STY)	



CHAPTER I  
INTRODUCTION  
Hyaluronic Acid

Hyaluronic acid (HA) **(1)** (Figure I-1), a linear, high-molecular weight polysaccharide, is comprised of alternating *N*-acetyl- $\beta$ -D-glucosamine **(2)** and  $\beta$ -D-glucosuronic acid **(3)** residues linked at 1-3 and 1-4 positions, respectively. Under physiological conditions it exists as the sodium salt form (HA-Na) **(4)**, is water soluble, and behaves as a weak polyelectrolyte. HA **(1)** is the primary component of synovial fluid and is thought to provide the lubricity of joint surfaces as well as the viscoelastic behavior of synovial fluid.<sup>1,2</sup> It is currently used in a wide range of biomedical applications, including post surgical adhesion prevention, rheology modification in orthopedic procedures, ophthalmic surgeries, tissue engineering, hydrogels and implants.<sup>3,4,5,6,7,8</sup> HA **(1)** is obtained commercially by either extraction from rooster comb or synthesis by microbial fermentation using streptococcus.<sup>9</sup>

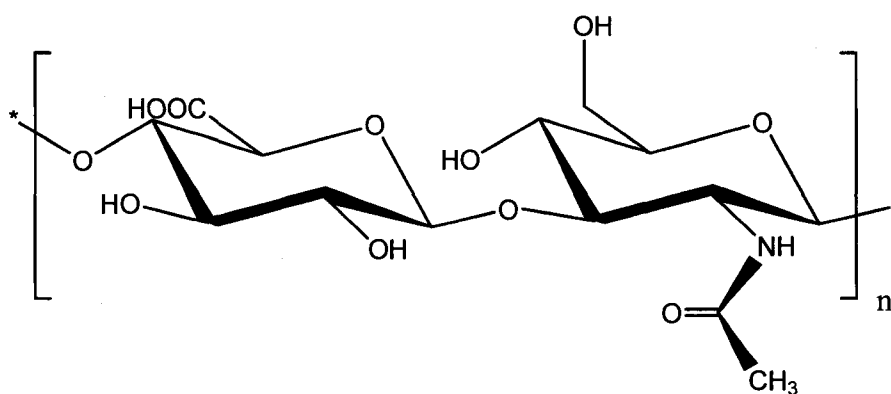


**Figure I-1. Hyaluronic Acid (1)**

Limitations of current systems include cost, allergy induction and reduced performance capabilities in comparison to native HA (1). Attempts to prepare surface coatings based on HA (1) *via* physisorption and chemisorption produced poorer than expected lubrication properties.<sup>4,10,11</sup> HA (1) is found with a range of molecular weights and molecular weight distributions. High molecular weight HA (1) has very high viscosity, and exhibits both pseudoplastic and rheopectic rheological behavior.<sup>12,13,14</sup> When the molecular weight of HA (1) is degraded, its viscosity is reduced, which is thought to result in decreased lubricity and function of the synovial fluid. It is of interest to prepare synthetic glycopolymer analogues to specifically target performance capabilities for biomedical applications.

### Glycopolymers

The term “glycopolymer” is used to describe synthetic polymers containing sugar moieties as pendant groups. Advances in controlled radical polymerization (CRP) allowing precise control of polymeric structures combined with increased understanding of structures required for specific biomimetic functions make glycopolymers promising candidates for biomedical applications. Glycopolymers have been investigated in diverse applications including macromolecular drugs, drug delivery systems, biocatalytic and biosensitive hydrogels, matrices for controlled cell culture, stationary phases for chromatographic purposes, and surface modifiers.<sup>15,16,17,18,19,20,21,22,23,24,25,26,27,28,29,30,31,32</sup> CRP can be used to prepare glycopolymers from unprotected monomers through post-polymerization modification strategies using reactive polymer precursors.<sup>29,33</sup> An alternate method for producing well-defined glycopolymers is the use of a

macromonomer, where a vinyl monomer carries the sugar moiety. There are advantages to both approaches. One of the main disadvantages of the post-polymerization method is that the conjugation of a pre-synthesized polymer backbone does not always result in 100% functionalization, resulting in an inhomogeneous sequence within the polymer chain.<sup>29</sup> On the other hand, with the post-polymerization approach it is possible to avoid the complex reaction and purification procedures often associated with carbohydrate monomer synthesis. The preparation of a reactive scaffold from a simple monomer, which can then be used to create a wide range of glycol-functionalized polymers through highly efficient post-polymerization reactions, is an attractive option. There are several successful examples in the literature of the post-polymerization modification approach applied to the synthesis of glycopolymers. For example, Haddleton et al. reported the polymerization of trimethylsilyl protected propargyl methacrylate *via* atom transfer radical polymerization (ATRP) and synthesis of well-defined glycopolymers with a high degree of conjugation utilizing “click” reactions between alkyne functionalized polymethacrylate and protected and unprotected glycosyl azides.<sup>34</sup> Hawker and coworkers reported the use of “click” reactions to successfully prepare asymmetric sugar functionalized dendrimers.<sup>35</sup> Matrix assisted laser desorption-ionization time of flight (MALDI-TOF) mass spectrometry was utilized to provide evidence that a single molecular species was obtained without side reactions. Liu and coworkers reported that poly(fluorenes) prepared by Sonogashira coupling of bromo-alkane functionalized monomers were glycosylated in near quantitative yield (98%) through the reaction of bromo-groups with a thio-sugar, using excess reagents.<sup>36</sup> Another important post-polymerization method for the synthesis of glycopolymers involves active esters.

Although this method often requires an excess of substrate as well as purification, it is effective.<sup>37</sup> Hu et al. reported ATRP of *N*-methacryloxysuccinimide using Cu(I)/bipy, which yielded low polydispersity and predicted number average molecular weight ( $M_n$ ) polymer, followed by quantitative substitution with gluco- and galactosamine.<sup>38</sup>

Well-defined primary amine-functionalized polymers were chosen as reactive polymer precursors due to their potential for post-polymerization modification reactions through primary amine pendant functionality. It was proposed that attachment of D-glucuronic acid sodium salt (**5**) to these polymers through the reductive amination reaction is possible, a mild reaction between the aldehyde functionality of the D-glucuronic acid sodium salt (**5**) and the primary amine functionalities of polymer precursors. Therefore, the controlled radical polymerization of primary amine functionalized polymers is of great interest for our goal of obtaining well-defined glycopolymers.

### Primary Amine Vinyl Monomers

Primary amine-functionalized methacrylate monomers are of interest for their potential utility in post-polymerization modification reactions, such as amide and imine formation, ring-opening reactions and Michael addition reactions, enabling advances in areas including new approaches for cross-linking micelles and hydrogels, synthesis of novel copolymers for biomimetic scaffold structures under mild conditions, preparation of well defined cationic latexes, and surface functionalization for bioconjugation.<sup>39,40,41,42,43,44,45,46,47,48,49</sup> For example, Alaissari *et al.* developed thermosensitive core-shell latex particles with a core of poly(methyl methacrylate)

(PMMA) and a positively charged shell prepared through statistical copolymerization of 2-aminoethyl methacrylate (AEMA) (**6**) and *N*-isopropylacrylamide (NIPAAm).<sup>50</sup> On absorption of rhodamine-labeled oligonucleotides, particles with temperature-selective fluorescent response were produced.<sup>51,52,53</sup> Armes and coworkers reported the synthesis of cyclic sugar modified methacrylates from the reaction of AEMA (**6**) with D-gluconolactone and lactobionolactone.<sup>54</sup> These monomers were further used by various research groups to produce well-defined glycopolymers utilized for the stabilization of gold nanoparticles.<sup>55,56,57</sup> Additionally, AEMA (**6**) copolymers have been evaluated for drug/gene delivery applications.<sup>58,59,60</sup> Dubruel *et al.* synthesized a series of polymethacrylates containing primary amine functionalities *via* conventional free radical copolymerization of dimethylaminoethyl methacrylate (DMAEMA), tertbutyl carbonate (tBoc) protected AEMA (**6**) and t-Boc protected 4-methyl-5-imidazolyl methyl methacrylate, which were subsequently used for the coupling of the fluorescent probe Oregon Green.<sup>61</sup> Hennick *et al.* synthesized random copolymers of DMAEMA with AEMA (**6**) through conventional radical polymerization, reacted the primary amine groups with protected thiol groups and subsequently conjugated the copolymers with decapeptide, reporting a coupling efficiency of 95%.<sup>62</sup> In these examples, AEMA (**6**) was copolymerized via conventional radical polymerization, or the primary amine was pre-functionalized prior to polymerization. It is of interest to directly polymerize AEMA (**6**) with preserved functionality in a controlled fashion, and to evaluate copolymers with precisely controlled architectures (i.e. crosslinked micelles, block ionomer complexes, and vesicles) for potential biomedical applications.

Controlled radical polymerization techniques such as ATRP<sup>63</sup> and RAFT<sup>64,65</sup> have provided facile routes for obtaining polymers of predetermined molecular weights and precise architectures for amine-based vinyl monomers. However, the controlled polymerization of primary amine containing monomers is challenging. In general, primary amine containing monomers should be protected in order to avoid unwanted side reactions. For example, AEMA (**6**) can be rapidly converted to 2-hydroxyethyl methacrylamide (**7**) at high pH through monomer rearrangement.<sup>58</sup> It has also been suggested that when the amine group is deprotonated, AEMA (**6**) can undergo Michael addition. In order to circumvent these side reactions, Dufresne and Leroux utilized t-Boc protected AEMA (**6**) for polymerization *via* ATRP, resulting in reasonably good control.<sup>66</sup> In addition, He *et al.* reported the direct polymerization of AEMA (**6**) under acidic conditions *via* ATRP in water, in a methanol-water mixture and in an isopropyl alcohol-water mixture, and also *via* RAFT polymerization in dimethyl sulfoxide (DMSO).<sup>67</sup> They reported slow polymerization rates in methanol. Even though polymerization rates were faster in water, the reaction exhibited poor control yielding a PDI of 1.41. However, when a cosolvent combination of 80:20 2-propanol:water was used, well-controlled polymerizations were achieved with PDIs lower than 1.25. For RAFT polymerization, polymers with well-defined molecular weights and PDIs between 1.25 and 1.29 were reported. The authors also reported synthesis of well-defined AEMA (**6**) based diblock copolymers using poly(ethylene oxide)-based ATRP macroinitiators and statistical copolymers of AEMA (**7**) with 2 N-(2-hydroxypropyl) methacrylamide (HPMA) (**8**) and DMAEMA. Further, preparation of shell cross-linked micelles with

pH-responsive cores consisting of PAEMA-*b*-PDAEMA copolymers with polyethylene glycol diacrylate crosslinking agent was reported.

Recently, the McCormick research group reported the aqueous RAFT polymerization of HPMA (**8**) and N-[3-(dimethylamino)propyl] methacrylamide (DMAPMA) (**9**).<sup>68</sup> Poly(2 N-(2-hydroxypropyl) methacrylamide) (PHPMA) (**10**) has been proposed as a nonviral carrier for drug delivery because of its biocompatibility and nonimmunogenicity.<sup>69,70,71,72,73,74,75,76</sup> Block copolymers of HPMA(**8**) have been shown to form micelles, vesicles and block ionomer complexes in aqueous environments, illustrating their potential to be used as nonviral drug/gene carriers.<sup>77</sup> McCormick and coworkers have also recently reported the aqueous RAFT generated block copolymer poly(HPMA-*b*-DMAPMA) (**11**), showing the formation of an electrostatic complex between the positively charged DMAPMA (**9**) block with negatively charged polynucleotides for gene delivery based applications.<sup>78</sup> In addition, McCormick and coworkers reported the aqueous RAFT polymerization of 3-aminopropyl methacrylamide hydrochloride (APMA) (**12**), a primary amine methacrylamide, in a dioxane-water mixture.<sup>79</sup> Homopolymers of APMA (**12**) were then chain extended with *N*-isopropylacrylamide (NIPAM) to produce temperature-responsive block copolymers that formed vesicles upon increasing the solution temperature.

Research has demonstrated that the synthesis of well-defined PAEMA and its copolymers with controlled architectures and narrow polydispersities is extremely challenging. The merits of aqueous RAFT polymerization may allow the direct synthesis of AEMA homo and block (co)polymers with controlled structures. The research in this thesis involves the attempt to polymerize unprotected AEMA via aqueous RAFT and its

subsequent incorporation into hydrophilic block copolymers. Since primary amine groups are amenable to a wide range of post-polymerization chemistries, this versatile primary amine functionalized polymer can undergo reductive amination reaction with sugars, resulting in new controlled glycopolymer architectures with multiple functionalities for biomedical and pharmaceutical applications.

### Reversible Addition-Fragmentation Chain Transfer (RAFT) Polymerization

RAFT is a controlled radical polymerization technique, first reported by Chiefari in 1998. RAFT is similar to conventional free radical polymerizations but the control is achieved upon the addition of a suitable chain transfer agent (CTA).<sup>80,81</sup> RAFT is a versatile polymerization technique, which is capable of polymerizing a variety of vinyl monomers and providing facile routes for obtaining polymers of predetermined molecular weights and precise architectures.<sup>82</sup> Scheme I-1 demonstrates the accepted mechanism for the RAFT polymerization.<sup>83</sup>

#### *The RAFT Mechanism*

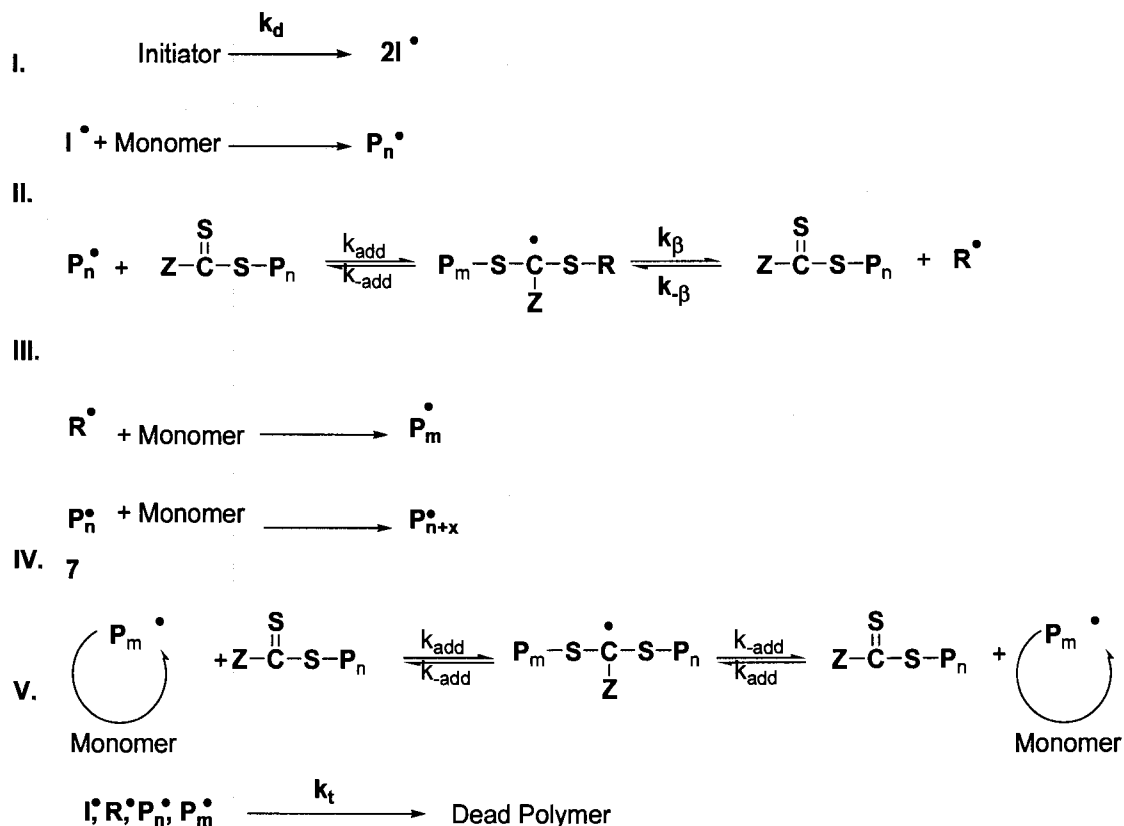
The RAFT mechanism resembles the conventional free radical polymerization mechanism. The difference in the RAFT mechanism is the presence of a series of reversible chain transfer reactions to give control. For this reason, in the initiation step, a primary radical source is needed to initiate polymerization.<sup>82,84,85,86,87</sup> Then, a pre-equilibrium step is achieved, where initiated oligomeric radical chains ( $P_n\cdot$ ) add rapidly to the CTA ( $k_{add}$ ) and form an intermediate radical species. A new radical ( $R\cdot$ ) is formed upon fragmentation of the intermediate by expelling the R group ( $k_{\beta}$ ) and producing a macro chain transfer agent (macroCTA). The new  $R\cdot$  re-initiates the polymerization. The



time of the pre-equilibrium period is directly associated to the time required for all R· fragments to add to monomer. Therefore, the R group must have the ability to effectively fragment and R· must be able to quickly re-initiate the polymerization in order to achieve narrow molecular weight distributions.<sup>88</sup> In the main equilibrium step, polymeric radicals react with the macroCTA to yield an intermediate species with two identical polymer sides. In this step, all chains have equal rates of addition, fragmentation, and propagation and most of the monomer conversion occurs.<sup>83,89</sup> The termination step includes radical coupling and disproportionation, which are directly related to the initiator's initial concentration.<sup>83</sup> The termination of the intermediate radicals was also observed.<sup>90</sup> The number of dead chains can be suppressed using a high [CTA]<sub>0</sub>/[initiator]<sub>0</sub> ratio.

#### *RAFT Chain Transfer Agent*

The CTA carries both R and Z groups which determine directly the CTA's capabilities in the fragmentation and re-initiation process.<sup>82</sup> The R group should be a good leaving group and capable of re-initiating polymerization during the pre-equilibrium stage.<sup>91,92</sup> The Z group has two different roles: the activation of the thiocarbonyl double bond for free radical addition and the stabilization of the intermediate species for successful fragmentation.<sup>93,94</sup> However, it was observed that a high stabilization can result in slow fragmentation of the intermediate radical adduct. This may cause both a decrease in speed of the polymerization<sup>95,96,97</sup> and side reactions that could lead to dead chains.<sup>98,99,100,101</sup> Figure I-2 shows common CTA's used for RAFT.



**Scheme I-1.** Accepted RAFT mechanism.<sup>11</sup>

### *Kinetic Behavior*

Ideally, the rate of polymerization observed for a RAFT process should be comparable to conventional free radical polymerizations. However, a low polymerization rate is observed for most RAFT systems.<sup>91,97,102,103</sup> This is related to the observed induction period, initialization period, and rate retardation period. The induction period describes the deviation from linear pseudo first-order kinetics during the early polymerization stages.<sup>83,94</sup> It has been shown that the main cause of the deviation is the poor fragmentation and reinitiating ability of the R group.<sup>104,105,106,107</sup> To minimize the induction period, less stabilizing Z groups have been employed.<sup>93,94,99,108</sup> The initialization period is the amount of time it takes for the starting CTA to be consumed.<sup>109</sup>

It was found that the initialization period is a function of both the R group and the specific monomer utilized.<sup>110,111,112</sup> RAFT polymerization also shows rate retardation, which is mainly dependent on the nature of monomer and CTA, and the concentration of the CTA. Possible reasons of rate of retardation might be a long lived intermediate radical species,<sup>113,114,115,116,117,118,119,120,121</sup> bimolecular termination reactions,<sup>122,123,124,125</sup> and slow reinitiation.<sup>126,127,128</sup>

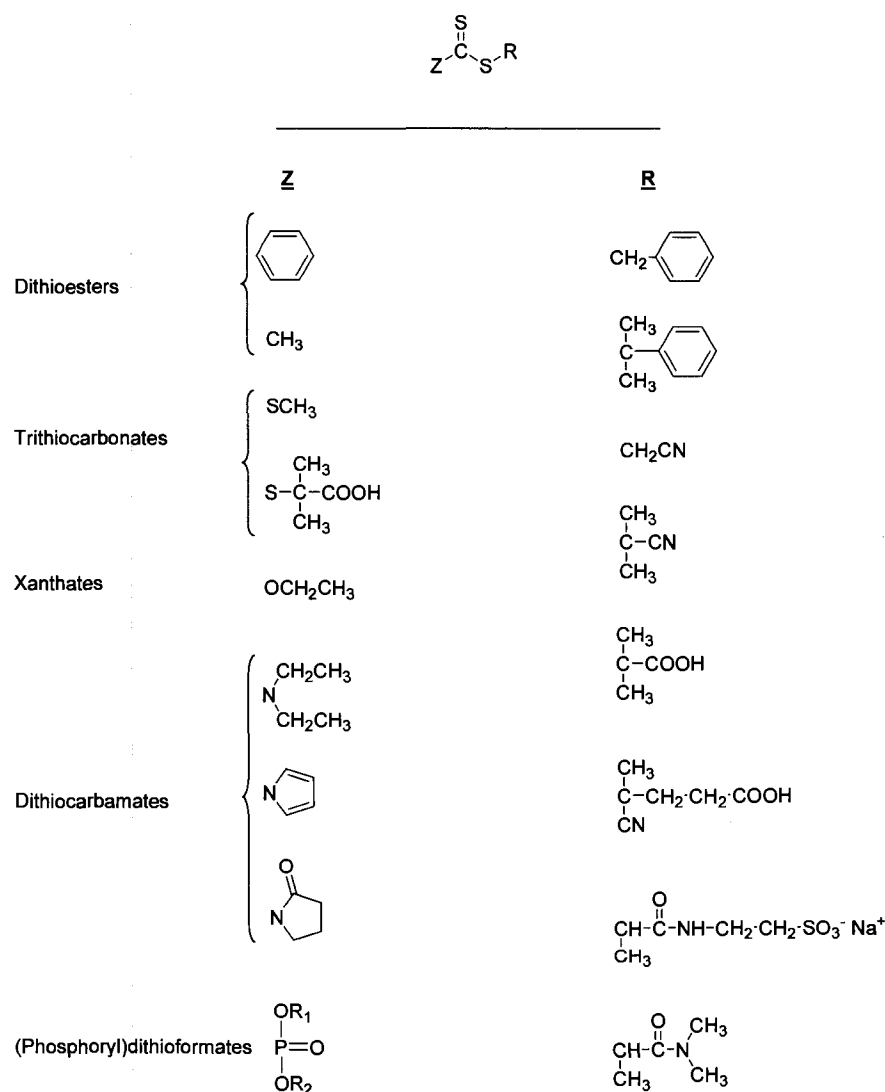


Figure I-2. Common thiocarbonylthio CTAs utilized in RAFT.<sup>82</sup>

Equation 1 defines the theoretical molecular weight calculation of the polymer,  $M_{n,th}$  in the RAFT polymerization process.

$$M_{n,th} = \left( \frac{[Monomer]_o}{[CTA] + 2f[I]_o(1 - e^{-k_d t})} \times MW_{Mon} \times Conversion \right) + MW_{CTA} \quad (1)$$

If the initiator concentration is kept very low compared to the CTA concentration, Equation 1 can be simplified into Equation 2.

$$M_{n,th} = \left( \frac{[Monomer]_o}{[CTA]_o} \times MW_{Mon} \times Conversion \right) + MW_{CTA} \quad (2)$$

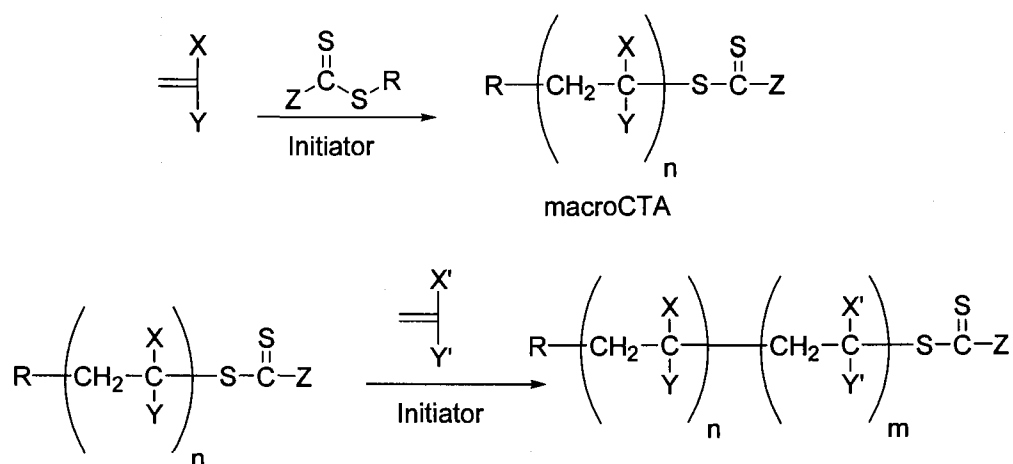
As shown in Equation 2, there is a linear relationship between molecular weight of polymer and conversion. This allows us to use Equation 2 to estimate required concentrations and conversion levels to achieve polymers with desired molecular weights and low polydispersities.<sup>82</sup>

The polydispersity of the resulting polymers can be estimated at 100 % conversion for a given CTA/monomer system through Equation 3 if the  $C_{tr}$  of the CTA is known.<sup>129</sup> deBrouwer and coworkers showed that  $C_{tr}$  must be  $\geq 10$  to achieve low polydispersity polymers.<sup>124,130</sup>

$$\frac{M_w}{M_n} = 1 + \frac{1}{C_{tr}} \quad (3)$$

### *Synthesis of Block Copolymers*

The preservation of the thiocarbonylthio group on the end of the polymer chain facilitates the preparation of AB, ABC and ABA block copolymer structures.<sup>82</sup> The desired block copolymers can be prepared upon the addition of a second monomer to a macroCTA (polymer carrying the thiocarbonylthio group). For successful block copolymerization, the preparation of the macroCTA is very important. The desired macroCTA is generally synthesized upon cessation of the polymerization before quantitative monomer conversion is achieved. The resulting macroCTA is carefully purified and used subsequently for block copolymerization with addition of the second monomer (Scheme I-2). For a successful block polymerization, the addition sequence of the monomers is crucial because the macroCTA's propagating radical must effectively fragment and attach to the second monomer.<sup>131,132</sup> In addition, well-defined block copolymers can also be prepared using transformation reactions, where previously prepared polymers (using different polymerization method) are functionalized with thiocarbonylthio groups. For example, Li and coworkers prepared poly(ethylene oxide)-block-poly(dimethylacrylamide)-block-poly(*N,N*isopropylacrylamide) from dithiobenzoate functionalized poly(ethylene oxide).<sup>133</sup>



**Scheme I-2.** Synthesis of AB diblock copolymers *via* RAFT.<sup>82</sup>

### *Aqueous RAFT Polymerization*

The first successful aqueous RAFT polymerization was reported by Chiefari et al. They polymerized 4-styrene sulfonate (NaSS) at 70 °C directly in water using 4, 4'-azobis (4-cyanopentanoic acid) (V-501) (**13**) as the primary radical source and 4-cyanopentanoic acid (CTP) (**14**) as the RAFT agent.<sup>84</sup> Subsequently, the McCormick research group reported aqueous polymerization behavior of NaSS with CTP (**14**) at 70 °C.<sup>134</sup> They also prepared the block copolymers of NaSS with 4-vinylbenzoic acid (VBA). The resulting block copolymers showed stimuli-responsive behavior with respect to pH. The McCormick group performed the aqueous RAFT polymerization of multiple water-soluble monomers, including those listed in Figure I-3, using various water soluble CTAs (Figure I-4). Sumerlin and coworkers first succeeded in the aqueous RAFT polymerization of acrylamido monomers.<sup>135,136</sup> Donovan and coworkers showed the aqueous RAFT polymerization of several zwitterionic monomers.<sup>139,137</sup> Thomas and coworkers polymerized acrylamide (AM), and observed significant retardation in the polymerization rate.<sup>138</sup> He and coworkers showed the successful polymerization of AM

using trithiocarbonate CTAs, which have higher intermediate fragmentation rates.<sup>90</sup>

Convertine and coworkers demonstrated the first room temperature aqueous RAFT polymerization of dimethyl acrylamide (DMA) and AM using 2-(1-carboxy-1-methylethylsulfanylthiocarbonylsulfanyl)-2-methyl-propioniacid (CMP) as CTA, resulting in narrow polydispersities.<sup>139</sup> Convertine and coworkers also demonstrated the controlled polymerization of *N*-isopropylacrylamide (NIPAM) in both organic and aqueous media, using room temperature RAFT conditions.<sup>140,141</sup>

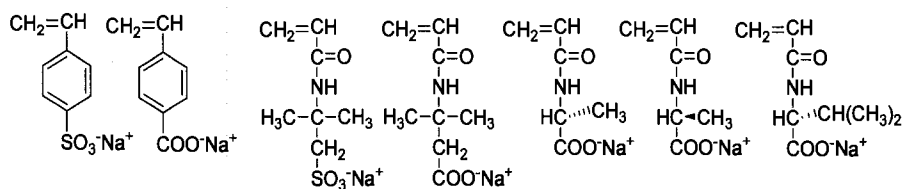
### *Synthesis of Polymeric Brushes*

RAFT polymerization can be also used for surface polymerization to form polymer brushes.<sup>142,143,144,145</sup> Polymer chains tethered by one end to a surface or an interface produce monolayer assemblies on the surface called polymer brushes. There are two successful routes for the preparation of well-defined polymer brushes through RAFT polymerization using the “grafting from” approach. The first method involves the attachment of the conventional radical initiator on the targeted surface and the polymerization is carried out from the surface with the addition of a CTA. In the second method, an appropriate CTA is directly attached on the surface from either R or Z groups.<sup>146,147,148,149</sup> There are also successful examples for the preparation of polymer brushes using the “grafting to method”.<sup>48,150,151,152</sup> In this method, telechelic polymers are first synthesized through the functionalization of the  $\alpha$ - or  $\omega$ -chain end. These telechelic polymers are then attached to a suitably functionalized surface.

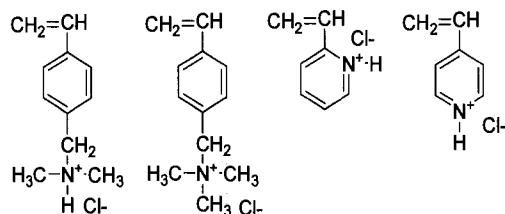
“Click” chemistry, described in the next section, has been recently employed for the modification of surfaces.<sup>153</sup> Surface modification using both “grafting to” and “grafting from” approaches is possible by combining “click” chemistry and RAFT

polymerization.<sup>154,155</sup> This approach can be experimentally simple and provide better control of the polymerization with high grafting density. This thesis explores the utilization of combined RAFT and “click” chemistry for the preparation of primary amine functionalized polymer brushes, which will enable further developments in surface modification, including surface attachment of bio-related materials such as glycopolymers.

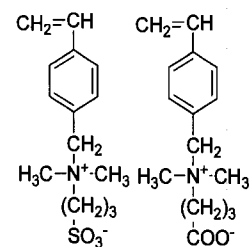
#### Anionic Monomers



#### Cationic Monomers



#### Zwitterionic Monomers



#### Neutral Monomers

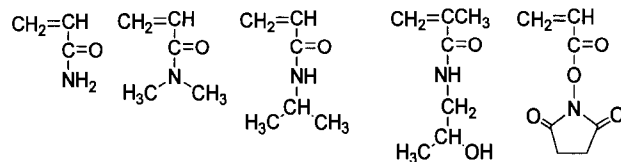


**Figure I-3.** Examples of water-soluble monomers polymerized by RAFT.<sup>8</sup>



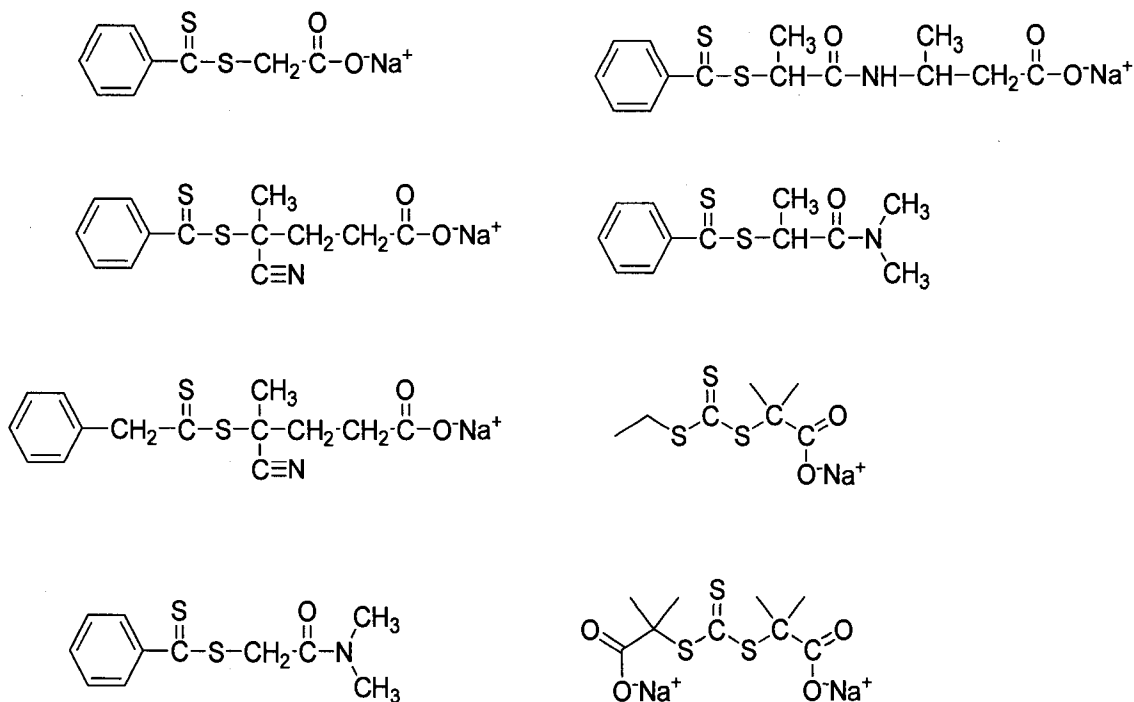
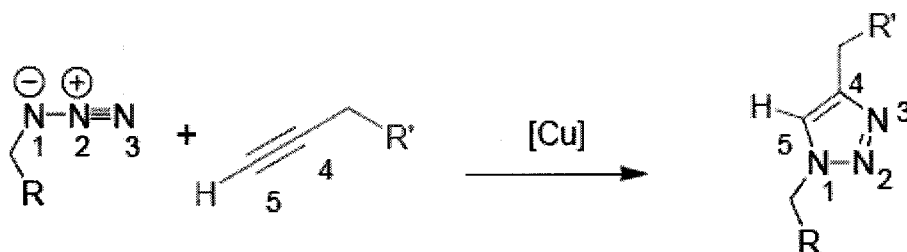


**Figure I-4.** Chain transfer agents employed in aqueous RAFT polymerizations.<sup>82</sup>

### “Click” Chemistry

Recent advancements in CRP techniques have resulted in the development of facile routes to obtain telechelic polymers with predetermined molecular weights and narrow molecular weight distributions. Although CRP has been used for the polymerization of a wide range of monomers, there is intense interest in synthesis of functional polymers with capabilities for post-polymerization modification. This method requires specific end group functionality that must be compatible with polymerization conditions.<sup>156,157</sup> As CRP polymerization provides predetermined chain end functionality that is easily controlled, there have been numerous reports of CRP preparation of functional polymers for post-modification applications such as fluorescently labeled chains, polymeric bioconjugates and surface-immobilized polymers.<sup>68,158,159,160,161</sup>

The term “click” chemistry was originally coined in a generic sense to mean reactions that are easy to perform, relatively unaffected by the presence of oxygen and water, and demonstrate high yield and facile isolation.<sup>162</sup> However, the Huisgen 1,3-dipolar cycloaddition of terminal alkynes with azides to give 1,2,3-triazoles has emerged as the leading “click” reaction.<sup>163,164</sup> The Huisgen 1,3-dipolar cycloaddition is a more versatile method, as the usage of copper (I) catalyst promotes both the speed and the regioselectivity of the reaction (Scheme I-3).<sup>165,166</sup> Most methods use Cu (I) salts directly, other methods generate the copper (I) species by reduction of Cu(II) salts using sodium ascorbate or metallic copper. Besides the copper catalyst, a base is added, mechanistically for promoting the formation of the copper(I)-acetylide.



**Scheme I-3.** Regioselective “click” chemistry in the presence of copper catalyst.

“Click” chemistry was originally used in organic synthesis, and more recently expanded to materials science. There are numerous reports of the use of “click” chemistry as a post-polymerization modification technique for functionalizing polymers prepared by CRP methods.<sup>167,168,169,170,171,172,173,174,175,176,177,178,179,180,181,182,183,184,185,186,187</sup> Given the telechelic nature of polymers prepared *via* CRP techniques, “click” chemistry is an attractive method for the functionalization of polymer chain ends. For example,

Agut et al. prepared  $\alpha$ -azide and alkyne functionalized poly[2-(dimethylamino)ethyl methacrylate] (PDMAEMA) through ATRP using  $\alpha$ - $\omega$ -functionalized initiators for the preparation of hybrid diblock copolymers.<sup>183</sup> These blocks were composed of a polypeptide PDMAEMA block that were covalently linked utilizing “click” chemistry. Lutz et al. recently reported ATRP synthesized polymers that were  $\omega$ -chain end functionalized with azides.<sup>184</sup> These azide functional polymers were subsequently reacted with various alkyne functional compounds to prepare  $\omega$ -hydroxy,  $\omega$ -carboxyl and  $\omega$ -methyl-vinyl functionalized polystyrene. In addition, the combination of ATRP and “click” chemistry was employed by Sumerlin et al. to prepare well-defined  $\omega$ -(meth)acryloyloxy functionalized poly(*n*-butyl acrylate) and  $\omega$ -acryloyloxy functionalized polystyrene macromonomers.<sup>185</sup> Unlike ATRP, the use of “click” chemistry for the post-polymerization modification of RAFT synthesized polymers has been minimal. One such example was carried out by Hawker et al. who reported the synthesis of alkyne-functionalized block copolymers *via* RAFT polymerization.<sup>186</sup> An alkynyl-functionalized RAFT chain transfer agent (CTA) was used directly for the sequential polymerization of tetrahydropyran acrylate and styrene (**15**), followed by selective cleavage of the tetrahydropyran esters to give  $\alpha$ -alkynyl-functionalized block copolymers that are capable of forming surface-functionalized “clickable” micelles in aqueous solutions. Another example utilizing RAFT polymers was reported by Sumerlin et al. who synthesized  $\alpha$ -azido terminal polymers using an  $\alpha$ -azido functionalized chain transfer agent (CTA) that allowed the preparation of a range of functional telechelics.<sup>187</sup>

“Click” chemistry has also been extensively employed for the modification of surfaces with different types of polymers. Meldal et al. were the first to demonstrate that “click” chemistry can be used to modify solid substrates.<sup>153</sup> They reported the successful synthesis of diversely 1,4-substituted [1,2,3]-triazoles in peptide backbones or side chains upon using the combination of “click” chemistry and solid-phase peptide synthesis. Given the success of Medal and coworkers, other researchers began to explore the attachment of CRP polymers to various surfaces. For example, Brittain et al. reported the immobilization of an  $\alpha$ -alkyne functionalized polymer, prepared *via* RAFT polymerization, to azide functionalized silica nanoparticles *via* “click” chemistry.<sup>154</sup> The same group also demonstrated a “grafting from” approach by first attaching  $\alpha$ -alkynyl functionalized CTA to azide functionalized silica nanoparticles followed by RAFT surface polymerization of styrene (**15**) and methyl methacrylate.<sup>155</sup> They achieved a grafting density of 1.2-1.3 RAFT agent/nm<sup>2</sup> for the immobilization of CTA onto silica nanoparticles, resulting in high density polymer brushes. Additionally, Drockenmuller et al. grafted  $\omega$ -azido functionalized polymers prepared through ATRP and nitroxide mediated radical polymerization (NMP) on alkynyl-fuctionalized silicon wafers using click chemistry.<sup>188</sup> Polymer brushes with a thickness of 6 nm and grafting densities of 0.2 chains/nm<sup>2</sup> were reported.

## Motivation for Research

Native carbohydrates and their synthetic analogues are the main interest of this research. As described in previous sections, the synthetic analogues of carbohydrates, also called glycopolymers, are important for studying the complex roles of native carbohydrates in many biological processes. To our knowledge, there are only two prior reports of the synthesis of charged glycopolymers, both of which involve complex reaction steps, protection chemistry and complex purification steps. Development of a facile, direct technique for synthesis of charged glycopolymers is therefore of interest.

Although the post-polymerization method is an attractive option for glycopolymer synthesis, as it can be performed without complex reactions and purification procedures, its application is limited due to the demand for a highly reactive polymer precursor and an efficient post-polymerization reaction. “Click” chemistry has been reported for the synthesis of neutral glycopolymers. However, this approach requires multiple reaction steps, including synthesis of alkynyl functionalized polymers, synthesis of azide functionalized sugars, and purification of resulting glycopolymers from transition metal impurities. Thus there is a need for demonstration of an alternative post-polymerization methodology with reduced complexity.

Primary amine-functionalized polymers are of interest for their potential utility in post-polymerization modification reactions, enabling synthesis of novel glycopolymers under mild conditions. However, the controlled polymerization of primary amine functionalized monomers is challenging. In general, primary amine containing monomers should be protected in order to avoid unwanted side reactions. Prior work has demonstrated that the synthesis of well-defined primary amine functionalized polymers

and their copolymers with controlled architectures and narrow polydispersities is extremely challenging. Therefore, there is a need to find an alternative method for the synthesis of well-defined homo and block copolymers of primary amine functionalized monomers directly, without the use of protecting groups.

There has been continuous interest in surface modification by glycopolymers. Although there are successful examples of the synthesis of glycopolymer brushes on solid substrates, these reports include multiple reaction steps and complex purification procedures. Therefore, there is a need to develop an alternative method to facilitate the synthesis of well-defined glycopolymer brushes.

In summary, the motivation for this study is to find alternative and simpler solutions for the current problems, which are:

- Direct synthesis of homopolymers and copolymers from primary amine-containing monomers without the use of protecting groups.
- Synthesis of well-defined primary amine functionalized polymers and their copolymers with controlled architectures and narrow polydispersities
- Synthesis of well-defined charged glycopolymers through post-polymerization reactions, avoiding multiple reaction steps and complex purification methods.
- Synthesis of well-defined glycopolymer brushes through an alternative method to reduce the complexity of reaction steps.

## Prospectus of Research

Glycosaminoglycans, HA (1) and heparin, are involved in a wide range of physiological processes, including cell proliferation and migration, modulation of angiogenesis and inflammatory responses.<sup>189,190,191</sup> Each of these processes are based on carbohydrate interactions. However, many of the physiological activities that are mediated by glycosaminoglycans have not been completely defined due to their diverse and complicated structures and capacity to interact with biologically active proteins. Therefore, their synthetic analogues are emerging as important tools for investigating carbohydrate-based interaction processes.<sup>192</sup> Combination of the synthetic diversity of polymers with the multivalency of saccharides results in a new class of synthetic bioconjugates, which allows mimicking of these carbohydrate interactions.<sup>193</sup> To date the reported synthesis of model glycosaminoglycans is limited to two examples, where conventional free radical chemistry was used for the polymerization of sulfate and amine functionalized macromonomers.<sup>194,195</sup> The resulting functionalized glycopolymers displayed high polydispersity.

Controlled radical polymerization (CRP) has emerged as an important polymerization method to obtain well-defined glycopolymers of controlled architecture.<sup>196</sup> CRP allows us to probe the effects of molecular architecture, topology, and molecular weight on biological function. Multiple reports of CRP methods have appeared in the literature for the synthesis of neutral glycopolymers. However, there have been no reports of synthesis of charged glycopolymers through CRP methods. Moreover, there are some issues that must be resolved. These include potential problems caused by transition metal impurities in glycopolymers remaining either from ATRP or “click”

reactions and the requirement for stringent purification methods during the synthesis of glycomonomers.

Most efforts toward the synthesis of well-defined glycopolymers have utilized the macromonomer route, which suffers from complex purification steps.<sup>197</sup> However, the post-polymerization method is an attractive option for glycopolymer synthesis that does not involve complex reaction and purification procedures. Therefore, it is of interest to prepare a reactive scaffold from a simple functionalized monomer, which can then be used to create a wide range of glyco-functionalized polymers through highly efficient reactions.

The success of the post-polymerization method is directly related to the reactivity of the polymer precursor and the efficiency of the post-polymerization reaction.<sup>197</sup> Well-defined primary amine functionalized polymers are promising candidates for the preparation of reactive scaffolds, due to the presence of primary amine functionality, which can easily undergo post-polymerization reactions under mild conditions. However, CRP of primary amine functionalized monomers is challenging. In the literature, there are limited examples showing the controlled polymerization of primary amine functionalized polymers in organic solvent.<sup>67, 69</sup> However, these reactions suffered from side reactions and long reaction times. Determining RAFT polymerization conditions that will result in controlled polymerization of primary amine functionalized monomers such as AEMA (**6**) and APMA (**12**) in aqueous solvent can lead to the development of facile preparation techniques for well-defined glycopolymers.



HA, an anionic glycosaminoglycan, is an important carbohydrate in the human body, performing key rolew in the regulation of many cellular and biological processes.<sup>4,10,11,12</sup> However, the industrial application of HA **(1)** has limitations including high cost, allergy induction and reduced performance capabilities in comparison to native HA **(1)**. It is of interest to prepare its synthetic polymer conjugate analogues to specifically target performance capabilities for biomedical applications. The reductive amination reaction between synthetic primary amine functionalized polymers and carboxylic acid functionalized sugars has the potential to provide a route for effective post-polymerization reactions to obtain well-defined carboxylic acid functionalized glycopolymers to mimic HA **(1)**.

The continuous evolution of polymer brush synthesis and other surface functionalization methods allow surface modification by glycopolymers, which has potential utility in glycomics and biocoating applications. Recently, researchers have used “click” chemistry to functionalize surfaces.<sup>186,187</sup> However, the attachment of glycopolymers to flat surfaces utilizing “click” chemistry has not been reported. The attachment of primary amine functionalized polymers on a surface using “click” chemistry and the subsequent post-polymerization reaction with carboxylic acid functionalized sugars has the potential to be a promising, practical method to create carboxylic acid functionalized glycopolymer brushes on a given substrate.

In this research, we intend to fill a gap in the area of glycopolymer research by proposing the synthesis of carboxylic acid functionalized glycopolymers through a practical one-step post-polymerization reaction between well-defined primary amine functionalized polymers and carboxylic acid functionalized sugars, without the need for

complex purification steps. We also propose to evaluate “click” chemistry methodology for the preparation of primary amine functionalized polymer brushes, which have potential application for the creation of surface attached glycopolymers.

## CHAPTER II

### RESEARCH GOAL AND OBJECTIVES

Carbohydrates are natural polymers, in which various monosaccharide building blocks are assembled in diverse chain lengths and architectures.<sup>197,198</sup> Because of their unlimited structural variations, carbohydrates carry a large density of information.<sup>199,200</sup> It is now clear that carbohydrates play a major role in recognition events, which are the key step in a variety of biological processes based on cell-cell interactions, such as blood coagulation, immune response, viral infection, inflammation, embryogenesis and cellular signal transfer.<sup>201</sup> Carbohydrates participate in complex biological functions, including the storage and transport of energy (e.g. starch, glycogen), the generation of structure and support (e.g. cellulose, chitin, chitosan), controlling osmotic pressure in connective tissues (e.g. proteoglycans), providing lubricating and cushioning properties in the extra cellular matrix (e.g. glycosaminoglycans such as HA (**1**)) and helping blood coagulation (the sulfated polysaccharide, heparin).<sup>202</sup>

The combination of synthetic polymer backbone with pendent mono or oligosaccharide segments allows preparation of synthetic carbohydrates resulting in polymers with unique properties. Such structures are generally called glycopolymers. Development of biomimetic polymers that could reproduce the lubricating, cushioning or anti-inflammatory properties of native carbohydrates is of intense interest.<sup>203,204,205,206,207,208</sup> However, the synthesis of glycopolymers with complex carbohydrate segments is still limited. Therefore, there is a need to achieve synthetic polymers with well-defined carbohydrate segments, capable of conveying sophisticated functions in biological systems.

Hyaluronic Acid (HA) **(1)**, an anionic glycosaminoglycan, is a linear polysaccharide consisting of alternating *N*-acetyl- $\beta$ -D-glucosamine **(2)** and  $\beta$ -D-glucosuronic acid **(3)** residues. HA **(1)** is widely studied due to its key role in the regulation of many cellular and biological processes, as well as its important physical properties such as hydration, lubricity, and viscosity control. HA **(1)** also plays an important role in protein-carbohydrate interaction during the regulation of cell activities.<sup>209</sup> The industrial application of HA **(1)** possesses some limitations including cost, allergy induction and reduced performance capabilities in comparison to native HA **(1)**. It is of interest to prepare synthetic polymer conjugate analogues of HA to specifically target performance capabilities for biomedical applications.

There are two main methods to prepare well-defined glycopolymers: the macromonomer route and the post-polymerization route.<sup>197</sup> The macromonomer route involves the controlled polymerization of a vinyl monomer carrying the sugar moiety at the pendant group. An alternative is the post-polymerization route where a reactive polymer precursor is prepared from a functional monomer and sugar molecules are attached to polymer chains using a highly efficient organic reaction. Both methods have advantages and disadvantages. The macromonomer route provides a well-defined homogeneous glycopolymer, but it suffers from stringent purification requirements during macromonomer synthesis. The post-polymerization method does not always result in 100% functionalization, yielding inhomogeneous polymer chains, but it does not require complex purification steps.<sup>197</sup> Therefore, the post-polymerization route with highly efficient reactions is an attractive method to synthesize a wide range of glycol-functionalized polymers.

The hypothesis of this study is that well-defined synthetic anionic glycosaminoglycans can be prepared easily using the post-polymerization strategy, where anionic sugar moieties are bioconjugated with the well-defined reactive polymer precursor. The overall goal of this research is to synthesize well-defined synthetic anionic glycosaminoglycans using a reductive amination reaction between carboxylic acid functionalized sugar, glucuronic acid sodium salt, and well-defined primary amine functionalized polymers such as poly(3-aminopropylmethacrylamide) (PAEMA) **(16)** and poly(2-aminoethylmethacrylate) (PAPMA) **(17)**. This approach will avoid stringent purification steps and provide a new bioinspired polymer, which can be used to model the protein-carbohydrate interactions and lubricity properties of anionic glycosaminoglycans.

To achieve this goal, the following objectives will be addressed:

1. Develop RAFT conditions to control the polymerization *N*-3-aminopropyl methacrylamide (APMA) **(12)** and 2-aminoethyl methacrylate (AEMA) **(6)** directly in aqueous medium;
2. Investigate the aqueous polymerization behavior of AEMA **(6)** and APMA **(12)** mediated by CTP **(14)**;
3. Investigate the block copolymerization behavior of AEMA **(6)** with HPMA **(8)** directly in aqueous medium;
4. Develop the reductive amination conditions for the post-polymerization reaction between two different primary amine functionalized polymers and glucuronic acid sodium salt **(5)**;
5. Synthesize carboxylic acid functionalized glycopolymer using reductive amination reaction.

6. Characterize the resulting synthetic carboxylic acid functionalized glycopolymer using nuclear magnetic resonance (NMR) and matrix assisted laser desorption-ionization (MALDI) mass spectroscopy;
7. Attach PAEMA (**16**) chains to the surface of silicon wafers using “click” chemistry and characterize the surface using atomic force microscopy (AFM), ATR-FTIR, and water contact angle measurements. Investigate the post-polymerization reaction capability of these chains with D-glucuronic acid sodium salt on the silicon-wafer surface.

## CHAPTER III

AQUEOUS RAFT POLYMERIZATION OF NON-PROTONATED 2-AMINOETHYL  
METHACRYLATE TO PRODUCE WELL-DEFINED, PRIMARY AMINE  
FUNCTION HOMO- AND COPOLYMERS FOR BIOMEDICAL APPLICATIONS

## Introduction

Primary amine-functionalized methacrylate monomers are of interest for their potential utility in post-polymerization modification reactions, such as amide and imine formation, ring-opening reactions and Michael addition reactions, enabling advances in areas including new approaches for cross-linking micelles and hydrogels, synthesis of novel copolymers for biomimetic scaffold structures under mild conditions, preparation of well defined cationic latexes, and surface functionalization for bioconjugation.<sup>39-49</sup> For example, Alaissari *et al.* developed thermosensitive core-shell latex particles with a core of poly(methyl methacrylate) (PMMA) and a positively charged shell prepared through statistical copolymerization of 2-aminoethyl methacrylate (AEMA) (**6**) and *N*-isopropylacrylamide (NIPAAm).<sup>50</sup> On absorption of rhodamine-labeled oligonucleotides, particles with temperature-selective fluorescent response were produced.<sup>51-53</sup> Armes and coworkers reported the synthesis of cyclic sugar modified methacrylates from the reaction of AEMA(**6**) with D-gluconolactone and lactobionolactone.<sup>54</sup> These monomers were further used by various research groups to produce well-defined glycopolymers utilized for the stabilization of gold nanoparticles.<sup>55,56,57</sup> Additionally, AEMA (**6**) copolymers have been evaluated for drug/gene delivery applications.<sup>58-60</sup> Dubruel *et al.* synthesized a series of polymethacrylates containing primary amine functionalities *via* conventional free radical

copolymerization of dimethylaminoethyl methacrylate (DMAEMA), tertbutyl carbonate (tBoc) protected AEMA (**6**) and t-Boc protected 4-methyl-5-imidazolyl methyl methacrylate, which were subsequently used for the coupling of the fluorescent probe Oregon Green.<sup>61</sup> Hennick *et al.* synthesized random copolymers of DMAEMA with AEMA (**6**) through conventional radical polymerization, reacted the primary amine groups with protected thiol groups and subsequently conjugated the copolymers with decapeptide, reporting a coupling efficiency of 95%.<sup>62</sup> In these examples, AEMA (**6**) was copolymerized via conventional radical polymerization, or the primary amine was pre-functionalized prior to polymerization. It is of interest to directly polymerize AEMA (**6**) with preserved functionality in a controlled fashion, and to evaluate copolymers with precisely controlled architectures (i.e. crosslinked micelles, block ionomer complexes, and vesicles) for potential biomedical applications.

Controlled radical polymerization techniques such as ATRP<sup>63</sup> and RAFT<sup>64,65</sup> have provided facile routes for obtaining polymers of predetermined molecular weights and precise architectures for amine-based vinyl monomers. However, the controlled polymerization of these monomers is challenging. In general, primary amine containing monomers should be protected in order to avoid unwanted side reactions. For example, AEMA (**6**) can be rapidly converted to 2-hydroxyethyl methacrylamide (**7**) at high pH through monomer rearrangement.<sup>58</sup> It has also been suggested that when the amine group is deprotonated, AEMA (**6**) can undergo Michael addition. In order to circumvent these side reactions, Dufresne and Leroux utilized t-Boc protected AEMA (**6**) for polymerization *via* ATRP, resulting in reasonably good control.<sup>66</sup> In addition, He *et al.* reported the direct polymerization of AEMA (**6**) under acidic conditions *via* ATRP in



water, in a methanol-water mixture and in an isopropyl alcohol-water mixture, and also *via* RAFT polymerization in dimethyl sulfoxide (DMSO).<sup>67</sup> They reported slow polymerization rates in methanol. Even though polymerization rates were faster in water, the reaction exhibited poor control yielding a PDI of 1.41. However, when a cosolvent combination of 80:20 2-propanol:water was used, well-controlled polymerizations were achieved with PDIs lower than 1.25. For RAFT polymerization, polymers with well-defined molecular weights and PDIs between 1.25 and 1.29 were reported. The authors also reported synthesis of well-defined AEMA based diblock copolymers using poly(ethylene oxide)-based ATRP macroinitiators and statistical copolymers of AEMA **(6)** with 2-hydroxypropyl methacrylate **(8)** and DMAEMA. Further, preparation of shell cross-linked micelles with pH-responsive cores consisting of PAEMA-*b*-PDAEMA copolymers with polyethylene glycol diacrylate crosslinking agent was reported.

The synthesis of functional block copolymers directly in aqueous media without using protection/deprotection chemistry is of particular interest for stimuli-responsive systems. RAFT polymerization has been widely used to yield water-soluble polymers with well-controlled structures.<sup>65</sup> For example, homopolymers and block copolymers with anionic,<sup>146,147,210</sup> cationic,<sup>159,211</sup> zwitterionic<sup>212,213</sup> and neutral<sup>103,105,145,151,152,214,152,151,215,216,217,218</sup> functionality have been synthesized directly in water without post-polymerization modification. Recently, the McCormick research group reported the aqueous RAFT polymerization of N-(2-hydroxypropyl) methacrylamide (HPMA) **(8)** and N-[3-(dimethylamino)propyl] methacrylamide (DMAPMA) **(9)**.<sup>31</sup> PHPMA **(10)** has been proposed as a nonviral carrier for drug delivery because of its biocompatibility and nonimmunogenicity.<sup>69-76</sup> Block copolymers

of HPMA (**8**) have been shown to form micelles, vesicles and block ionomer complexes in aqueous environments, illustrating their potential to be used as nonviral drug/gene carriers.<sup>77</sup> McCormick and coworkers have also recently reported the aqueous RAFT generated block copolymer poly(HPMA-*b*-DMAPMA), showing the formation of an electrostatic complex between the positively charged DMAPMA block with negatively charged polynucleotides for gene delivery based applications.<sup>78</sup> In addition, this same group reported the aqueous RAFT polymerization of 3-aminopropyl methacrylamide hydrochloride (APMA) (**12**) in a dioxane-water mixture.<sup>79</sup> Homopolymers of AMPA (**12**) were then chain extended with *N*-isopropylacrylamide (NIPAM) to produce temperature-responsive block copolymers that formed vesicles upon increasing the solution temperature.

Herein we report, for the first time, the unprotected controlled aqueous RAFT polymerization of AEMA (**6**) yielding near monodisperse homopolymers. Well-defined block copolymers of AEMA-*b*-HPMA (**18**) were also prepared directly in aqueous solution through the chain extension of AEMA (**6**) macroCTA with HPMA (**8**).

## Experimental

*Materials.* All reagents were used without further purification unless otherwise noted. Methacryloyl chloride (>97%), ethanolamine (>98%) and hydroquinone (99%) were purchased from Aldrich. Phenylmagnesium bromide solution (3M in diethyl ether) was purchased from Fluka. Acetic acid, sodium acetate, sodium bicarbonate, diethylether, ethylacetate, hexane, and hydrochloric acid were purchased from Fisher. Carbon disulfide and potassium ferric cyanide were purchased from Acros Organics. 2,2'-Azobis(2-imidazolinylpropane) dihydrochloride (VA-044) (**19**) was purchased from Wako Pure Products and recrystallized from methanol. 4,4'-Azobis(4-cyanovaleric acid) (V-501) (**13**) was purchased from Fluka and recrystallized from methanol. 4-Cyanodithiobenzoic acid (CTP) (**14**) was synthesized according to literature procedure.<sup>145</sup> 2-Aminoethyl methacrylate (AEMA) (**6**) was synthesized using a previously reported procedure.<sup>54</sup> N-(2-hydroxypropyl methacrylamide) (HPMA) (**8**) was synthesized according to Kopecek et al.<sup>219</sup>

*Aqueous RAFT homopolymerization of AEMA (6).* The aqueous RAFT polymerization of AEMA (**6**) was conducted at 70°C and 50°C. The polymerization of AEMA (**6**) at 50 °C was performed using VA-044 (**19**) as the radical initiator and CTP (**14**) as the RAFT chain transfer agent (CTA). An initial monomer concentration ( $[M]_0$ ) of 1 M was used with a monomer to CTA ratio ( $[M]_0/[CTA]_0$ ) of 400. The CTA to initiator ratio ( $[CTA]_0/[I]_0$ ) was 5:1. A typical procedure is as follows: in a 10 ml round bottom flask, CTP (**14**) (3.5 mg, 0.0125 mmol) and AEMA (0.825 g, 5 mmol) were dissolved in 0.6 ml of acetate buffer (pH=5, 0.27 mol/L acetic acid and 0.73 mol/L sodium acetate), followed by the addition of VA-044 (**19**) (0.7 mg, 0.0025 mmol). The

solution was diluted to 5 ml with acetate buffer. The flask was sealed with a rubber septum and purged with nitrogen for 30 min, and placed in a 50 °C water bath. Aliquots for kinetic analysis were removed at predetermined time intervals and quenched by rapid cooling in liquid nitrogen.

For the homopolymerization at 70 °C, V-501 (**13**) was employed as the primary radical source and CTP (**14**) was used as the CTA. The polymerization was performed directly in acetate buffer (pH=5, 0.27 mol/L acetic acid and 0.73 mol/L sodium acetate) with an initial monomer concentration ( $[M]_0$ ) of 1 M. The initial  $[M]_0/[CTA]_0$  was 400, while the CTA to initiator ratio was 5:1. The homopolymerization was conducted by dissolving AEMA (**6**) (1.65 g, 10 mmol), CTP (**14**) (6.2 mg, 0.022 mmol) and V-501 (**13**) (1.25 mg, 0.004 mmol) in a 25 ml round-bottom flask and diluting the resulting mixture to a final volume of 10 ml with acetate buffer. The reaction solution was purged with nitrogen for 45 minutes and subsequently placed in a water bath at 70 °C. Aliquots for kinetic analysis were removed from the polymerization solution at appropriate time intervals and immersed in liquid nitrogen to terminate the polymerization.

*Synthesis of MacroCTA of AEMA (**20**).* AEMA (**6**) (8.3g, 0.05 mol), CTP (**14**) (31.1 mg, 0.11 mmol), and VA-044 (**19**) (6.23 mg, 0.022 mmol) were added to a 100 ml, round bottom flask and dissolved with 5 ml of acetate buffer (pH=5, 0.27 mol/L acetic acid and 0.73 mol/L sodium acetate). The solution was then diluted to a final volume of 50 ml. The flask was sealed with a rubber septum and cooled in an ice bath. The contents were purged with nitrogen for 30 min at 5 °C. The flask was subsequently immersed in a water bath at 50 °C. The polymerization was allowed to proceed for 75 minutes before

being quenched by rapid cooling in liquid nitrogen. The PAEMA macro-CTA (**20**) was then purified by dialysis against deionized water and then lyophilized.

$^1\text{H}$  NMR ( $\text{D}_2\text{O}$ ):  $\delta$  4.21 (br, 2H,  $-\text{OCH}_2$ );  $\delta$  3.31 (br, 2H,  $-\text{NH}_2\text{CH}_2$ );  $\delta$  1.95 (br, 2H,  $-\text{CH}_2$ );  $\delta$  0.83-1.36 (br, 3H,  $-\text{CH}_3$ ).  $^{13}\text{C}$  NMR ( $\text{D}_2\text{O}$ ):  $\delta$  184.6 (C=O);  $\delta$  68.4 (C-O);  $\delta$  58.7 (C);  $\delta$  49.5 (C-N);  $\delta$  43.6 ( $\text{CH}_2$ );  $\delta$  23.3 ( $\text{CH}_3$ ).

*Chain extension of PAEMA MacroCTA (**20**) with HPMA (**8**).* Block copolymers of PAEMA (**16**) and HPMA (**8**) were prepared directly in acetate buffer by dissolving V-501 (**13**) (1.49 mg, 0.006 mmol), PAEMA macroCTA (**20**) (0.827 g, 0.03 mmol), and HPMA (**8**) (1.718 g, 12 mmol) in 12 ml of buffer. The resulting polymerization solution was divided into four separate 5 ml round bottom flasks (3 ml in each flask) and each flask was subsequently sealed and purged with nitrogen for 30 minutes. The flasks were then placed in a water bath at 70 °C and removed from the water bath at predetermined time intervals. Upon removal, the flasks were exposed to oxygen and quenched by rapid cooling in liquid nitrogen.

*(Co)polymer Characterization.* PAEMA macroCTAs (**20**) and AEMA-b-HPMA (**18**) copolymers were characterized by aqueous size exclusion chromatography (ASEC-MALLS) at ambient temperature using Eprogen CATSEC columns (100, 300, and 1000 °Å; Eichrom Technologies, Inc). A Wyatt Optilab DSP interferometric refractometer ( $\lambda = 690$  nm) and a Wyatt DAWN DSP multiangle laser light scattering detector ( $\lambda = 633$  nm) were employed using 1 wt % acetic acid/0.1 M  $\text{Na}_2\text{SO}_4$  (aq) solution as the eluent at a flow rate of 0.25 ml/min. The  $dn/dc$  of the PAEMA (**16**) was determined to be 0.153 in the above eluent at 25 °C using a Bausch and Lomb refractometer. Conversions in each system were determined by comparing the area of the UV signal corresponding to

monomer at  $t_0$  to the area at  $t_x$ . Absolute molecular weights and polydispersities were calculated using the Wyatt ASTRA SEC/LS software package.

A Varian 300 MHz NMR equipped with a standard 5 mm  $^1\text{H}/^{13}\text{C}$  probe was utilized to identify the structure of PAEMA (**16**) *via*  $^1\text{H}$  NMR (256 scans with a relaxation delay of 1.0 second and a pulse angle of 45 degrees) and  $^{13}\text{C}$  NMR (512 scans with a relaxation delay of 1 second and a pulse angle of 45 degrees).

A Varian 500 MHz NMR equipped with a standard 5 mm  $^1\text{H}/^{13}\text{C}$  probe was utilized to identify the homopolymer structure of PAEMA (**16**) (nt = 64, d1 = 3.1  $\mu\text{s}$ , pw90 = 16  $\mu\text{s}$ , at = 1.89  $\mu\text{s}$ ). The degree of polymerization and molecular weight were determined *via*  $^1\text{H}$  NMR through integration of the relative intensities of methylene-protons resonance at 3.31 ppm and phenyl-protons of CTP (**14**) between 7.51 and 7.89 ppm.

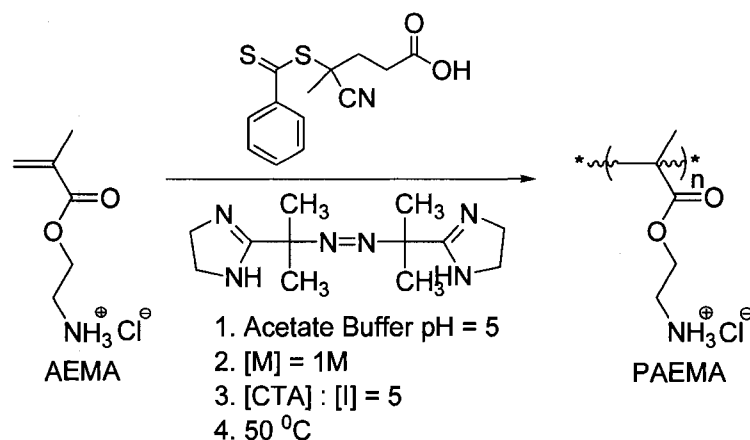
The copolymer structures, degrees of polymerization and molecular weights were identified *via*  $^1\text{H}$  NMR (nt = 32, d1 = 4.1  $\mu\text{s}$ , pw90 = 15.3  $\mu\text{s}$ , at = 1.89  $\mu\text{s}$ ) by integration of the relative intensities of methyne-proton resonances at 3.8 ppm (HPMA) (**8**) and methylene-proton resonances at 4.2 ppm (PAEMA) (**16**). Samples were prepared at 5 wt% in deuterated water ( $\text{D}_2\text{O}$ ). All pH measurements were performed with accuracy  $\pm 0.02$  with 900A (Orion) pH meter.

## Results and Discussion

*Aqueous RAFT Homopolymerization of AEMA (6)*. The careful selection of the chain transfer agent (CTA) and reaction conditions for the monomer of interest are key points for a successful RAFT polymerization.<sup>103,212,213</sup> McCormick and coworkers have previously shown the polymerization of a wide range of amine containing monomers *via* aqueous RAFT polymerization.<sup>65,77</sup> However, it is necessary to optimize reaction conditions because the CTA may be susceptible to hydrolysis and aminolysis. These side reactions result in a loss of active chain ends and diminish control while increasing the polydispersity of the resulting polymers. After careful examination of CTP (**14**) for the aqueous RAFT polymerization of AM, it was shown that the solution pH has a strong influence on the rate of hydrolysis and aminolysis. This study suggested that aqueous RAFT polymerization of amine containing monomers should be performed at pH values below 7. Recently, McCormick and coworkers reported the successful homopolymerization and block copolymerization of methacrylamido monomers bearing both tertiary and primary amines *via* aqueous RAFT polymerization.<sup>65,77,79,103,146,151</sup> In a typical homopolymerization procedure, monomers were polymerized in an aqueous buffer employing CTP (**14**) as chain transfer agent at 70 °C and pH 5 to reduce hydrolysis and aminolysis.

Considering the above issues, AEMA (**6**) polymerizations were carried out at 50 °C using VA-044 (**19**) as the radical source and CTP (**14**) as the CTA in an acetic acid/sodium acetate buffer (pH = 5) (SchemeIII-1). For the polymerizations, the initial ratio of  $[M]_0$  to  $[CTA]_0$  was maintained at 400 /1 and a  $[CTA]_0/[I]_0$  ratio of 5/1 was

employed. Molecular weights, polydispersities and conversion data are shown in Table III-1.



**Scheme III-1.** Aqueous RAFT polymerization of AEMA (**6**) at 50 °C.

ASEC-MALLS evaluation revealed shifts to lower elution volumes as a function of polymerization time, indicating increasing molecular weight (Figure III-1). The traces are unimodal and free from high molecular weight termination products, providing a first indication of controlled polymerization. A plot of  $\ln([M_0]/[M])$  as a function of reaction time is given in Figure III-2. A short inhibition period is observed, which may be related to: (i) slow fragmentation of CTP (**14**) just after first addition of initiated polymer chains, (ii) slow reinitiation following first fragmentation in the pre-equilibrium stage, or (iii) tendency of the expelled radical to add to the CTA rather than the monomer.<sup>220</sup> The rate of fragmentation and the reinitiation of the leaving group of the CTA just after first fragmentation depend on the radical reactivity.<sup>90,212,213</sup> The more stable, bulky R radical leaving group of CTP (**14**) should add to AEMA (**6**) significantly slower than the



monomer radical adds to AEMA (**6**), and is more likely to add back to CTP (**14**) again.<sup>90,212,213</sup> After this inhibition period, a linear relationship is observed indicating pseudo first order kinetic behavior, providing further evidence of controlled polymerization. This also indicates that PAEMA (**16**) radical is inherently a good leaving group, though the weaker P<sub>n</sub>-S bond of polymeric CTA results in a moderate rate of polymerization. For polymerization times longer than 240 minutes, a deviation from linearity is observed that can be attributed to a decrease in the radical concentration (most likely due to termination) in the polymerization medium at higher conversion.<sup>152</sup>

**Table III-1.** Aqueous RAFT polymerization of AEMA (**6**) at 50 °C.

Time (min)	$M_n \times 10^4$ <sup>1</sup>	$M_n \times 10^4$ <sup>2</sup>	PDI <sup>1</sup>	Conv. <sup>1</sup> (%)
30	1.5	0.37	1.19	5.1
45	2.1	0.95	1.15	14
60	2.6	1.6	1.13	23
90	3.8	2.2	1.11	34
120	4.8	2.8	1.11	43
150	5.5	3.3	1.10	50
180	6.3	3.8	1.10	58
240	7.0	4.5	1.12	69
300	7.7	4.9	1.13	75
360	8.1	5.1	1.14	77
420	8.3	5.3	1.14	80
460	8.4	5.5	1.17	83
540	8.7	5.6	1.15	84

1. Determined by ASEC/MALLS
2. Theoretical molecular weight
3. [M]:[CTA]:[I] = 400:1:0.2

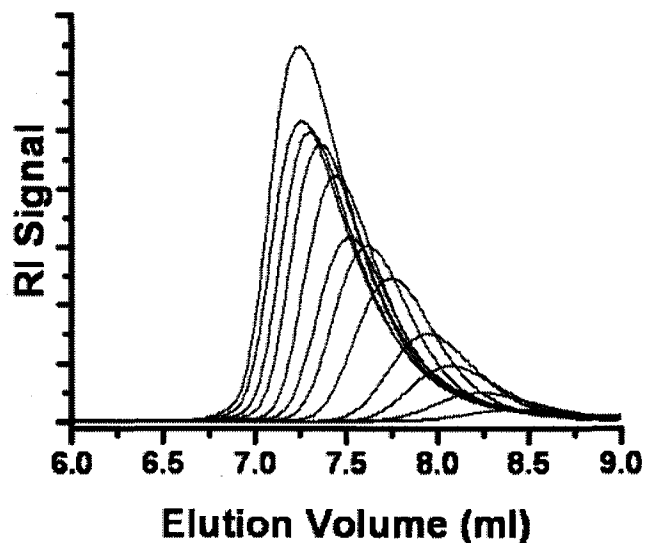


**Figure III-1.** ASEC traces for the homopolymerization of AEMA (**6**) at 50 °C showing the RI signal as a function of elution volume.

The apparent molecular weight values as a function of time are given in Figure III-3. The low polydispersities (Table III-1) and the linear increase in apparent  $M_n$  with increasing conversion indicate the controlled synthesis of PAEMA (**16**) in an aqueous solvent. The apparent molecular weights are higher than the theoretical molecular weights. Similar molecular weight overshoots have also been reported for the polymerization of other amine containing polymers. In an ideal RAFT polymerization, the chain transfer process should be fast and intermediate RAFT-adduct radical should be short-lived. Because of the rapid transfer of the growing polymeric radicals between free

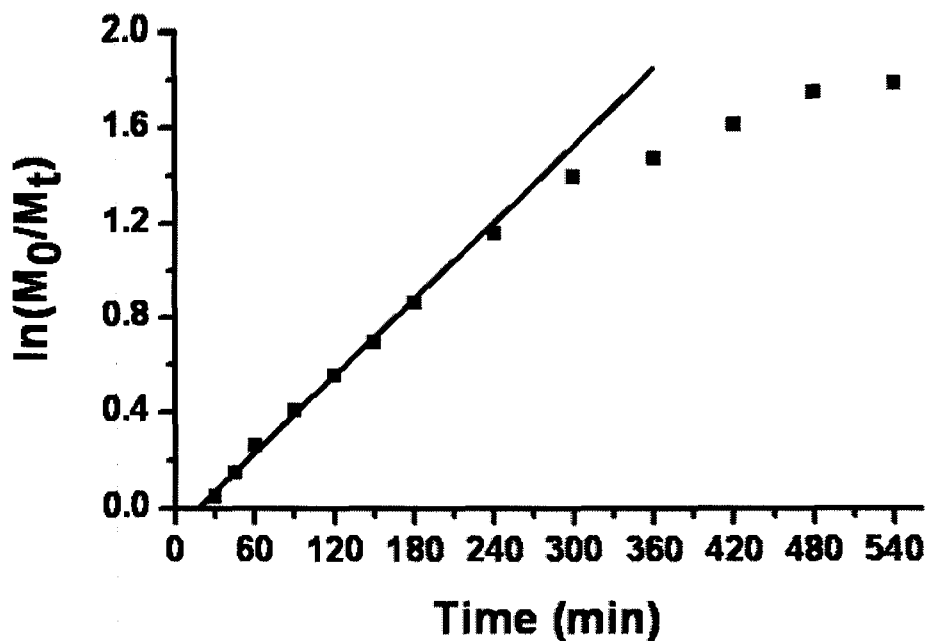


**Figure III-2.** Pseudo-first-order kinetic plot for the homopolymerization of AEMA (6) at 50 °C.

and dormant forms, unwanted radical-radical termination processes are minimized without reducing the rate of the polymerization.<sup>90</sup> However, we observe a significant inhibition period, which is strongly related to the nature of the CTA. One possible explanation for this observation is that after addition of oligomeric radicals to the RAFT CTA, the resulting intermediate radical is short-lived allowing it to undergo bimolecular termination. Another possibility is that the poor initiating and fragmentation ability of R group radicals can lead to bimolecular termination of the intermediate radical resulting in higher than predicted molecular weights.<sup>90,212,213</sup>

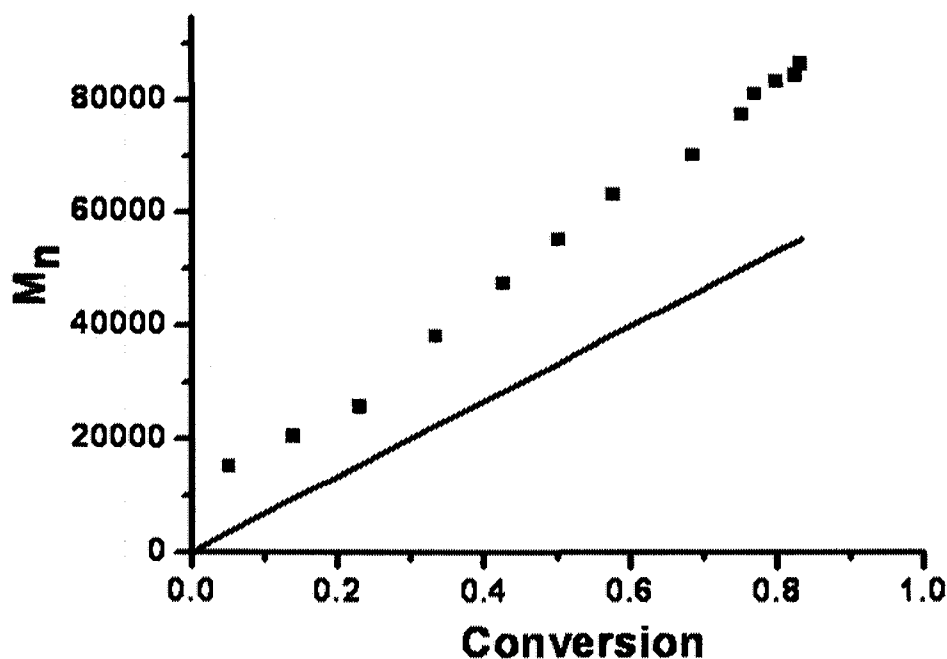


**Figure III-3.**  $M_n$  determined by GPC as a function of conversion for the aqueous homopolymerizations of AEMA (**6**) at 50 °C.

AEMA (**6**) polymerizations were also performed at 70 °C using V-501 (**13**) as the initiator with [CTA]/[I] ratios of 5/1. To avoid CTA hydrolysis in basic conditions ( $pK_a$  of AEMA (**6**) = 8.8) and possible aminolysis of CTA due to the monomer hydrolysis, an acetic acid/sodium acetate buffer ( $pH = 5$ ) was used as the buffer. Experimental data for the homopolymerization of AEMA (**6**) at 70 °C are summarized in Table III-2. Shown in Figure III-4 is the evaluation of molecular weight, as determined by ASEC-MALLS, for aliquots taken from the AEMA (**6**) homopolymerization. The molecular weight of resulting aliquots increases with time and unimodal peaks are observed at decreasing elution volumes. However, a broadening is observed in molecular weight distribution curves after 90 minutes.

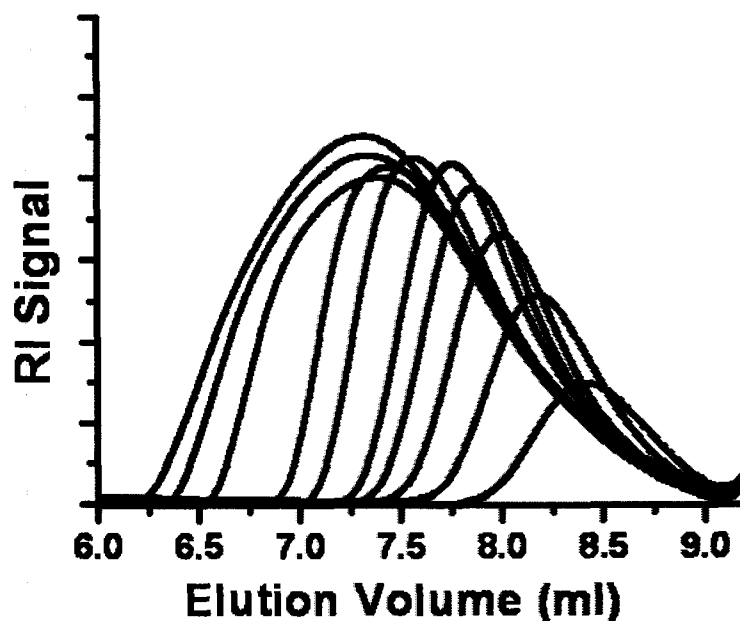


**Figure III-4.** ASECs traces for the homopolymerization of AEMA (**6**) at 70 °C showing refractive index as a function of elution volume.

**Table III-2.** Aqueous RAFT polymerization of AEMA (**6**) at 70 °C.

Time (min)	$M_n \times 10^{4,1}$	$M_n \times 10^{4,2}$	PDI*	Conv.* (%)
30	1.2	0.44	1.24	6
45	2.0	1.2	1.16	17
60	2.5	2.1	1.26	31
75	3.1	1.9	1.26	28
90	4.3	2.6	1.21	39
120	5.7	2.9	1.27	45
150	6.7	3.6	1.35	54
180	7.4	4.0	1.46	59
240	8.7	5.0	1.62	74
300	8.9	5.4	1.84	82
360	9.7	5.7	1.89	85

1. Determined by ASEC/MALLS
2. Theoretical molecular weight
3.  $[M]:[CTA]:[I] = 400:1:0.2$

The kinetic plot shows, for polymerization times longer than 45 minutes, a deviation from linearity that can be attributed to termination reactions in the polymerization medium at higher conversions (Figure III-5). Actual molecular weight is greater than predicted molecular weight (Figure III-6) and an increase in polydispersity (PDI) is observed over time (Table III-2). It was also observed that the polymerization solution changed from pink to colorless within one hour. This suggests loss of CTA during the reaction, resulting in an increase in the monomer to CTA ratio and production of polymers with higher molecular weights than predicted. Continued increase in PDI with time is also indicative of a non-controlled polymerization. Recently, Le et al. reported the RAFT polymerization of AEMA (**6**) in DMSO at 70 °C using dithiocumyl ester.<sup>67</sup> We suggest that the relatively high PDI's reported by Le et al. are due to the high polymerization temperature, which resulted in side reactions that broadened molecular weight distribution. The loss of control we observe at 70 °C for aqueous polymerization of AEMA (**6**) may be related to increase of the equilibrium rate between unprotonated and protonated primary amine groups with consequent side reactions such as Micheal addition or aminolysis reactions, where the unprotonated primary amine group undergoes reaction with either AEMA (**6**) monomer or the chain transfer agent. The controlled polymerization of AEMA (**6**) in an aqueous solvent thus depends not only on the solution pH but also on the polymerization temperature.

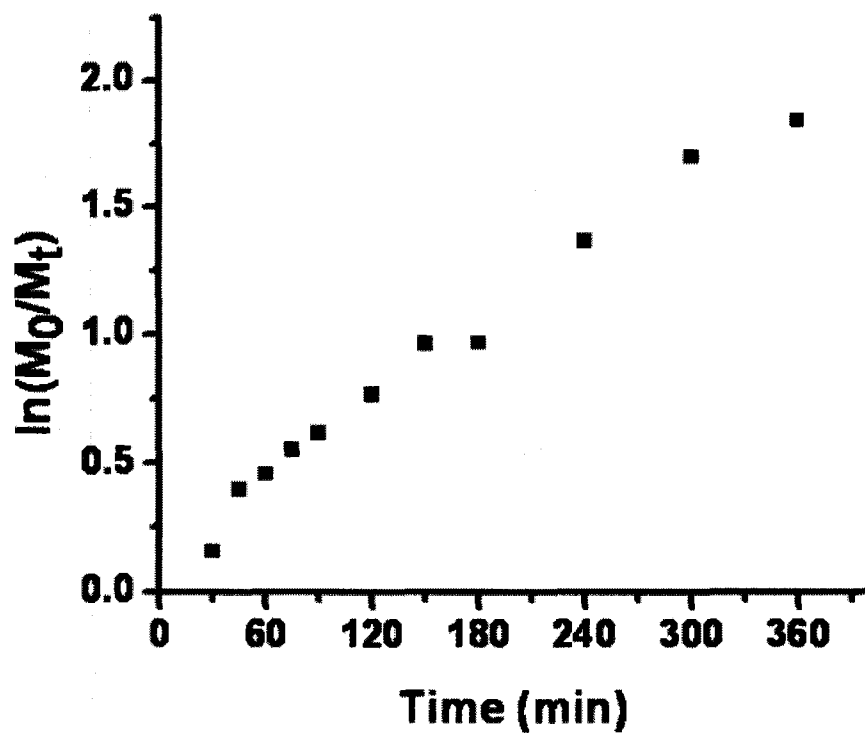


**Figure III-5.** Pseudo-first-order kinetic plot for the homopolymerization of AEMA (6) at 70 °C.

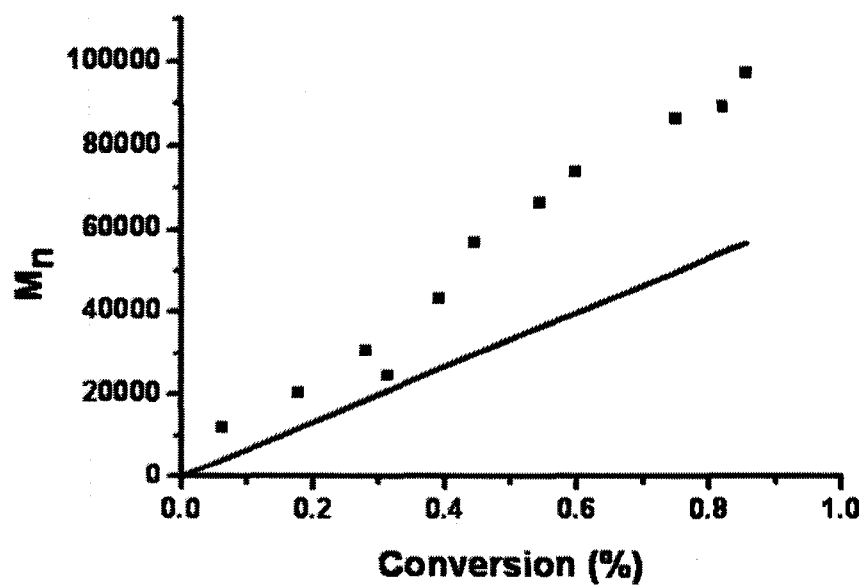


**Figure III-6.**  $M_n$  determined by GPC as a function of conversion for the aqueous homopolymerization of AEMA (6) at 70 °C.

Copolymerization of AEMA (**6**) with HPMA (**8**). Having established conditions for the controlled polymerization of AEMA (**6**) in aqueous solvent, AEMA macroCTAs (**20**) were prepared at both 50 and 70 °C (Table III-3). The  $M_n$  of the resulting macroCTAs, calculated through proton NMR, is close to that obtained from ASEC/MALLS for both macroCTAs. However, the polydispersity of the macroCTA synthesized at 70 °C is greater, presumably due to side reactions as mentioned in the previous section.

In order to demonstrate the presence of active chain ends, the AEMA macroCTA (**20**) prepared at 50 °C was chain extended with HPMA (**8**) to form an AB diblock copolymer. Reaction conditions,  $[CTA]/[I] = 5/1$  and 70 °C, were chosen to mimic previously reported conditions for the block copolymerization of DMAPMA (**9**) and HPMA (**8**) (Scheme III-2).<sup>216</sup>

**Table III-3.** Conditions for synthesis and physical properties of AEMA MacroCTA (**20**) at 50 and 70 °C.

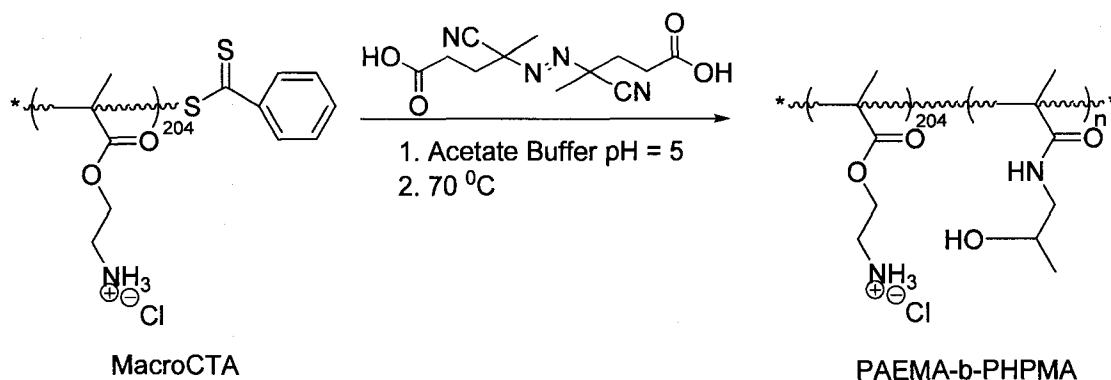
[M]:[CTA]:[I]	Time (min)	Temp. (°C)	$M_n^1$	$M_n^2$	$M_n^3$	PDI <sup>1</sup>	Conv. <sup>1</sup> (%)	DP <sup>2</sup>
400:1:0.2	60	70	24900	24000	21000	1.12	31	145
450:1:0.2	75	50	31200	34100	34900	1.05	47	204

1. Calculated through GPC.

2. Calculated through <sup>1</sup>H NMR.

3. Theoretical molecular weight.





**Scheme III-2.** Block copolymerization of AEMA (**6**) with HPMA (**8**).

Figure III-7 shows ASEC-MALLS chromatograms presenting the controlled chain extension of the macroCTA with HPMA (**8**) under aqueous conditions. The traces are unimodal and shift to lower elution volumes as a function of time indicating high blocking efficiency. Table III-4 lists the conversion, molecular weight, and polydispersity data for each block copolymer. These data indicate that AEMA macroCTAs (**20**) were extended in a controlled fashion, resulting in diblock copolymers with low PDIs (<1.1).

**Table III-4.** PAEMA-*b*-PHPMA (**18**) copolymerization and physical properties.

Time (min)	Temp. (°C)	$M_n^1$	$M_n^2$	PDI <sup>1</sup>	Conv. <sup>2</sup> (%)	DP <sup>2</sup>
60	70	43000	44100	1.05	18	70
120	70	48400	51000	1.05	33	130
180	70	53700	57100	1.07	44	177
240	70	55400	65100	1.05	54	216

1. Calculated through GPC.

2. Calculated through  $^1\text{H}$  NMR.

3.  $[\text{M}]:[\text{CTA}]:[\text{I}] = 400:1:0.2$

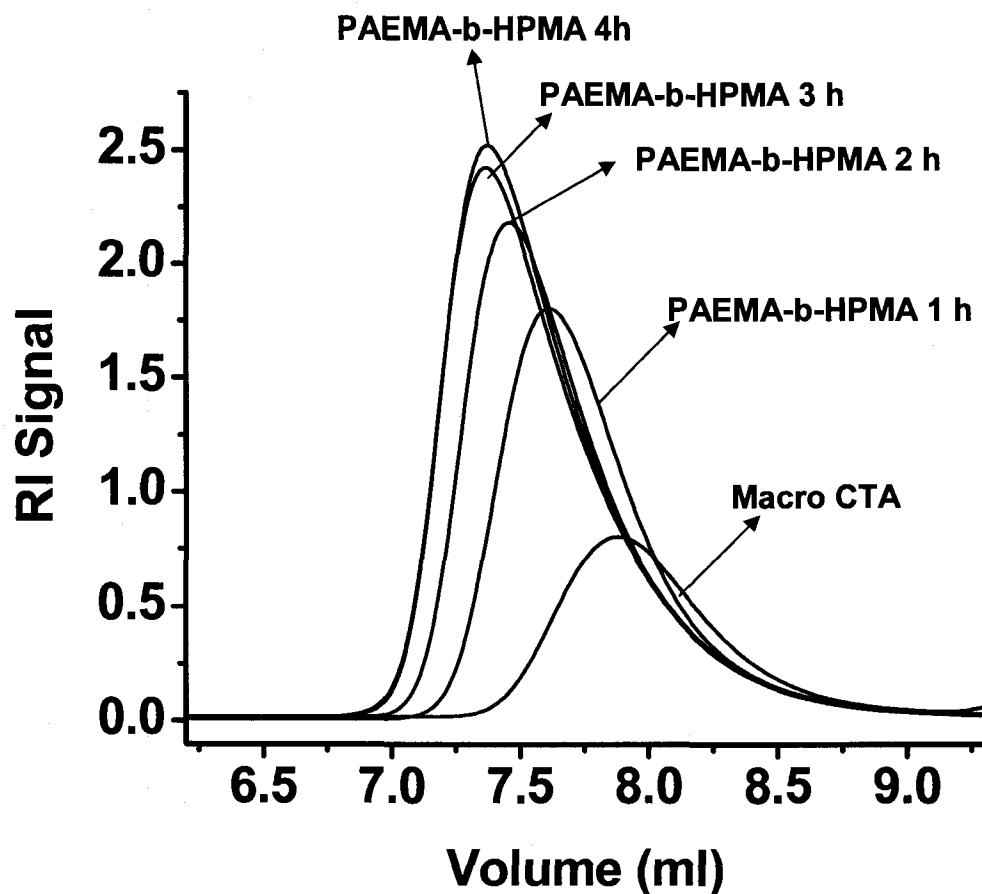


**Figure III-7.** ASEC RI traces for diblock copolymers of AEMA (**6**) and HPMA (**8**) and the corresponding AEMA homopolymer macroCTA (**20**).

Copolymer compositions and experimental molecular weights were determined by comparing relative normalized resonances of the methyne proton peaks at 3.8 ppm of PHPMA (**10**) and methylene peaks at 4.2 ppm of PAEMA (**16**) (Figure III-8). The experimentally derived molecular weights are slightly larger than theoretical molecular weights, attributed to a loss of active chain ends throughout the polymerization, but are still in good agreement. Thus the higher temperature conditions do not appear to cause significant side reactions or loss of control for HPMA (**8**) block copolymerization.

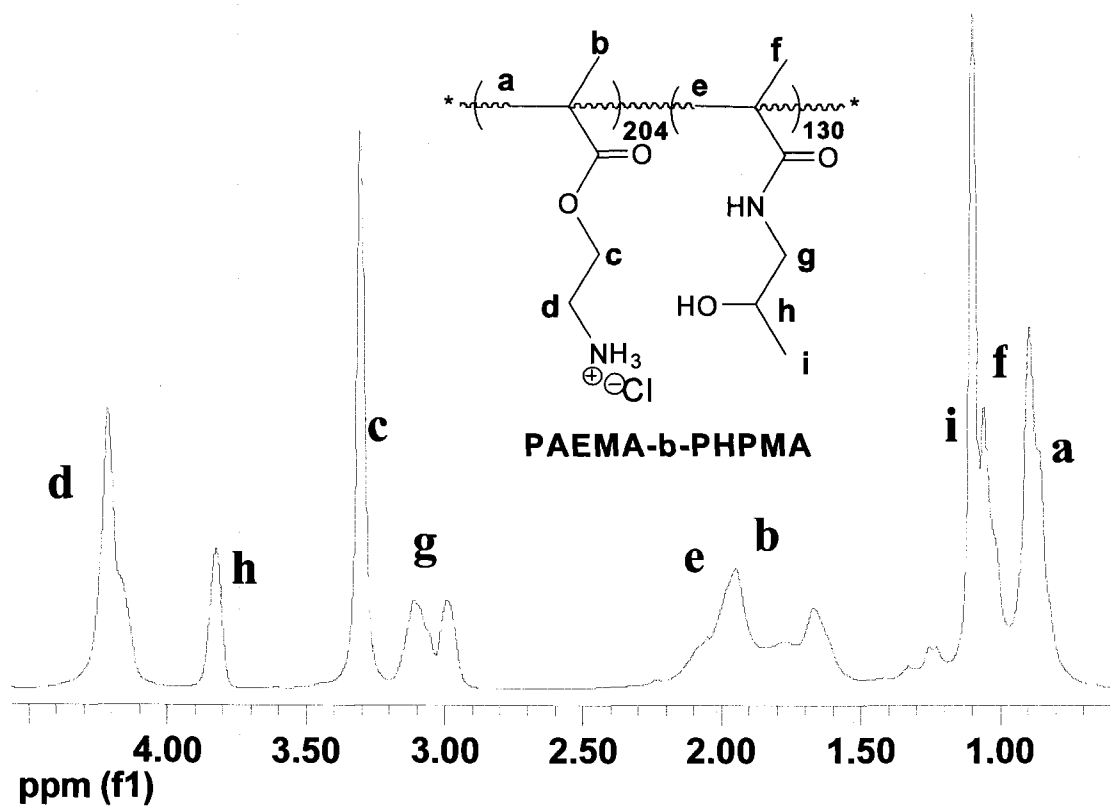


Figure III-8. <sup>1</sup>H NMR spectrum of PAEMA-*b*-PHPMA (18).

## Conclusions

Well-defined, narrowly dispersed homopolymer and diblock copolymers of AEMA (**6**) have been synthesized *via* aqueous RAFT polymerization. Specifically, AEMA (**6**) monomer has been homopolymerized directly in aqueous solution with PDIs below 1.2 and conversions up to 95%. To our knowledge, this is the first report of aqueous AEMA (**6**) RAFT polymerization with very low polydispersity and good control without the necessity of protecting group chemistry. The resulting PAEMA (**16**) was also chain extended with HPMA (**8**) to produce well defined diblock copolymers with high blocking efficiency and PDIs lower than 1.1. Building on our earlier work and recent literature reports, we show for the first time a series of novel, well-defined block copolymers of AEMA (**6**) and HPMA (**8**) with high conversion. Since primary amine groups are amenable to a wide range of post-polymerization chemistries, such as rapid formation of amides and imines, ring-opening of epoxy groups and Micheal addition, we believe that this study will enable developments in several areas, including synthesis of controlled architecture, bio-inspired polymers through the conjugation of the primary amine pendant groups with targeted sugars, peptides or amino acids. Improved crosslinking strategies for shell cross-linked micelles, and robust surface functionalization for various surface chemistries are also possible. Diblock copolymers of AEMA (**6**) and HPMA (**8**) may prove useful as drug/gene delivery vehicles through electrostatic complexation of the positively charged AEMA (**6**) block with the negatively charged phosphate backbone of polynucleotides. In addition, the susceptibility of the AEMA (**6**) block to post-polymerization reactions facilitates the conjugation of this diblock-copolymer with targeted drugs or bio-molecules.

## CHAPTER IV

BIOCONJUGATION OF D-GLUCURONIC ACID SODIUM SALT TO WELL-  
DEFINED PRIMARY AMINE CONTAINING HOMO- AND BLOCK COPOLYMERS  
FOR POTENTIAL BIOMEDICAL APPLICATIONS

## Introduction

Hyaluronic acid (HA) **(1)**, a linear, high-molecular weight polysaccharide, is comprised of alternating *N*-acetyl- $\beta$ -D-glucosamine **(2)** and  $\beta$ -D-glucosuronic acid residues linked **(3)** at 1-3 and 1-4 positions, respectively. Under physiological conditions it exists as the sodium salt form (HA-Na), is water soluble, and behaves as a weak polyelectrolyte. HA **(1)** is the primary component of synovial fluid and is thought to provide the lubricity of joint surfaces as well as the viscoelastic behavior of synovial fluid.<sup>1,2</sup> It is currently used in a wide range of biomedical applications, including post surgical adhesion prevention, rheology modification in orthopedics, ophthalmic procedures, tissue engineering, hydrogels and implants.<sup>3-8</sup> HA **(1)** is obtained commercially by either extraction from rooster comb or synthesis by microbial fermentation using streptococcus.<sup>9</sup> Limitations of current systems include cost, allergy induction and reduced performance capabilities in comparison to native HA. Attempts to prepare surface coatings based on HA **(1)** *via* physisorption and chemisorption produced poorer than expected lubrication properties.<sup>4,10,11</sup> HA **(1)** is found with a range of molecular weights and molecular weight distributions. High molecular weight HA **(1)** has very high viscosity, and exhibits both pseudoplastic and rheopectic rheological behavior.<sup>12,13,14</sup> When the molecular weight of HA **(1)** is degraded, its viscosity is reduced, which is thought to result in decreased lubricity and function of the synovial

fluid. It is of interest to prepare synthetic glycopolymer analogues to specifically target performance capabilities for biomedical applications.

The term “glycopolymer” is used to describe synthetic polymers containing sugar moieties as pendant groups. Advances in controlled radical polymerization (CRP) allowing precise control of polymeric structures combined with increased understanding of structures required for specific biomimetic functions make glycopolymers promising candidates for biomedical applications, glycomics, medicine, biotechnology, sensors and separation science. Glycopolymers have been investigated as macromolecular drugs, drug delivery systems, biocatalytic and biosensitive hydrogels, matrices for controlled cell culture, stationary phases for chromatographic purposes, and surface modifiers.<sup>15-32</sup> CRP can be used to prepare glycopolymers from unprotected monomers through post-polymerization modification strategies using reactive polymer precursors.<sup>29,33</sup> An alternate method for producing well-defined glycopolymers is the use of a macromonomer, where a vinyl monomer carries the sugar moiety. There are advantages to both approaches. One of the main disadvantages of the post-polymerization method is that the conjugation of a pre-synthesized polymer backbone does not always result in 100% functionalization, resulting in an inhomogeneous sequence within the polymer chain.<sup>29</sup> On the other hand, with the post-polymerization approach it is possible to avoid the complex reaction and purification procedures often associated with carbohydrate monomer synthesis. The preparation of a reactive scaffold from a simple monomer, which can then be used to create a wide range of glycol-functionalized polymers through highly efficient post-polymerization reactions is an attractive option.

There are several successful examples in the literature of the post-polymerization modification approach applied to the synthesis of glycopolymers. For example, Haddleton et al. reported the polymerization of trimethylsilyl protected propargyl methacrylate *via* atom transfer radical polymerization (ATRP) and synthesis of well-defined glycopolymers with a high degree of conjugation utilizing “click” reactions between alkyne functionalized polymethacrylate and protected and unprotected glycosyl azides.<sup>34</sup> Hawker and coworkers reported the use of “click” reactions to successfully prepare asymmetric sugar functionalized dendrimers.<sup>35</sup> MALDI-TOF mass spectrometry was utilized to provide evidence that a single molecular species was obtained without side reactions. Liu and coworkers reported that poly(fluorenes) prepared by Sonogashira coupling of bromo-alkane functionalized monomers were glycosylated in near quantitative yield (98%) through the reaction of bromo-groups with a thio-sugar, using excess reagents.<sup>36</sup> Another important post-polymerization method for the synthesis of glycopolymers involves active esters. Although this method often requires an excess of substrate as well as purification, it is effective.<sup>37</sup> Hu et al. reported ATRP of *N*-methacryloxysuccinimide using Cu(I)/bipy, which yielded low polydispersity and predicted number average molecular weight ( $M_n$ ) polymer, followed by quantitative substitution with gluco- and galactosamine.<sup>38</sup>

Primary amine-functionalized vinyl monomers have attracted great interest recently due to the potential for post-polymerization modification reactions through primary amine pendant functionality.<sup>39-49</sup> For example, Armes and coworkers reported the synthesis of well-defined glycopolymers upon the controlled radical polymerization of sugar modified methacrylates, prepared from the reaction of 2-aminoethyl

methacrylate (AEMA) **(6)** with D-gluconolactone and lactobionolactone.<sup>54-57</sup>

Additionally, AEMA **(6)** and *N*-(3-aminopropyl)methacrylamide (APMA) **(12)** copolymers have been used for post-polymerization reactions in drug/gene delivery applications.<sup>58-60</sup> Peptide conjugated random copolymers have been prepared by Hennick and coworkers through the reaction of primary amine moieties of random copolymers of DMAEMA with AEMA **(6)** with protected thiol groups, yielding a coupling efficiency of 95%.<sup>62</sup> Jindrich, Kopecek and coworkers have also reported the synthesis of copolymers containing APMA **(6)** and *N*-(2-hydroxypropyl)methacrylamide (HPMA) **(8)** to prepare cell penetrating peptide (CPP) conjugates after bioconjugation of primary amine functionalized copolymers with targeted CPPs.<sup>221,222,223,224</sup>

The development of controlled radical polymerization techniques such as ATRP<sup>63</sup> and RAFT<sup>64,65,159,225,226,227</sup> polymerizations have provided a facile route to obtain polymers of predetermined molecular weights and precise architectures for amine-based vinyl monomers. However, the controlled polymerization of primary amine-based monomers is challenging. Recently, in our laboratories, we reported for the first time the unprotected controlled aqueous RAFT polymerization of AEMA **(6)** yielding near monodisperse homopolymers.<sup>228</sup> Well-defined block copolymers of AEMA-*b*-HPMA **(18)** were also prepared directly in aqueous solution through the chain extension of AEMA macroCTA **(20)** with HPMA **(8)**. Recently, the McCormick research group reported the aqueous RAFT polymerization of APMA **(12)** in a dioxane-water mixture.<sup>79</sup> Homopolymers of APMA **(12)** were then chain extended with *N*-isopropylacrylamide (NIPAM) to produce temperature-responsive block copolymers that formed vesicles upon increasing the solution temperature.



Herein, we report for the first time the synthesis of well-defined carboxylic acid functionalized glycopolymers prepared via the reductive amination reaction between PAPMA (**17**), synthesized by aqueous RAFT polymerization, and D-glucuronic acid sodium salt. The bioconjugation is effective, giving near quantitative yields. We also report the bioconjugation of PAEMA (**16**) and PAEMA-*b*-PHPMA (**18**) using the same method, resulting in poorer yields (60-82%).

## Experimental

*Materials.* All reagents were used without further purification unless otherwise noted. Methacryloyl chloride (>97%), ethanolamine (>98%), D-Glucuronic acid sodium salt monohydrate (**5**) and hydroquinone (99%) were purchased from Aldrich. Phenylmagnesium bromide solution (3M in diethyl ether), boric acid and sodium cyanoborohydride (NaCNBH<sub>3</sub>) were purchased from Fluka. Acetic acid, sodium acetate, sodium bicarbonate, diethylether, ethylacetate, hexane, and hydrochloric acid were purchased from Fisher. Carbon disulfide and potassium ferric cyanide were purchased from Acros Organics. 2,2'-Azobis(2-imidazolinypropene) dihydrochloride (VA-044) (**19**) was purchased from Wako Pure Products and recrystallized from methanol. *N*-3-Aminopropyl methacrylamide (APMA) (**12**) was purchased from Polysciences, Inc. 4'-Azobis(4-cyanovaleric acid) (V-501) (**13**) was purchased from Fluka and recrystallized from methanol. 4-Cyanodithiobenzoic acid (CTP) (**14**) was synthesized according to reported procedure.<sup>145</sup> 2-Aminoethyl methacrylate (AEMA) (**6**) was synthesized using a previously reported procedure.<sup>54</sup> *N*-2-Hydroxypropyl methacrylamide (HPMA) (**8**) was synthesized according to Kopecek et al.<sup>211</sup>

*Synthesis of PAPMA (17).* The aqueous RAFT polymerization of APMA (12) was performed at 70 °C. V-501 (13) was employed as the primary radical source and CTP (14) was used as the CTA. The polymerization was performed directly in acetate buffer (pH=5, 0.27 mol/L acetic acid and 0.73 mol/L sodium acetate) with an initial monomer concentration ( $[M]_0$ ) of 2 M. The initial  $[M]_0/[CTA]_0$  was 200, while the CTA to initiator ratio was 5:1. The homopolymerization was conducted by dissolving APMA (40) (1.65 g, 10 mmol), CTP (14) (28 mg, 0.1 mmol) and V-501 (13) (5.61 mg, 0.004 mmol) in a 25 ml round-bottom flask and diluting the resulting mixture to a final volume of 10 ml with acetate buffer. The reaction solution was purged with nitrogen for 45 minutes and subsequently placed in a water bath at 70 °C. The polymerization was allowed to proceed for 60 minutes before being quenched by rapid cooling in liquid nitrogen. The PAPMA (17) was then purified by dialysis against deionized water followed by lyophilization.

$^1\text{H NMR (D}_2\text{O)}$ :  $\delta$  3.11 (br, 2H,  $-\text{NH}_2\text{CH}_2$ );  $\delta$  2.94 (br, 2H,  $-\text{NH}_2\text{CH}_2$ );  $\delta$  1.79 (br, 2H,  $-\text{CH}_2$ ); 1.63 (br, 2H,  $-\text{CH}_2$ );  $\delta$  0.85-1.16 (br, 3H,  $-\text{CH}_3$ ).  $^{13}\text{C NMR (D}_2\text{O)}$ :  $\delta$  184.6 (C=O);  $\delta$  68.4 (C-O);  $\delta$  58.7 (C);  $\delta$  49.5 (C-N);  $\delta$  43.6 ( $\text{CH}_2$ );  $\delta$  23.3 ( $\text{CH}_3$ ).

*Synthesis of PAEMA (16).* PAEMA (6) was synthesized according to previous chapter. Molecular weights, polydispersities and conversion data are shown in Table IV-1.

$^1\text{H NMR (D}_2\text{O)}$ :  $\delta$  4.21 (br, 2H,  $-\text{OCH}_2$ );  $\delta$  3.31 (br, 2H,  $-\text{NH}_2\text{CH}_2$ );  $\delta$  1.95 (br, 2H,  $-\text{CH}_2$ );  $\delta$  0.83-1.36 (br, 3H,  $-\text{CH}_3$ ).  $^{13}\text{C NMR (D}_2\text{O)}$ :  $\delta$  184.6 (C=O);  $\delta$  68.4 (C-O);  $\delta$  58.7 (C);  $\delta$  49.5 (C-N);  $\delta$  43.6 ( $\text{CH}_2$ );  $\delta$  23.3 ( $\text{CH}_3$ ).

*Preparation of PAEMA-*b*-PHPMA (18).* PAEMA-*b*-PHPMA (18) was synthesized according to previous chapter. Molecular weights, polydispersities and conversion data are shown in Table IV-1.

$^1\text{H NMR (D}_2\text{O)}$ :  $\delta$  4.21 (br, 2H, -OCH<sub>2</sub>);  $\delta$  3.82 (br, H, -CHOH);  $\delta$  3.31 (br, 2H, -NH<sub>2</sub>CH<sub>2</sub>);  $\delta$  3.29-2.99 (br, 2H, -NH<sub>2</sub>CH<sub>2</sub>);  $\delta$  2.05 (br, 2H, -CH<sub>2</sub>);  $\delta$  1.95 (br, 2H, -CH<sub>2</sub>);  $\delta$  1.10 (br, 3H, -CH<sub>3</sub>);  $\delta$  1.06 (br, 3H, -CH<sub>3</sub>);  $\delta$  0.83-1.36 (br, 3H, -CH<sub>3</sub>).  $^{13}\text{C NMR (D}_2\text{O)}$ :  $\delta$  184.6 (C=O);  $\delta$  183.5 (C=O);  $\delta$  71.0 (CH);  $\delta$  68.4 (C-O);  $\delta$  58.7 (C);  $\delta$  58.2 (C);  $\delta$  56.7 (C-N);  $\delta$  49.5 (CH<sub>2</sub>); 48.9 (CH<sub>2</sub>);  $\delta$  43.6 (C-N);  $\delta$  25.4 (CH<sub>3</sub>);  $\delta$  23.3 (CH<sub>3</sub>);  $\delta$  23.0 (CH<sub>3</sub>).

*Model Study for Bio-conjugation of (Co)polymers with D-Glucuronic Acid Sodium Salt (5).* A model study was conducted by attachment of D-Glucuronic acid sodium salt to the APMA (12) through reductive amination reaction. APMA (12) (0.382 g, 2.14 mmol), D-Glucuronic acid sodium salt (5) (1 g, 4.27 mmol), sodium cyanoborohydride (NaCNBH<sub>3</sub>) (0.268 g, 4.27 mmol) and hydroquinone (0.024 g, 0.217 mmol) were dissolved in 15 ml of sodium borate buffer solution (0.1 M, pH 8.5) containing 0.5 M sodium chloride (NaCl). The flask was sealed with a rubber septum. The contents were purged with nitrogen for 30 min. The flask was subsequently immersed in an oil bath at 40 °C. The reaction was allowed to proceed for 4 days under continuous stirring. The solution was precipitated in selective solvent acetone and passed through a silica plug using water as eluent.

**<sup>1</sup>H NMR (D<sub>2</sub>O) of APMA (12):** δ 5.55 (1H, =CH); δ 5.29 (1H, =CH) δ 3.16 (2H, -NH<sub>2</sub>CH<sub>2</sub>); δ 2.86 (2H, -NH<sub>2</sub>CH<sub>2</sub>); δ 1.79 (2H, -CH<sub>2</sub>); δ 1.72 (3H, -CH<sub>3</sub>). **<sup>13</sup>C NMR (D<sub>2</sub>O) of APMA (12):** δ 172.3 (C=O); δ 138.5 (=C); δ 120.4 (=C); δ 37.4 (C-N); δ 35.6 (C-N); δ 25.9 (CH<sub>2</sub>); δ 16.3 (CH<sub>3</sub>).

**<sup>1</sup>H NMR (D<sub>2</sub>O) of D-glucuronic acid sodium salt (5):** δ 5.12 (1H, 1αCH); δ 4.53 (1H, 1βCH); δ 3.95 (1H, 5αCH); δ 3.61 (1H, 5βCH); δ 3.46-3.34 (1H, 3βCH, 3αCH, 4βCH, 4αCH, 2αCH); δ 3.15 (1H, 2βCH). **<sup>13</sup>C NMR (D<sub>2</sub>O) of D-glucuronic acid sodium salt (5):** δ 180.6 (6αC=O); δ 179.4 (6βC=O); δ 98.9 (1βC); δ 94.9 (1αC); δ 79.8-73.7 (2βC, 2αC, 3βC, 3αC, 4βC, 4αC, 5βC, 5αC).

**<sup>1</sup>H NMR (D<sub>2</sub>O) of Bio-conjugated APMA (21):** δ 5.63 (1H, =CH); δ 5.38 (1H, =CH); δ 4.11 (1H, 5αCH); δ 3.94 (1H, 5βCH); δ 3.84-3.44 (1H, 3βCH, 3αCH, 4βCH, 4αCH, 2αCH); 3.22 (1H, 2βCH); δ 3.93 (2H, -NH<sub>2</sub>CH<sub>2</sub>); δ 3.00 (2H, -NH<sub>2</sub>CH<sub>2</sub>); δ 1.89 (2H, -CH<sub>2</sub>); δ 1.82 (3H, -CH<sub>3</sub>). **<sup>13</sup>C NMR (D<sub>2</sub>O) of Bio-conjugated APMA (21):** δ 183.8 (6αC=O); δ 181.8 (6βC=O); δ 175.7 (C=O); δ 138.5 (=C); δ 120.4 (=C); δ 98.9 (1βC); δ 94.9 (1αC); δ 79.8-73.7 (2βC, 2αC, 3βC, 3αC, 4βC, 4αC, 5βC, 5αC), δ 37.4 (C-N); δ 35.6 (C-N); δ 25.9 (CH<sub>2</sub>); δ 16.3 (CH<sub>3</sub>).

*Bio-conjugation of (Co)polymers with D-Glucuronic Acid Sodium Salt (5).*

PAEMA (16), PAPMA (17) and PAEMA-*b*-HPMA (18) were bio-conjugated with D-glucuronic acid sodium salt (5) through reductive amination reaction. In a typical experimental protocol, PAPMA<sub>86</sub> (16) (M<sub>n</sub> = 15,400) (100 mg, 6.5 x 10<sup>-3</sup> mmol), D-glucuronic acid sodium salt (5) (10 times mole equivalent of primary amine group in polymer) (1.31 g, 5.59 mmol), NaCNBH<sub>3</sub> (10 times mole equivalent of D-glucuronic acid sodium salt (5)) (3.18 g, 0.051 mol) were dissolved in 25 ml of sodium borate buffer

solution (0.1 M, pH 8.5) containing 0.5 M NaCl. The flask was sealed with a rubber septum and the contents were purged with nitrogen for 30 min. The flask was subsequently immersed in an oil bath at 45 °C. The reaction was allowed to proceed for 4 days under constant stirring, followed by dialysis against a 0.5 M NaCl aqueous solution using a Spectra/Por 7 membrane (molecular weight cutoff of 14000) to remove excess sugar. The solution was desalted by dialysis against DI water, and the resulting bio-conjugated polymer was obtained by lyophilization.

**<sup>1</sup>H NMR (D<sub>2</sub>O) of Bio-conjugated PAPMA (22):** δ 3.10 (br, 2H, -NHCH<sub>2</sub>); δ 2.94 (br, 2H, -NH<sub>2</sub>CH<sub>2</sub>); δ 4.28-3.13 (br, 1H, 5 $\alpha$ CH, 5 $\beta$ CH, 1 $\alpha$ CH, 1 $\beta$ CH); δ 3.13-2.82 (br, 1H, 3 $\beta$ CH, 3 $\alpha$ CH, 4 $\beta$ CH, 4 $\alpha$ CH, 2 $\alpha$ CH, 2 $\beta$ CH); δ 1.79 (br, 2H, -CH<sub>2</sub>); δ 1.62 (br, 2H, -CH<sub>2</sub>); δ 0.99-0.84 (br, 3H, -CH<sub>3</sub>). **<sup>13</sup>C NMR (D<sub>2</sub>O) of Bio-conjugated PAPMA (22):** 191.2-189.1 (6 $\alpha$ , 6 $\beta$  C=O) δ 182.6 (C=O); δ 82.6-68.9 (1 $\alpha$ C, 1 $\beta$ C, 2 $\beta$ C, 2 $\alpha$ C, 3 $\beta$ C, 3 $\alpha$ C, 4 $\beta$ C, 4 $\alpha$ C, 5 $\beta$ C, 5 $\alpha$ C); δ 55.4 (C); δ 47.2 (C-N); δ 48.1 (C-N); δ 40.1 (CH<sub>2</sub>); δ 28.6 (CH<sub>2</sub>); δ 19.0 (CH<sub>3</sub>).

**<sup>1</sup>H NMR (D<sub>2</sub>O) of PAEMA (16):** δ 4.21 (br, 2H, -OCH<sub>2</sub>); δ 3.31 (br, 2H, -NH<sub>2</sub>CH<sub>2</sub>); δ 1.95 (br, 2H, -CH<sub>2</sub>); δ 0.83-1.36 (br, 3H, -CH<sub>3</sub>). **<sup>13</sup>C NMR (D<sub>2</sub>O) of PAEMA (101):** δ 184.6 (C=O); δ 68.4 (C-O); δ 58.7 (C); δ 49.5 (C-N); δ 43.6 (CH<sub>2</sub>); δ 23.3 (CH<sub>3</sub>).

**<sup>1</sup>H NMR (D<sub>2</sub>O) of Bio-conjugated PAEMA (23):** δ 4.03 (br, 2H, -OCH<sub>2</sub>); δ 3.82 (br, 2H, -NH<sub>2</sub>CH<sub>2</sub>); δ 3.98-3.52 (br, 1H, 5 $\alpha$ CH, 5 $\beta$ CH, 1 $\alpha$ CH, 1 $\beta$ CH); δ 3.29-2.40 (br, 1H, 3 $\beta$ CH, 3 $\alpha$ CH, 4 $\beta$ CH, 4 $\alpha$ CH, 2 $\alpha$ CH, 2 $\beta$ CH); δ 1.95 (br, 2H, -CH<sub>2</sub>); δ 0.76-1.31 (br, 3H, -CH<sub>3</sub>). **<sup>13</sup>C NMR (D<sub>2</sub>O) of Bio-conjugated PAEMA (23):** δ 188.7-185.0 (6 $\alpha$ , 6 $\beta$  C=O); δ 182.8 (C=O); δ 98.9 (1 $\beta$ C); δ 94.9 (1 $\alpha$ C); δ 80.3-71.3 (2 $\beta$ C, 2 $\alpha$ C, 3 $\beta$ C, 3 $\alpha$ C, 4 $\beta$ C, 4 $\alpha$ C, 5 $\beta$ C, 5 $\alpha$ C); δ 68.4 (C-O); δ 58.7 (C); δ 49.5 (CH<sub>2</sub>); δ 76.1 (C-N); δ 23.3 (CH<sub>3</sub>).

*Characterization.* PAPMA (**17**), PAEMA (**16**) and PAEMA-*b*-PHPMA (**18**) copolymers were characterized by aqueous size exclusion chromatography (ASEC-MALLS) at ambient temperature using Eprogen CATSEC columns (100, 300, and 1000 Å). A Wyatt Optilab DSP interferometric refractometer ( $\lambda = 690$  nm) and a Wyatt DAWN DSP multiangle laser light scattering detector ( $\lambda = 633$  nm) were employed using 1 wt % acetic acid/0.1 M Na<sub>2</sub>SO<sub>4</sub> (aq) solution as the eluent at a flow rate of 0.25 ml/min. The  $dn/dc$  of the PAEMA (**16**) was determined to be 0.153 and the  $dn/dc$  of the PAPMA (**17**) was determined to be 0.181 in the above eluent at 25 °C using a Bausch and Lomb refractometer. Conversions in each system were determined by comparing the area of the UV signal corresponding to monomer at  $t_0$  to the area at  $t_x$ . Absolute molecular weights and polydispersities were calculated using the Wyatt ASTRA SEC/LS software package.

The conjugated polymers were incompatible with the GPC columns, so MALDI-TOF was used to determine the peak molecular weight values and the degree of conjugation. MALDI-TOF mass spectrometry was performed on a Bruker Microflex equipped with a 337 nm N<sub>2</sub> laser in linear mode and 20 kV acceleration voltage. Pulsed ion extraction (200 ns) was employed during the collection of all data. 2,5-Dihydroxybenzoic acid (DHB, Fluka, 99.5%) was used as the matrix and trifluoroacetic acid (TFA) was used as the charging agent. The matrix and samples were prepared in HPLC H<sub>2</sub>O without addition of a charging agent. Samples were then mixed (10  $\mu$ l polymer/10  $\mu$ l Matrix) in separate microcentrifuge tubes and 1.0  $\mu$ l of the mixture was spotted directly on a stainless steel target. Due to the propensity of the conjugated polymers to precipitate upon addition of TFA, 0.5  $\mu$ l of 0.5 % TFA in acetonitrile was added once the sample had been spotted on the target to facilitate charging and drying.

Two different external calibration standards were used for polymers (Bruker, Protein Standard I) and for conjugated polymers (Bruker, Protein Standard II). For each sample, an average of 800 laser shots was taken. The peak molecular weight values of the polymers were determined by mass spectrometry and compared to GPC values.

A Varian 500 MHz NMR equipped with a standard 5 mm  $^1\text{H}/^{13}\text{C}$  probe was utilized to identify the homopolymer structure of PAEMA (**16**), PAPMA (**17**), PAEMA-*b*-PHPMA (**18**) and bio-conjugated polymers (nt = 64, d1 = 3.1  $\mu\text{s}$ , pw90 = 16  $\mu\text{s}$ , at = 1.89  $\mu\text{s}$ ). The degree of polymerization and molecular weight were determined *via*  $^1\text{H}$  NMR through integration of the relative intensities of methylene-protons resonance at 3.31 ppm of PAEMA (**16**) and 3.10 ppm of PAPMA (**17**) and phenyl-protons of CTP (**14**) between 7.51 and 7.89 ppm.

The copolymer structures, degrees of polymerization and molecular weights were identified *via*  $^1\text{H}$  NMR (nt = 32, d1 = 4.1  $\mu\text{s}$ , pw90 = 15.3  $\mu\text{s}$ , at = 1.89  $\mu\text{s}$ ) by integration of the relative intensities of methylene-proton resonances at 3.78 ppm (HPMA) (**8**) and methylene-proton resonances at 4.2 ppm (PAEMA (**16**)). Samples were prepared at 5 wt% in deuterated water ( $\text{D}_2\text{O}$ ). All pH measurements were performed with  $\pm 0.02$  accuracy with a 900A (Orion) pH meter.

## Results and Discussion

*Aqueous RAFT Homopolymerization of APMA (12) and AEMA (6).* The aqueous RAFT polymerization of primary amine containing monomers is challenging because the chain transfer agent and the monomer are susceptible to side reactions due to the moderate nucleophilic character of the primary.<sup>103,213,214</sup> For example, AEMA (6) is rapidly rearranged to 2-hydroxyethyl methacrylamide (7) at alkaline pH through the attack of the deprotonated amine group on its own carbonyl group, forming a stable six member ring intermediate. It has also been suggested that AEMA (6) can undergo Micheal addition, through the intermolecular nucleophilic attack of the deprotonated primary amine group on the double bond. Considering these issues, primary amine containing monomers are generally polymerized using protecting group chemistry. However, recent advances in aqueous RAFT polymerization provide a facile route for the controlled polymerization of primary amine containing monomers. Our research group has recently reported the direct synthesis of well-defined PAEMA (16) through aqueous RAFT polymerization without the necessity of protecting group chemistry.<sup>228</sup> Specifically, AEMA (6) monomer was homopolymerized directly in aqueous solution at 50 °C with polydispersities (PDIs) below 1.2 and conversions up to 95%. Additionally, it was deduced that the controlled polymerization of AEMA (6) depends on polymerization temperature. AEMA (6) polymerization performed at 70 °C resulted in loss of the CTA within 45 minutes leading to an increase in PDI. Our results suggested that the relatively high PDIs reported by previous groups<sup>67</sup> are due to the high polymerization temperature, which resulted in various side reactions that led to broadened molecular weight distributions. We also demonstrated the synthesis of well-defined PAEMA-*b*-PHPMA



**(18)** block copolymers upon the chain extension of PAEMA **(16)** with HPMA **(8)**.

Based upon our previously reported results, well-defined PAEMA **(16)** and PAEMA-*b*-PHPMA **(18)** were prepared.<sup>228</sup> Molecular weights, polydispersities and conversion data of resulting PAEMA **(16)** and PAEMA-*b*-PHPMA **(18)** are shown in Table IV-1.

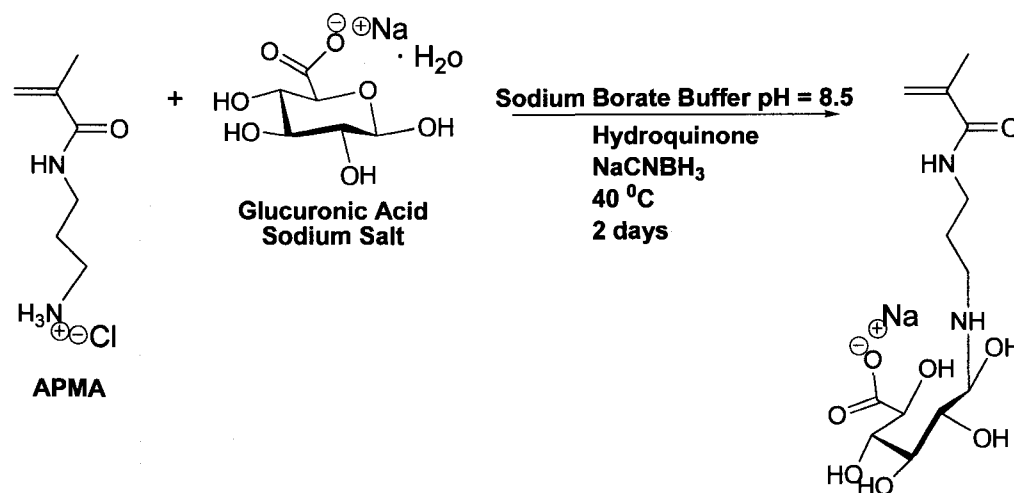
**Table IV-1.** (Co)polymers results.

<i>Polymer</i>	Time (min)	Temp. (°C)	$M_n^1$	$M_n^2$	$M_n^3$	PDI <sup>1</sup>	Conv. <sup>1</sup> (%)
<i>PAPMA</i> <sub>86</sub>	60	70	15000	15400	21000	1.08	31
<i>PAEMA</i> <sub>216</sub>	75	50	33000	35000	33500	1.05	47
<i>PAEMA</i> <sub>204</sub> - <i>b</i> - <i>PHPMA</i> <sub>130</sub>	120	70	48400	51000		1.05	33

1. Calculated through GPC.
2. Calculated through <sup>1</sup>H NMR.
3. Theoretical molecular weight.

In the current research, APMA **(12)** polymerization was evaluated in comparison to AEMA **(6)**. APMA **(12)** exhibits higher stability in alkaline medium when compared to AEMA **(6)**. Owing to its longer pendant group, APMA **(12)** is not susceptible to rearrangement reactions. McCormick and coworkers recently reported the successful homopolymerization and copolymerization of APMA **(12)** *via* RAFT polymerization using dioxane-water mixture as a solvent.<sup>79</sup> In this study, APMA polymerizations were carried out at 70 °C using V-501 **(13)** as the radical source and CTP **(14)** as the CTA in an acetic acid/sodium acetate buffer (pH = 5). For the polymerizations, the initial ratio of  $[M]_0$  to  $[CTA]_0$  was maintained at 200 /1 and a  $[CTA]_0/[I]_0$  ratio of 5/1 was employed. Molecular weights, polydispersities and conversion data are shown in Table IV-1.

*Model Study for Bioconjugation of PAPMA (17) with D-Glucuronic Acid Sodium Salt (5).* In order to gain understanding of expected chemical shifts in  $^1\text{H}$  and  $^{13}\text{C}$  NMR spectra after bioconjugation, a model study was performed reacting APMA (12) monomer with D-glucuronic sodium salt (5) (Scheme IV-1).



**Scheme IV-1.** Model Study for bioconjugation of D-glucuronic acid sodium salt (5) with PAPMA (17).

The reductive amination reaction was carried out in a sodium borate buffer (pH = 8.5) in the presence of NaCNBH<sub>3</sub> reducing agent. The  $^{13}\text{C}$  NMR spectra of APMA (12) monomer, D-glucuronic acid sodium salt (5) and bio-conjugated APMA (22) with D-glucuronic acid sodium salt (5) are given in Figure IV-1. The reductive amination reaction is evidenced by the chemical shift upfield of the carbon atoms of D-glucuronic acid sodium salt (5) labeled as  $1\alpha\text{C}$  and  $1\beta\text{C}$ .<sup>54,229</sup> In addition, a significant downfield chemical shift is observed for the carbon atom of APMA (12) labeled as **c**. The  $^1\text{H}$  NMR spectra (Figure IV-2) also provide evidence for the success of the reaction with the

chemical shifts of  $1\alpha\text{H}$  and  $1\beta\text{H}$  of the D-glucuronic acid sodium salt (**5**) upfield and the shift of **c** and **d** protons of APMA (**12**) downfield. It is difficult to label the exact chemical shifts of  $1\alpha\text{H}$  and  $1\beta\text{H}$  due to the broadness of the sugar peaks. A potential reason for this peak broadening is hydrogen bonding between carboxylic acid and secondary amine functionalities.

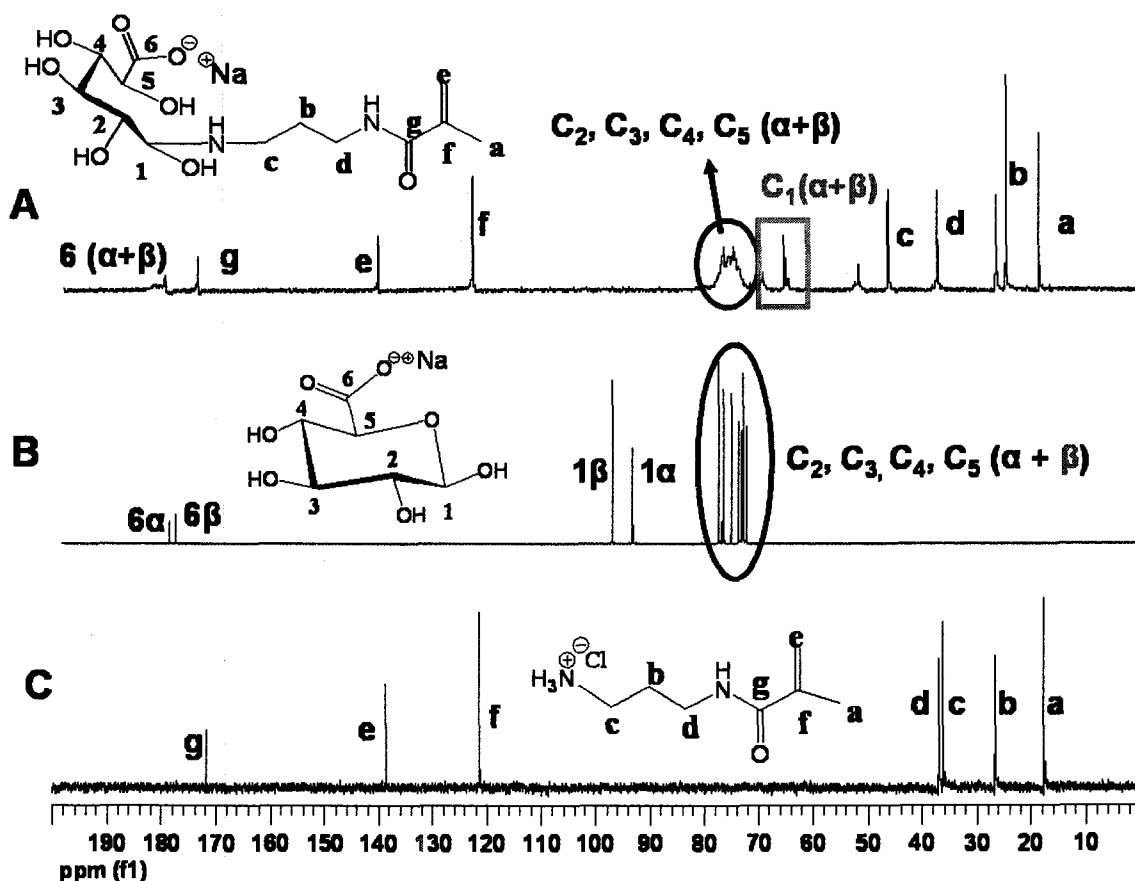
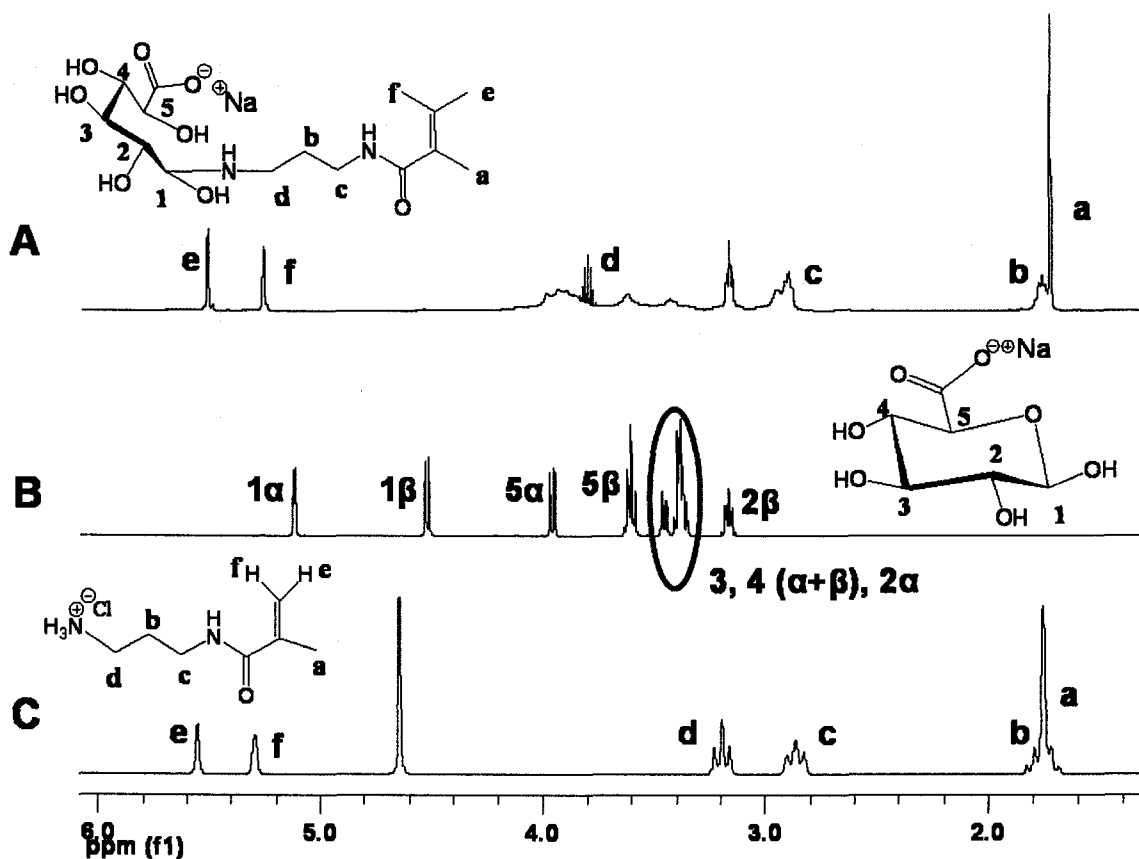


Figure IV-1.  $^{13}\text{C}$  NMR spectra of A. Bioconjugated APMA (**21**) with D-glucuronic acid sodium salt (**5**); B. D-Glucuronic acid sodium salt (**5**); and C. APMA monomer (**12**).

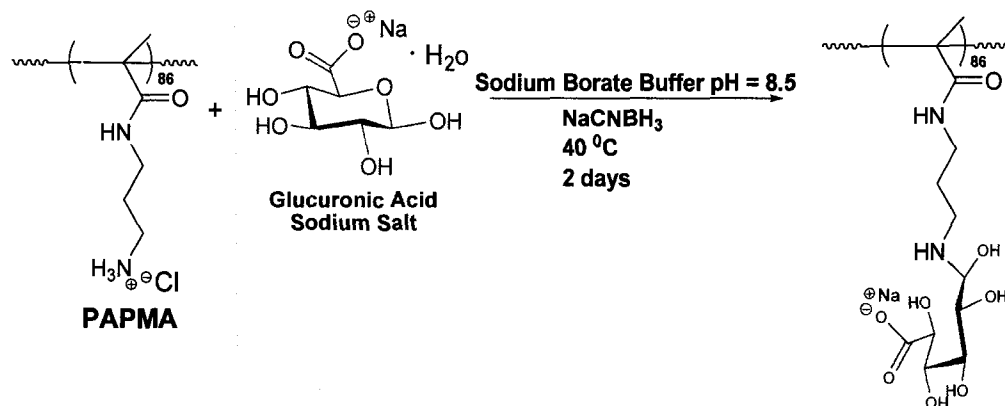


**Figure IV-2.** <sup>1</sup>H NMR spectra of A. Bioconjugated APMA (**21**) with D-glucuronic acid sodium salt (**5**); B. D-Glucuronic acid sodium salt (**5**); and C. APMA monomer (**12**).

*Bio-conjugation of PAPMA (**17**) with D-Glucuronic Acid Sodium Salt (**5**).*

PAPMA (**17**) (Table IV-1) was reacted with ten times molar excess of D-glucuronic acid sodium salt in the presence of NaCNBH<sub>3</sub> reducing agent in alkaline medium (Scheme IV-2). The ionic strength of the medium was increased (0.5-1 M NaCl) to suppress the formation of an ion complex with D-glucuronic acid sodium salt. The resulting polymer mixture was dialyzed against water to remove excess sugar. <sup>13</sup>C NMR spectra of PAPMA (**17**) and bioconjugated PAPMA (**22**) are given in Figure IV-3. The appearance of sugar peaks between 82.6 and 68.9 ppm in the <sup>13</sup>C NMR spectrum of bioconjugated PAPMA

(22) verifies the conjugation. Further, the upfield chemical shifts of  $1\alpha\text{C}$  and  $1\beta\text{C}$  of D-glucuronic acid sodium salt and the upfield chemical shift of the e carbon of PAPMA (17) provide evidence for the successful bioconjugation reaction.



Scheme IV-2. Bioconjugation of PAPMA (22) with D-glucuronic acid sodium salt (5).

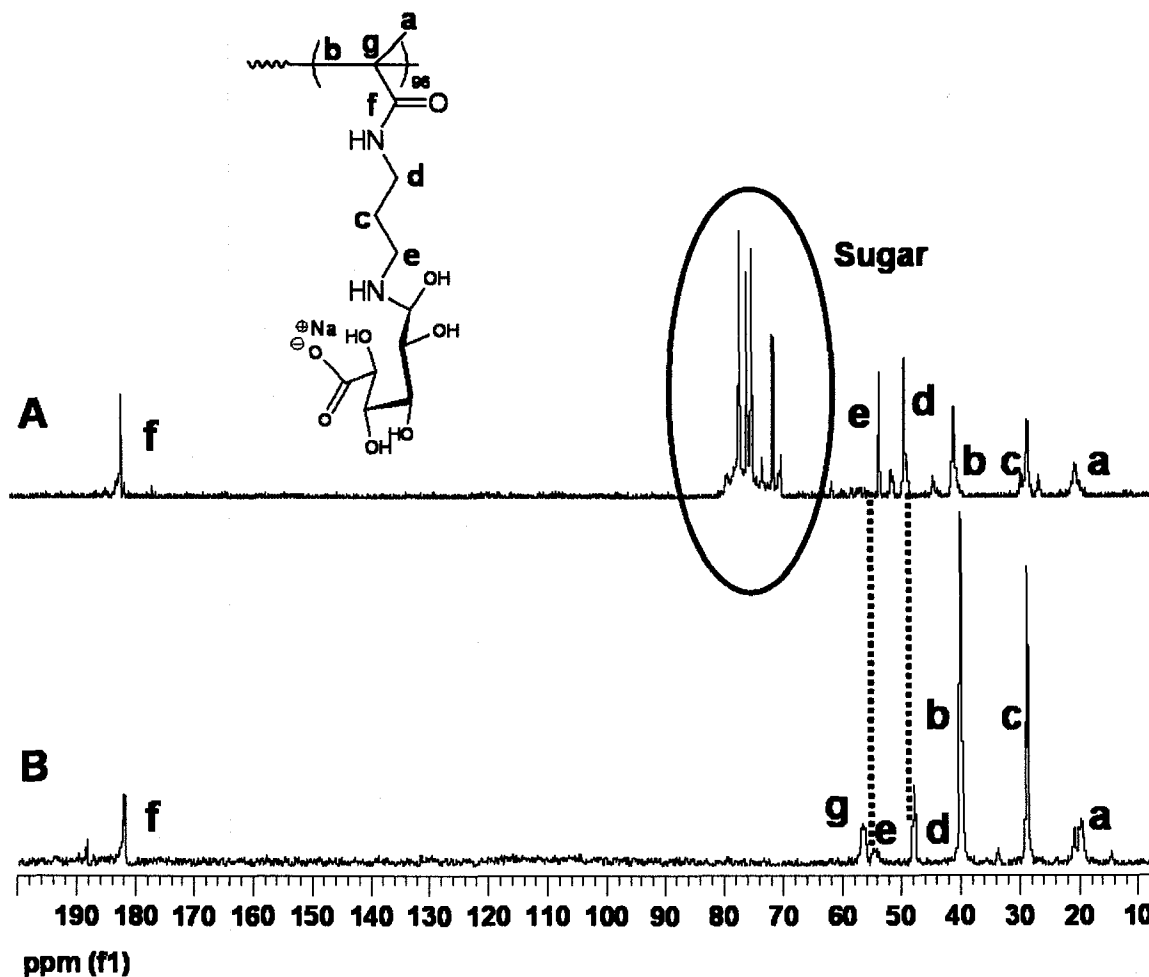


**Figure IV-3.**  $^{13}\text{C}$  NMR spectra of A. Bioconjugated PAPMA (**22**) with D-glucuronic acid sodium salt (**5**); B. PAPMA (**17**).

The  $^1\text{H}$  NMR spectra (Figure IV-4) shows the characteristic signals of both D-glucuronic acid sodium (**5**) and PAPMA (**17**) moieties. The integration value of proton resonances appearing between 4.2 and 2.6 ppm matches the number of protons which correspond to e, d and sugar unit protons (9 protons). The integration value of proton resonances appearing between 2.0 and 0.8 ppm matches the number of protons corresponding to a, b, c, and d units (7 protons). Comparing the integration values of the resonances to the number of protons in each unit yields a conversion of nearly 100%.

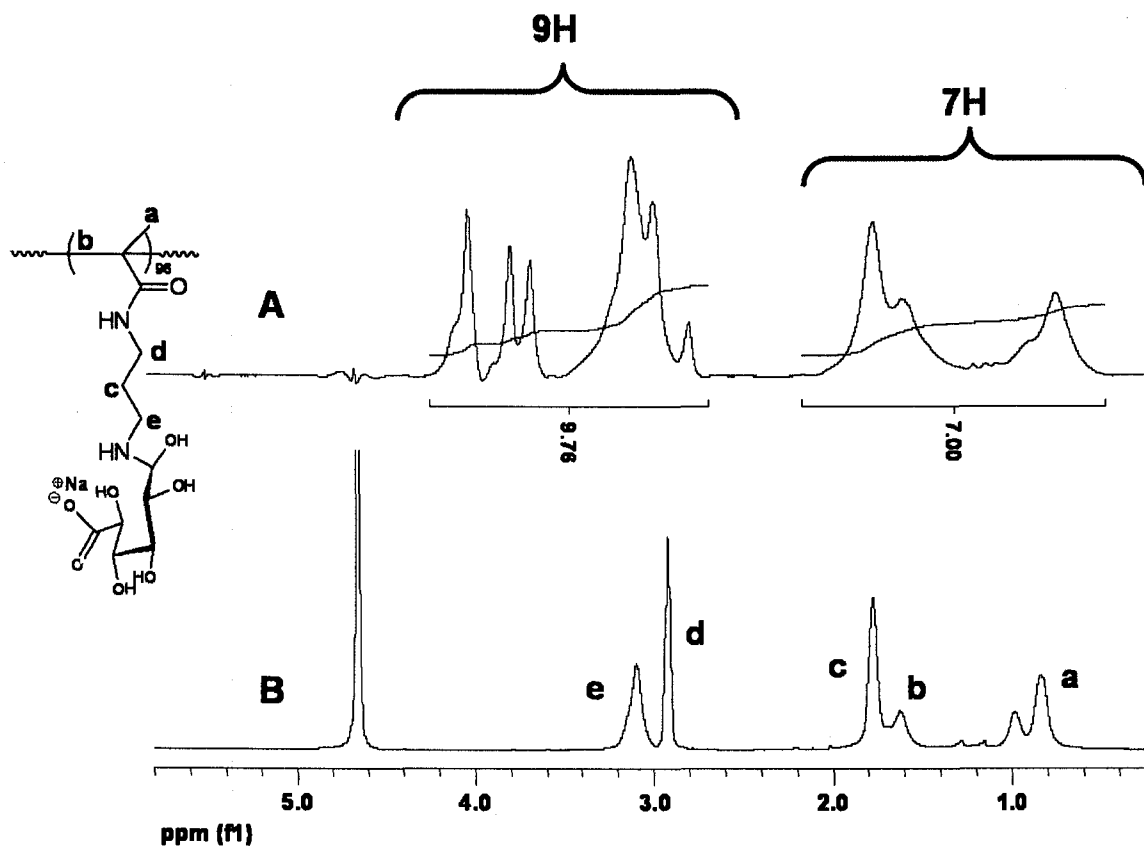


**Figure IV-4.** <sup>1</sup>H NMR spectra of A. Bioconjugated PAPMA (**22**) with D-glucuronic acid sodium salt (**5**); B. PAPMA (**17**).

Further evidence of high conversion is observed qualitatively in MALDI TOF analysis. As shown in Figure IV-5, MALDI TOF analysis of PAPMA (**17**) yields a narrow, unimodal mass distribution with peak molecular weight of 13,917. A small shoulder is observed in the lower mass region indicating the presence of terminated, low molecular weight chains during the early stage of the RAFT polymerization. The MALDI TOF mass spectrum of bioconjugated PAPMA (**22**) is given in Figure IV-6. A unimodal mass distribution is observed, with a peak molecular weight value of 34,052. The theoretical molecular weight for 100% substituted PAPMA (**17**) with starting molecular weight of 13,917 is 34,000. The close agreement of the theoretical value with

the peak molecular weight obtained through MALDI TOF analysis indicates near 100% conversion. A small high mass distribution is also observed in the bioconjugated PAPMA (22) MALDI TOF spectrum, which shows a peak molecular weight approximately two times that of the main peak. This is attributed to either disulfide formation between the polymer chains upon reduction of the dithioester end group or ion complexation of two charged polymer chains with a single charged sodium cation.

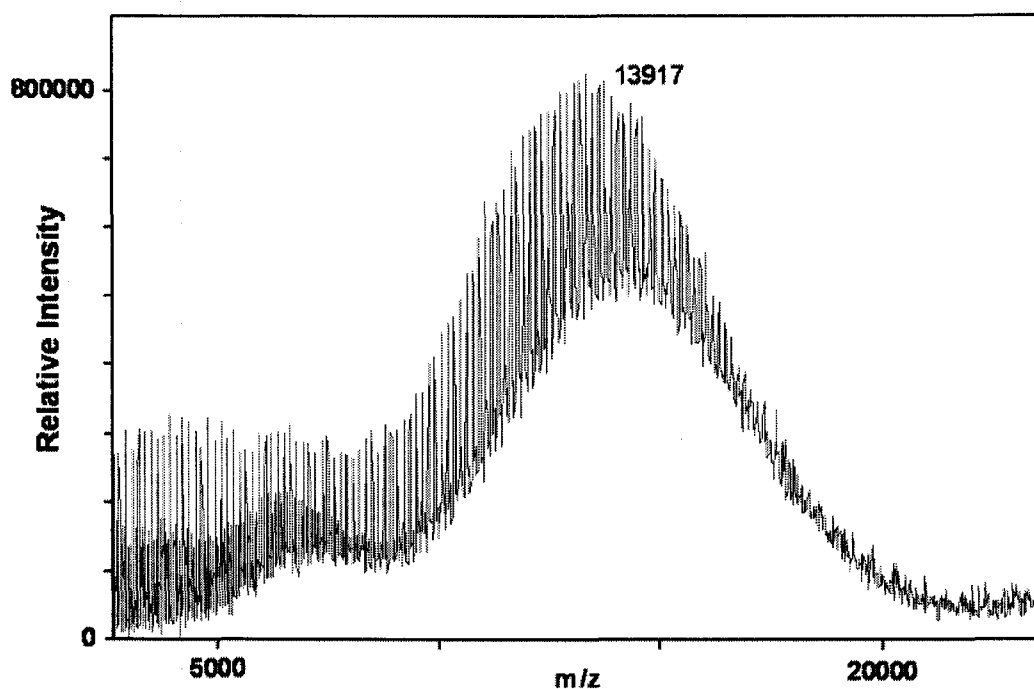
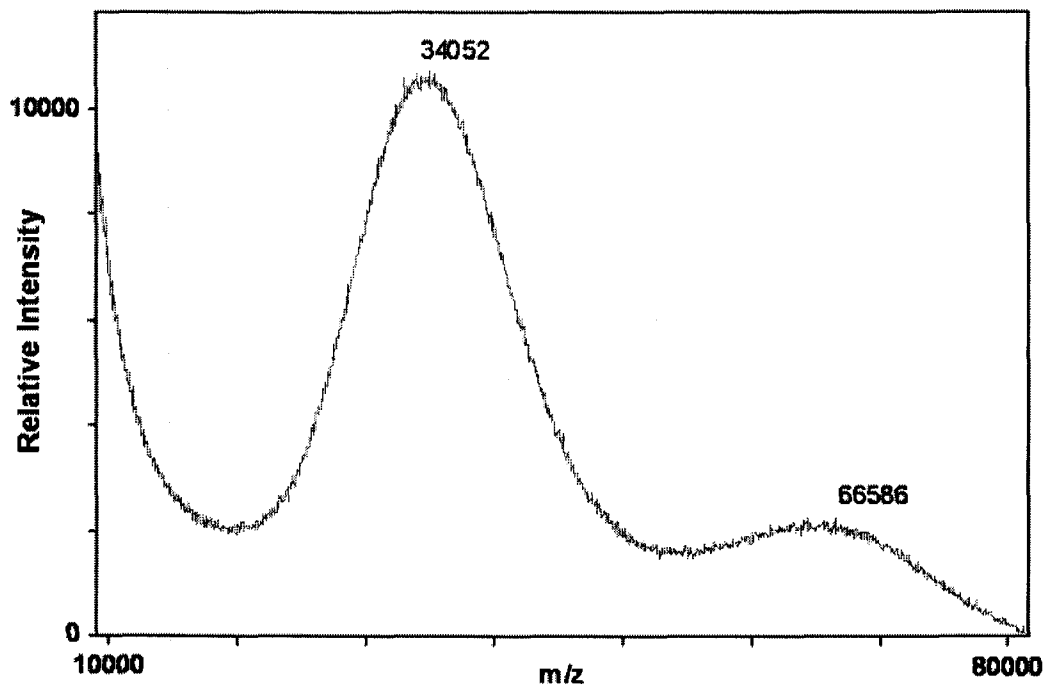


Figure IV-5. MALDI TOF mass spectrum of PAPMA (17).





**Figure IV-6.** MALDI TOF mass spectrum of bio-conjugated PAPMA (**22**) with D-glucuronic acid sodium salt (**5**).

*Bio-conjugation of PAEMA (**16**) with D-Glucuronic Acid Sodium Salt (**5**).*

PAEMA (**16**) (Table IV-1) was also bioconjugated with D-glucuronic acid sodium salt (**5**) through the method described previously. Figure IV-7 shows the  $^{13}\text{C}$  NMR spectra recorded for PAEMA (**16**) and bioconjugated PAEMA (**23**). The sugar incorporation is evidenced by the carbon resonances observed between 82.6 and 68.9 ppm. In addition, a significant chemical shift is observed for the f carbon resonance of PAEMA (**16**) from 44 ppm to 64 ppm due to the reaction of the primary amine groups with the reducing end of the of D-glucuronic acid sodium salt (**5**).

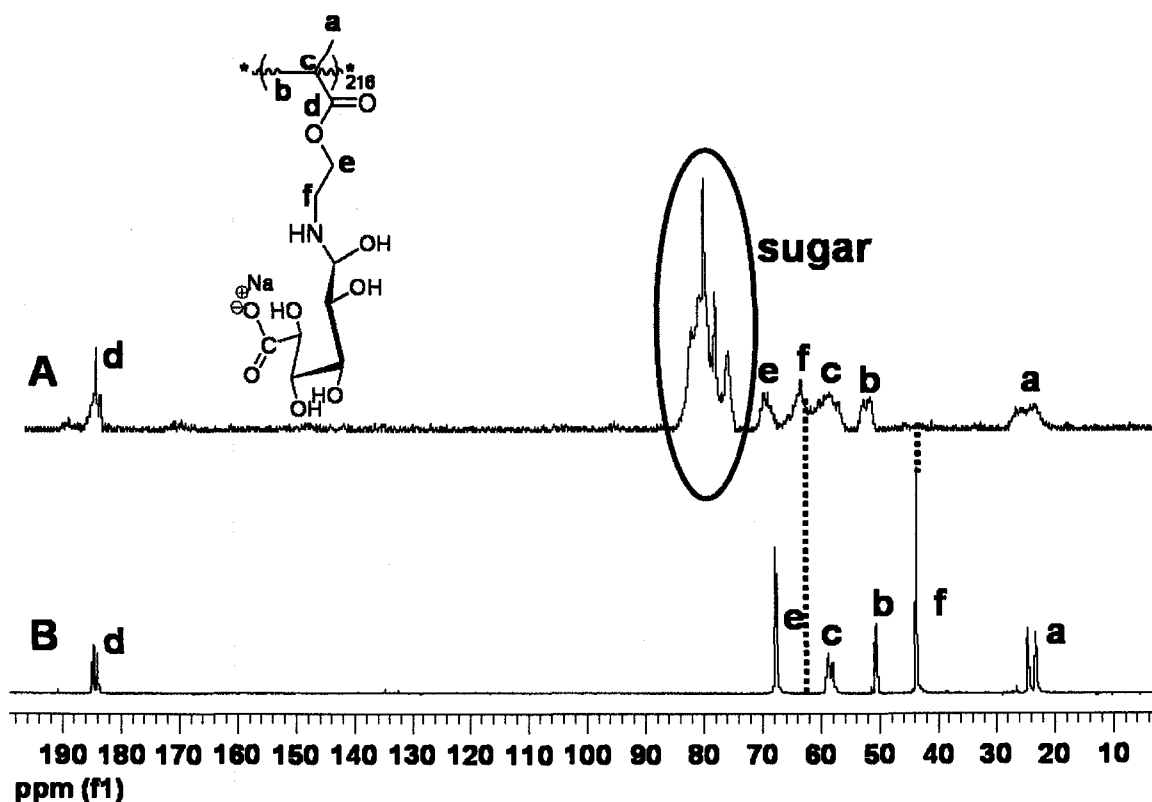


**Figure IV-7.**  $^{13}\text{C}$  NMR spectra of A. Bio-conjugated PAEMA (**23**) with D-glucuronic acid sodium salt (**5**); B. PAEMA (**16**).

Further evidence of the incorporation of the D-glucuronic acid sodium salt (**5**) with PAEMA (**16**); is observed in  $^1\text{H}$  NMR analysis (Figure IV-8).  $1\alpha\text{H}$  and  $1\beta\text{H}$  proton resonances of D-glucuronic acid sodium salt are shifted upfield after reaction. In addition, the **d** proton resonance of PAEMA (**16**) (3.31 ppm) is shifted downfield, also indicating the successful incorporation of D-glucuronic acid sodium salt (**5**). It is difficult to calculate the extent the reaction from the  $^1\text{H}$  NMR spectra due to overlapping of the resonance peak of  $\text{D}_2\text{O}$  with the resonance peaks of sugar and **c** proton resonances of PAEMA (**16**). After comparing the relative intensities of all peaks, we roughly calculated a yield of 95%.

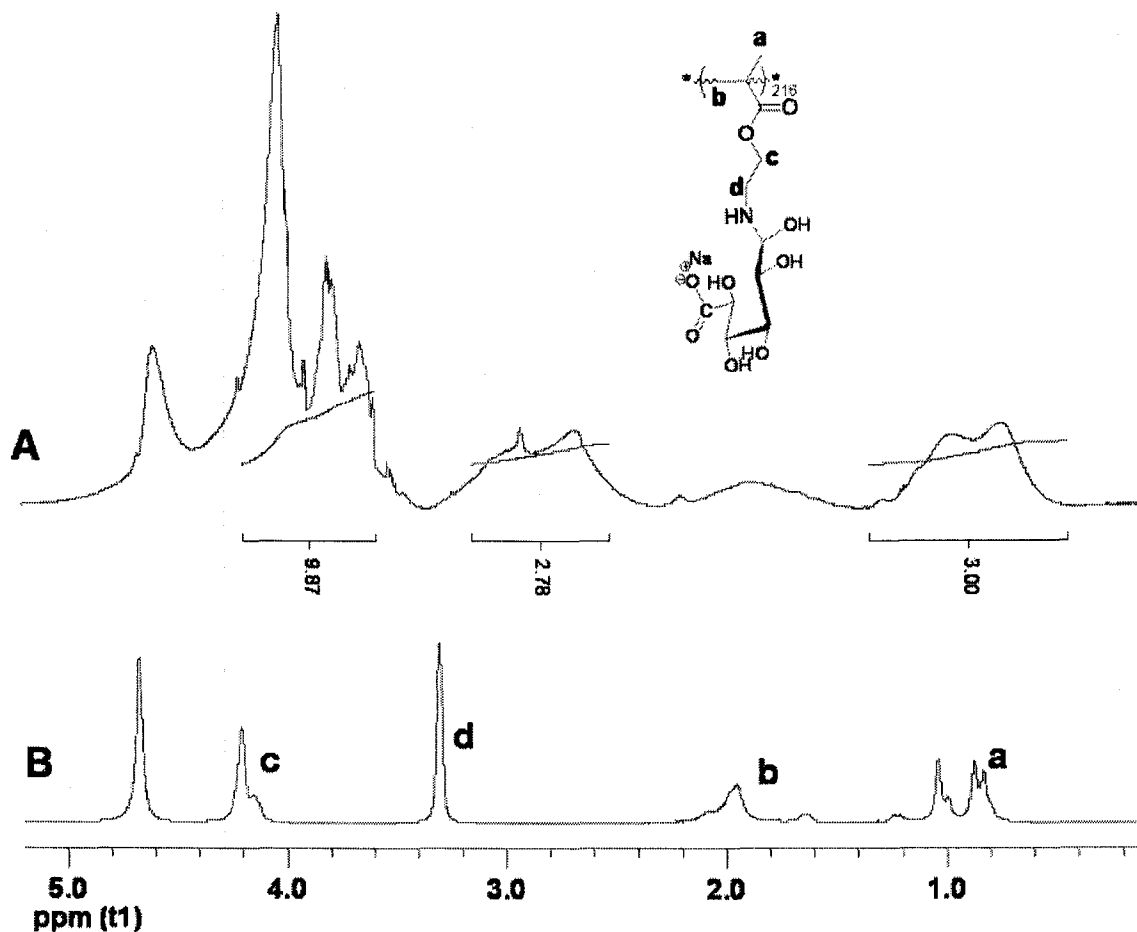


**Figure IV-8.**  $^1\text{H}$  NMR spectra of A. Bioconjugated PAEMA (**23**) with D-glucuronic acid sodium salt (**5**); B. PAEMA (**16**).

However, a peak molecular weight shift from 30697 to 64337 is observed from the mass spectra of PAEMA (**16**) and bioconjugated PAEMA (**23**) (Figure IV-9), suggesting a yield of 67%. The reason for such a low conversion might be the rearrangement reaction of PAEMA (**16**) in alkaline medium (pH 8.5), where some deprotonated primary amine groups attack the carbonyl group rather than reacting with D-glucuronic acid sodium salt (**5**), yielding unreacted hydroxyethyl methacrylamide pendant groups. He et al. recently reported the degradation of PAEMA (**16**) in alkaline solutions at 20 °C.<sup>67</sup> They found

that PAEMA (**16**) is very stable at pH 9, but slow degradation occurred over long time periods in more alkaline solution. In our case, even though the pH of the medium was held at 8.5, PAEMA (**16**) is still susceptible to degradation reactions due to the higher reaction medium temperature.

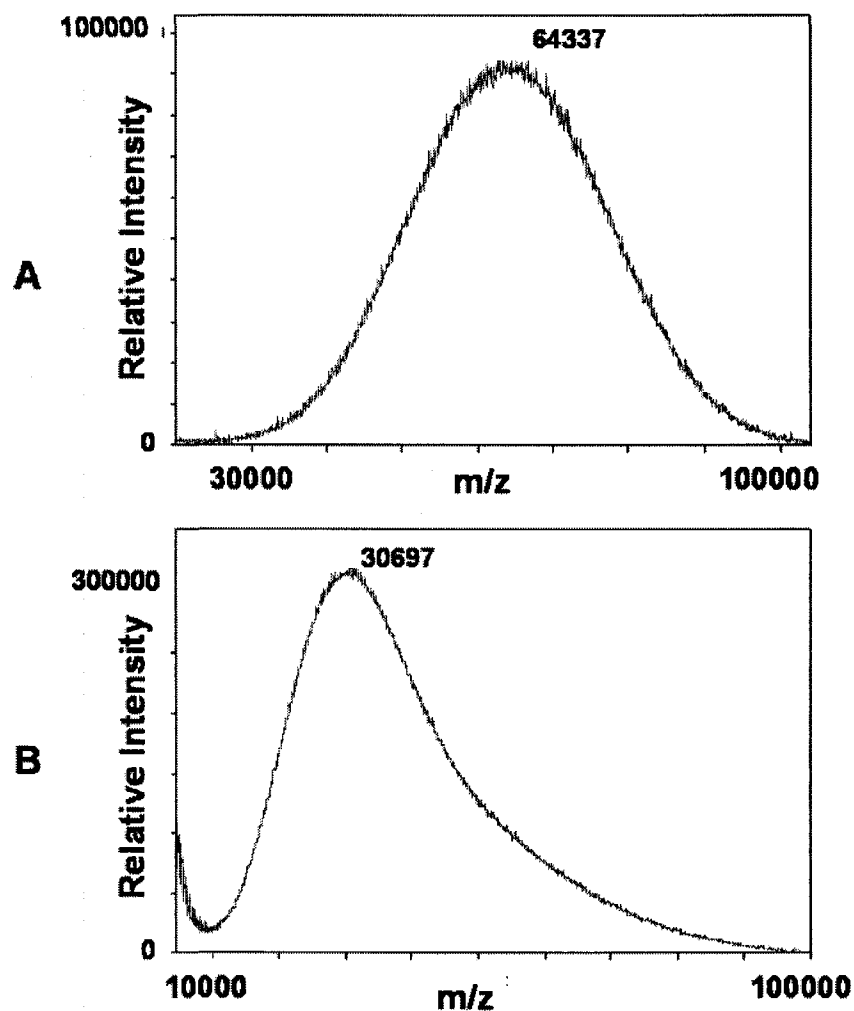


**Figure IV-9.** MALDI TOF mass spectra of A. Bio-conjugated PAEMA (**23**) with D-glucuronic acid sodium salt (**5**); B. PAEMA (**16**).

*Bioconjugation of PAEMA-*b*-PHPMA (18) with D-Glucuronic Acid Sodium Salt*

(5). PAEMA-*b*-PHPMA (18) was bioconjugated with D-glucuronic acid sodium salt (5) to prepare glycoblock copolymers *via* post-polymerization reactions. The bioconjugation was evidenced through  $^{13}\text{C}$  and  $^1\text{H}$  NMR (Figure IV-10, Figure IV-11). The appearance of D-glucuronic acid sodium salt (5) resonances between 83.2 and 72.9 ppm in the  $^{13}\text{C}$  NMR spectra indicates successful conjugation (Figure IV-10). Further evidence of the reaction is provided by the upfield chemical shifts of  $1\alpha\text{C}$  and  $1\beta\text{C}$  of D-glucuronic acid sodium salt (5) and the downfield chemical shift of the **f** carbon of PAEMA (16) block from 43 ppm to 66 ppm.

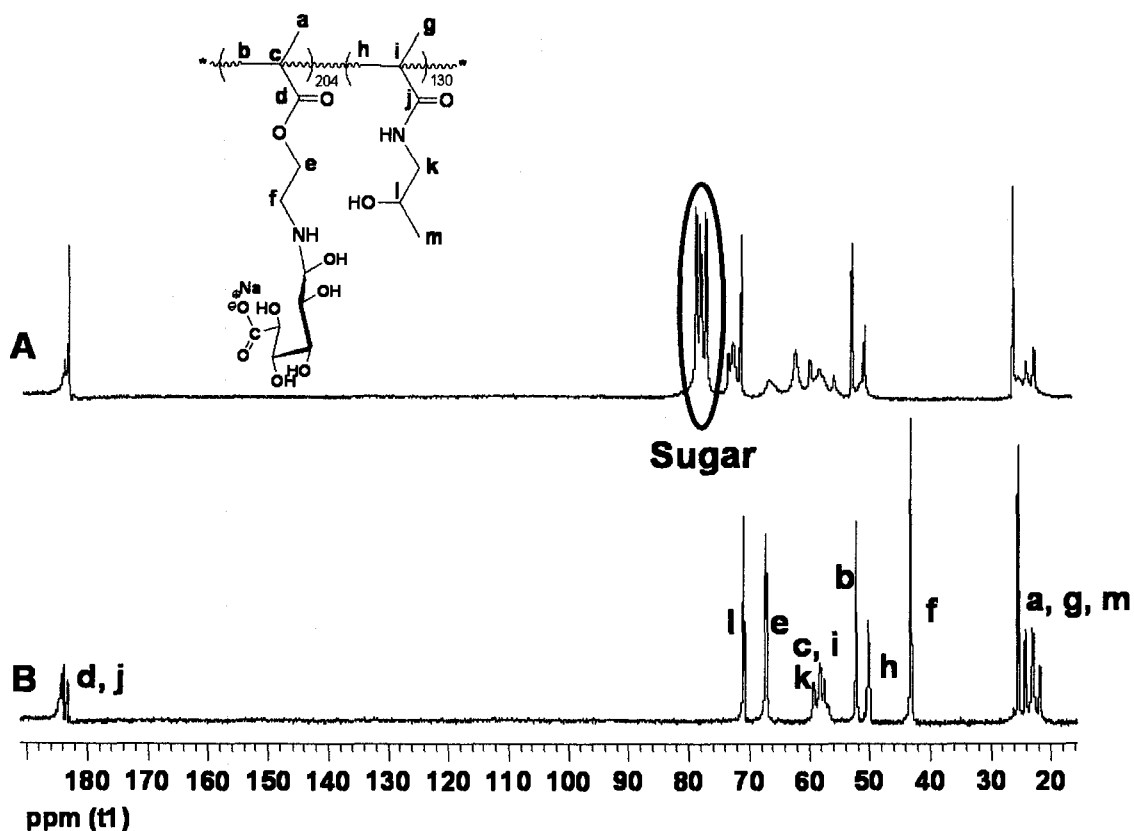


**Figure IV-10.**  $^{13}\text{C}$  NMR spectra of A. Bioconjugated PAEMA-*b*-PHPMA (24) with D-glucuronic acid sodium salt (5); B. PAEMA-*b*-PHPMA (18).

The incorporation of the D-glucuronic acid sodium salt (**5**) with PAEMA (**16**) block is also evidenced through  $^1\text{H}$  NMR analysis (Figure IV-11).  $1\alpha\text{H}$  and  $1\beta\text{H}$  proton resonances of D-glucuronic acid sodium salt (**5**) are shifted upfield upon the reductive amination reaction with PAEMA (**16**) block. Furthermore, the **d** proton resonance of PAEMA block is shifted downfield from 3.32 ppm to 3.73 ppm, suggesting the successful conjugation of D-glucuronic acid sodium salt (**5**).

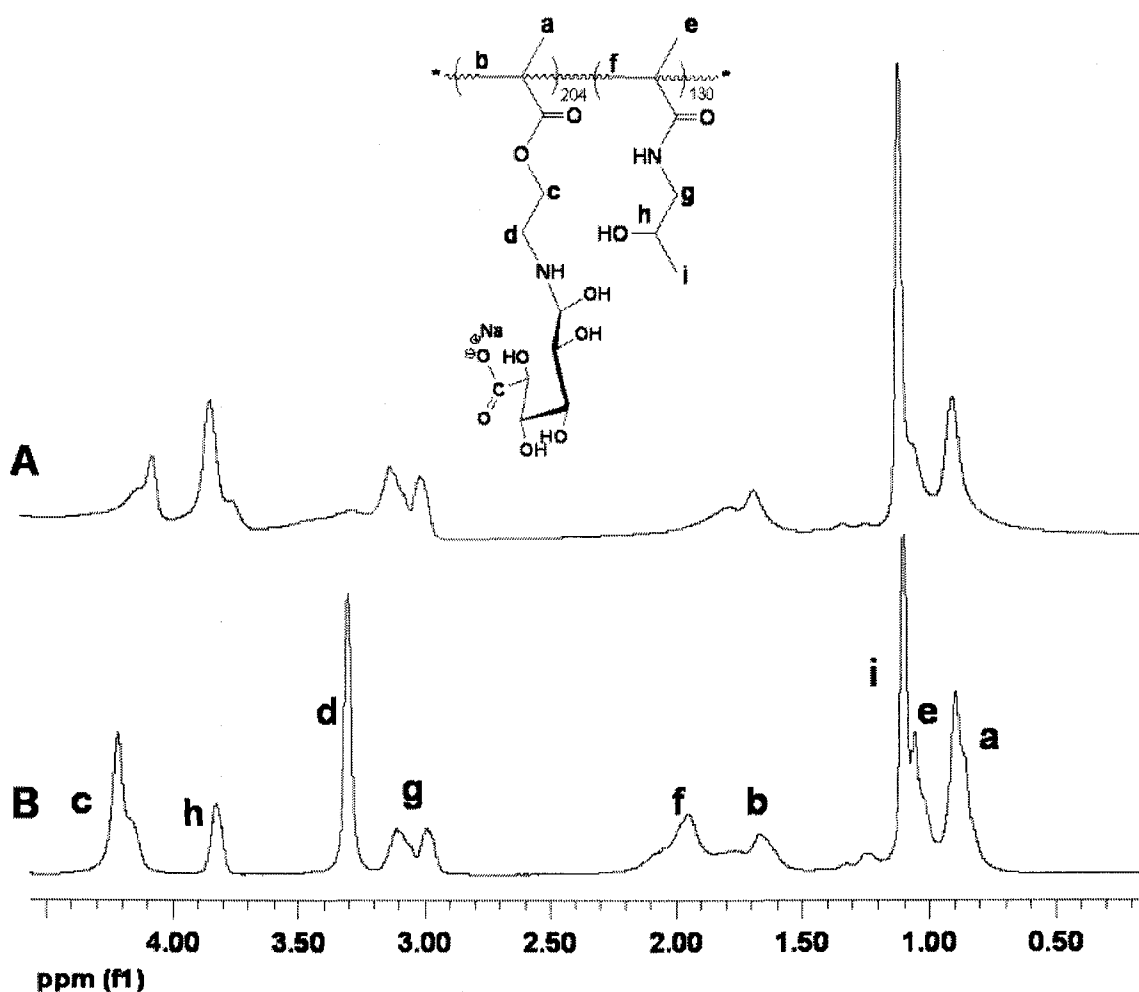


**Figure IV-11.**  $^1\text{H}$  NMR spectra of A. Bioconjugated PAEMA-*b*-PHPMA (**24**) with D-glucuronic acid sodium salt (**5**); B. PAEMA-*b*-PHPMA (**18**).

The mass distributions of PAEMA-*b*-PHPMA (**18**) and bioconjugated PAEMA-*b*-PHPMA (**24**) are shown in Figure IV-12. A molecular weight increase of 39392 was obtained, indicating 82% of the primary amine pendant groups were bioconjugated. The relatively low conversion is attributed to rearrangement reactions of the PAEMA (**16**), as discussed in the previous section.

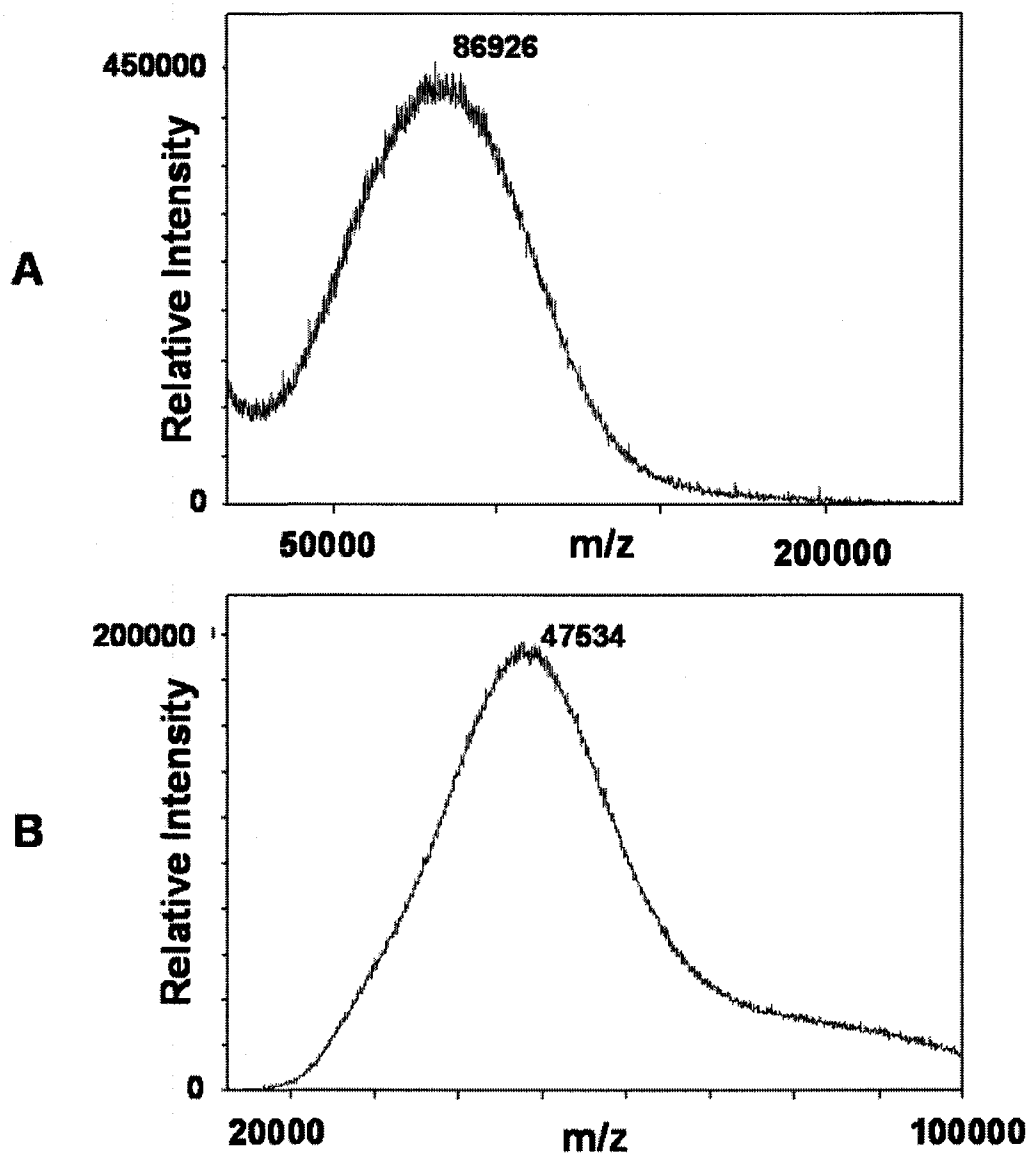


**Figure IV-12.** MALDI TOF mass spectra of A. PAEMA-*b*-PHPMA (**18**); B. Bioconjugated PAEMA-*b*-PHPMA (**24**) with D-glucuronic acid sodium salt (**5**).

## Conclusions

The synthesis of well-defined, carboxylic acid functionalized glycopolymers has been accomplished through high yield post-polymerization modification approaches. Specifically, APMA (**12**) monomer was homopolymerized directly in aqueous solution with PDIs below 1.1 through aqueous RAFT polymerization. The well-defined, narrowly dispersed PAPMA (**17**) was bioconjugated with D-glucuronic acid sodium salt (**5**) via a reductive amination reaction pathway in alkaline medium to obtain well-defined glycopolymers with near quantitative substitution.

In addition, the bioconjugation of PAEMA (**16**) and PAEMA-b-PHPMA (**18**) with D-glucuronic acid sodium salt (**5**) was demonstrated. Lower yields of bioconjugation were achieved, likely due to the degradation of PAEMA (**16**) under alkaline conditions at high temperature. The resulting glycopolymers appear to include inhomogeneous sequences within the chain.

Building on our earlier work and recent literature reports, we show for the first time well-defined carboxylic acid functionalized glycopolymers via one step, high-yield post-polymerization modification. PAPMA (**17**) is demonstrated to be a versatile primary amine functionalized polymer which readily undergoes reductive amination reactions with sugars with high yields. We believe that this study will enable new capabilities in the synthesis of controlled architecture glycopolymers with multiple functionalities for biomedical and pharmaceutical applications, without the need for stringent purification methods.



## CHAPTER V

SURFACE MODIFICATION OF  $\alpha$ -ALKYNYL-FUNCTIONALIZED POLY(2-AMINOETHYL METHACRYLATE) VIA “CLICK” CHEMISTRY TO PRODUCE PRIMARY AMINE FUNCTIONALIZED SURFACES

## Introduction

The recent development of controlled radical polymerization (CRP) techniques such as atom transfer radical polymerization (ATRP)<sup>63</sup> and reversible addition-fragmentation chain transfer polymerization (RAFT)<sup>64,65</sup> polymerization have provided a facile route to obtain telechelic polymers with predetermined molecular weight and narrow molecular weight distributions. Although CRP has been used for the polymerization of a wide range of monomers, post-polymerization modification is an important method that requires specific end group functionality that must be compatible with polymerization conditions.<sup>156,157</sup> Since the chain end functionality of CRP polymers is predetermined and easily controlled, there has been numerous reports on the preparation of fluorescently labeled chains, polymeric bioconjugates and surface-immobilized polymers.<sup>68,158-161</sup>

The Cu(I) catalyzed 1,3-dipolar cycloaddition reaction between azide and alkyne groups results in very stable 1,4-disubstituted 1,2,3-triazole products.<sup>165,166</sup> Due to its high thermodynamic driving force, this reaction can be performed in high yield under ambient conditions. This coupling process can be conducted in aqueous or organic media and is tolerable to various functional groups. Due to its simplicity and efficiency, the term “click” chemistry was given to this category of reactions by Sharpless and coworkers in 2001.<sup>162</sup>

In the literature, “Click” chemistry has been used extensively as a post-polymerization modification technique for functionalizing polymers prepared by CRP methods.<sup>167-187</sup> Given the telechelic nature of polymers prepared *via* CRP techniques, “click” chemistry is an attractive method for the functionalization of polymer chain ends. For example, Agut et al. prepared  $\alpha$ -azide and alkyne functionalized poly[2-(dimethylamino)ethyl methacrylate] (PDMAEMA) through ATRP using  $\alpha$ - $\omega$ -functionalized initiators for the preparation of hybrid diblock copolymers.<sup>183</sup> These blocks were composed of a polypeptide and poly[2-(dimethylamino)ethyl methacrylate] (PDMAEMA) block that were covalently linked utilizing “click” chemistry. Lutz et al. recently reported ATRP synthesized polymers that were  $\omega$ -chain end functionalized with azides.<sup>184</sup> These azide functional polymers were subsequently reacted with various alkyne functional compounds to prepare  $\omega$ -hydroxy,  $\omega$ -carboxyl and  $\omega$ -methyl-vinyl functionalized polystyrene. In addition, the combination of ATRP and “click” chemistry was employed by Sumerlin et al. to prepare well-defined  $\omega$ -(meth)acryloyloxy functionalized poly(*n*-butyl acrylate) and  $\omega$ -acryloyloxy functionalized polystyrene macromonomers.<sup>185</sup> Unlike ATRP, the use of “click” chemistry for the post-polymerization modification of RAFT synthesized polymers has been minimal. One such example was carried out by Hawker et al. who synthesized alkyne-functionalized block copolymers *via* RAFT polymerization.<sup>186</sup> An alkynyl-functionalized RAFT chain transfer agent (CTA) was directly used for the sequential polymerization of tetrahydropyran acrylate and styrene, followed by selective cleavage of the tetrahydropyran esters to give  $\alpha$ -alkynyl-functionalized block copolymers that are capable of forming surface-functionalized “clickable” micelles in aqueous solutions. Another example utilizing

RAFT polymers was performed by Sumerlin et al. who synthesized  $\alpha$ -azido terminal polymers using an  $\alpha$ -azido functionalized chain transfer agent (CTA) that allowed the preparation of a range of functional telechelics.<sup>187</sup>

“Click” chemistry has also been extensively used for the modification of surfaces with various polymers. Meldal et al. was the first to demonstrate that “click” chemistry can be used to modify solid substrates.<sup>153</sup> They succeeded in synthesizing diversely 1,4-substituted [1,2,3]-triazoles in peptide backbones or side chains upon using the combination of “click” chemistry and solid-phase peptide synthesis. Given the success of Medal and coworkers, other researchers began to explore the attachment of CRP polymers to various surfaces. For example, Brittain et al. reported the immobilization of an  $\alpha$ -alkyne functionalized polymer, prepared *via* RAFT polymerization, to azide functionalized silica nanoparticles *via* “click” chemistry.<sup>154</sup> The same group also demonstrated a “grafting from” approach by first attaching  $\alpha$ -alkynyl functionalized CTA to azide functionalized silica nanoparticles followed by RAFT surface polymerization of styrene and methyl methacrylate.<sup>155</sup> They achieved a grafting density of 1.2-1.3 RAFT agent/nm<sup>2</sup> for the immobilization of CTA onto silica nano particles, resulting in high density polymer brushes. Additionally, Drockenmuller et al. grafted  $\omega$ -azido functionalized polymers prepared through ATRP and nitroxide mediated radical polymerization (NMP) on alkynyl-functionalized silicon wafers using click chemistry.<sup>188</sup> Polymer brushes with a thickness of 6 nm and grafting densities of 0.2 chains/nm<sup>2</sup> were synthesized.

The use of primary amine-functionalized methacrylates are of interest for the potential utility in post-polymerization modification reactions, such as amide and imine formation, ring-opening reactions and Micheal addition reactions, enabling advances in areas that include new approaches for cross-linking micelles and hydrogels, synthesis of novel copolymers for biomimetic scaffold structures, and bioconjugation.<sup>39-49</sup> However, the controlled polymerization of 2-aminoethyl methacrylate (AEMA) (**6**) is challenging because it is susceptible to side reactions such as Micheal addition in alkaline medium.<sup>230</sup> Recent developments in RAFT polymerization provide a facile route for the controlled polymerization of AEMA (**6**) without using protecting group chemistry. Our research group recently reported the aqueous RAFT polymerization of AEMA (**6**) yielding near monodisperse homopolymers.<sup>228</sup>

Herein, we report the direct synthesis of  $\alpha$ -alkynyl functionalized PAEMA (**26**) through RAFT polymerization yielding near monodisperse homopolymers. In addition, the successful surface attachment of  $\alpha$ -alkynyl functionalized PAEMA (**26**) on azide functionalized silicon wafers was achieved through “click” chemistry using the “grafting to” approach. PAEMA (**6**) modified surfaces were characterized through ellipsometry, contact angle measurements, attenuated total reflectance-Fourier transform infrared spectroscopy (ATR-IR), and atomic force microscopy (AFM).

## Experimental

*Materials.* All reagents were used without further purification unless otherwise noted. Methacryloyl chloride (>97%), propargyl alcohol (99%), 3-bromopropyltrichlorosilane (96%), anhydrous toluene, copper sulfate, azidotrimethylsilane ( $\text{Si}(\text{CH}_3)_3\text{N}_3$ ) (95%), sodium ascorbate (>98%) ethanolamine (>98%) and hydroquinone (99%) were purchased from Aldrich. 4-Dimethylamino-pyridine (99%) (DMAP) and *N,N'*-dicyclohexyl-carbodiimide (99%) (DCC) were purchased from Acros Organics. Phenylmagnesium bromide solution (3M in diethyl ether) was purchased from Fluka. Dimethylsulfoxide (DMSO), 30% hydrogen peroxide ( $\text{H}_2\text{O}_2$ ), sulfuric acid ( $\text{H}_2\text{SO}_4$ ), diethylether, ethylacetate, hexane, and hydrochloric acid were purchased from Fisher. 2,2'-Azobis(2,4-dimethyl-4-methoxyvaleronitrile) (V-70) (**27**) was purchased from Wako Pure Products and recrystallized from methanol. Silicon wafers were purchased from Silicon Inc., and cut into 1 x 2 cm pieces using a diamond-tipped glass cutter. 4-Cyanodithiobenzoic acid (CTP) (**14**) was synthesized according to literature procedure.<sup>145</sup> 2-Aminoethyl methacrylate (AEMA) (**6**) was synthesized using a previously reported procedure.<sup>54</sup>  $\alpha$ -Alkynyl-Functionalized CTP (**25**) was synthesized according to literature procedure.<sup>231</sup>

*Preparation of  $\alpha$ -Alkynyl-Functionalized PAEMA (**26**).*  $\alpha$ -Alkynyl-functionalized PAEMA (**26**) was prepared *via* RAFT polymerization. The RAFT polymerization of AEMA (**6**) was conducted at 45 °C using V-70 (**27**) as the radical initiator and  $\alpha$ -alkynyl-functionalized CTP (**25**) as the RAFT chain transfer agent (CTA). An initial monomer concentration ( $[\text{M}]_0$ ) of 1 M was used with a monomer to CTA ratio ( $[\text{M}]_0/[\text{CTA}]_0$ ) of 400. The CTA to initiator ratio ( $[\text{CTA}]_0/[\text{I}]_0$ ) was 10:1. A typical procedure is as follows:

in a 30 ml round bottom flask,  $\alpha$ -alkynyl functionalized CTP (**25**) (23.8 mg, 0.075 mmol), AEMA (**6**) (4.952 g, 30.0 mmol) and V-70 (**27**) (2.31 mg, 0.0075 mmol) were dissolved in 30 ml of DMSO. The flask was sealed with a rubber septum and purged with nitrogen for 30 min at 5 °C, and placed in a 45 °C water bath. The polymerization was allowed to proceed for various time intervals before being quenched by rapid cooling in liquid nitrogen. The  $\alpha$ -alkynyl-functionalized PAEMA (**26**) was purified by dialysis against deionized water followed by lyophilization.

*Purification of Silicon Wafers.* Silicon wafers were cleaned using piranha solution (30:70 v/v solution of 30% hydrogen peroxide and concentrated sulfuric acid). The solution was heated for 2 h at 100 °C. *Caution: piranha solution is extremely caustic.* Wafers were cleaned in HPLC water, ethanol and acetone sequentially, characterized through ellipsometry, water contact angle, and atomic force microscopy (AFM), and used immediately for subsequent modification.

*Deposition of 3-Bromopropyltrichlorosilane on Silicon Wafers.* Cleaned wafers were placed in clean, dry glass tubes (in glove box) containing 20 mL of anhydrous toluene. 3-Bromopropyltrichlorosilane (0.2 ml, 1 wt %) was directly added *via* syringe, and the tubes were sealed. Wafers were removed after 45 minutes and sequentially cleaned with toluene, ethanol, and acetone and dried in a stream of air.

*Synthesis of Azide Modified Silicon Wafers.* The azide modified silicon wafer was prepared by the substitution of a bromo-terminated monolayer with azidotrimethylsilane ( $\text{Si}(\text{CH}_3)_3\text{N}_3$ ). The bromo-functionalized silicon wafer was placed in clean, dry glass tubes (in glove box) containing 20 mL of anhydrous toluene.  $\text{Si}(\text{CH}_3)_3\text{N}_3$  (0.4 ml, 2%) was added directly into the toluene by a syringe and the tubes were sealed. The reaction

was heated at 80 °C for 48 hours. The substrate was removed and rinsed with toluene, ethanol, and acetone and dried in a stream of air.

*Click Coupling between PAEMA (16) and Azide Modified Silicon Wafers.* A previously published procedure for the modification silica nanoparticles through “click” chemistry was implemented.<sup>187</sup> A large excess of PAEMA (16) (0.5 g, 0.017), 0.005 g (0.031 mmol) of CuSO<sub>4</sub>, 0.015 g (0.75 mmol) of sodium ascorbate and 20 mL of DMSO were combined in a round-bottomed flask and stirred until the  $\alpha$ -alkynyl functionalized PAEMA (16) was dissolved. The azide modified silicon wafer was placed in the flask. The mixture was heated in an oil bath at 80 °C for 2 days. Following the reaction, the silicon wafer was placed in a Soxhlet extractor and extracted with water for 18 h.

*Polymer and Surface Characterization.*  $\alpha$ -alkynyl functionalized PAEMA (26) was characterized by aqueous size exclusion chromatography (ASEC-MALLS) at ambient temperature using Eprogen CATSEC columns (100, 300, and 1000 °Å). A Wyatt Optilab DSP interferometric refractometer ( $\lambda = 690$  nm) and a Wyatt DAWN DSP multiangle laser light scattering detector ( $\lambda = 633$  nm) were employed using 1 wt % acetic acid/0.1 M Na<sub>2</sub>SO<sub>4</sub> (aq) solution as the eluent at a flow rate of 0.25 ml/min. Conversions in each system were determined by comparing the area of the UV signal corresponding to monomer at  $t_0$  to the area at  $t_x$ . Absolute molecular weights and polydispersities were calculated using the Wyatt ASTRA SEC/LS software package.

A Varian 500 MHz NMR equipped with a standard 5 mm <sup>1</sup>H/<sup>13</sup>C probe was utilized to identify the homopolymer structure of  $\alpha$ -alkynyl functionalized PAEMA (26) (nt = 64, d1 = 3.1  $\mu$ s, pw90 = 16  $\mu$ s, at = 1.89  $\mu$ s). The degree of polymerization and molecular weight were determined *via* <sup>1</sup>H NMR through integration of the relative

intensities of the  $\alpha$ -alkynyl functionalized PAEMA (**26**) methylene-proton resonances at 3.31 ppm and phenyl-protons of CTP (**14**) between 7.51 and 7.89 ppm.

Ellipsometric measurements were carried out on a Gaertner ellipsometer, model L116C, with a 632.8 nm heliumneon laser at a  $70^\circ$  angle of incidence. Refractive indices were fixed at 1.455 for all respective surface modifications. Contact angle measurements were performed utilizing a Rame-Hart goniometer with a 10.0  $\mu\text{l}$  syringe. Static ( $\theta_a$ ) water contact angles were recorded at  $0^\circ$  from horizontal. Five measurements were taken across each sample, with their average being used for analysis. Attenuated total reflectance Fourier transform infrared (ATR FTIR) spectra were collected using a Bio-Rad FTS- 6000 FT-IR single beam spectrometer set at a  $4\text{ cm}^{-1}$  resolution equipped with a deuterated triglycine sulfate (DTGS) detector and a  $45^\circ$  face angle Ge crystal. Each spectrum represents 400 co-added scans ratioed against a reference spectrum obtained by recording 400 co-added scans of an empty ATR cell. All spectra were corrected for spectral distortions using Q-ATR software.<sup>232</sup>

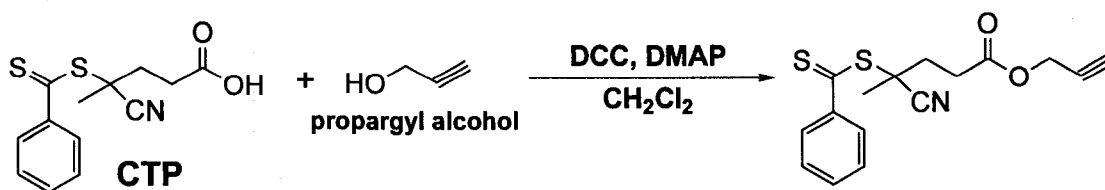
Tapping mode atomic force microscopy (AFM) measurements were performed with an Agilent 5500 PicoPlus microscope (Agilent Technologies Inc., Santa Clara, CA, USA). Experiments were conducted at room temperature in the presence of air (20–25  $^\circ\text{C}$ ). Images were taken with 1 and 5  $\mu\text{m}^2$  scan areas. Standard phosphorous doped silicon cantilevers (RTESPW cantilevers, Veeco Probe Center, Santa Barbara, CA, USA), with a nominal spring constant of 20-80 N/m and a typical radius of curvature  $\leq 10\text{ nm}$ , were used as received. The scan rate was 0.7 Hz, and as an additional precaution to eliminate artifacts, images were obtained from at least three macroscopically separated areas of each sample. All images were processed using PicoView 1.4 AFM software and the



Gwyddion 2.7 SPM data analysis framework. All experiments were performed at  $22 \pm 1$  °C unless specified otherwise. Surface roughness analysis was performed Nanoscope version 5.30 r2 image analysis software. To verify the reproducibility, two sets of readings were taken for each sample and an average value is reported. The difference between the two readings was less than 1%.

## Results and Discussion

*Preparation of  $\alpha$ -Alkynyl-Functionalized PAEMA (26).* By virtue of the accepted mechanism for RAFT-mediated polymerization, the degenerative chain transfer process that involves a CTA allows one to prepare polymers that carry the respective Z and R groups at the  $\alpha, \omega$ -termini of the polymer chains.<sup>233</sup> Thus, by synthetically modifying the R group of the CTA, a variety of end-functionalized polymers can be obtained. Due to its carboxylic acid functionality, CTP (**14**) has been widely used for modifying the R group yielding various functionalized CTAs.<sup>234</sup> In this work, we prepared  $\alpha$ -alkynyl-functionalized CTP (**25**) by the conversion of the terminal carboxyl group of CTP (**14**) to an alkyne group *via* DCC/DMAP-mediated esterification with propargyl alcohol (70% yield) (Scheme V-1). The product structure was confirmed by <sup>1</sup>H NMR as shown in Figure V-1 confirming the attachment of propargyl alcohol to CTP (**14**).



**Scheme V-1.** Preparation  $\alpha$ -alkynyl-functionalized CTP (**25**).

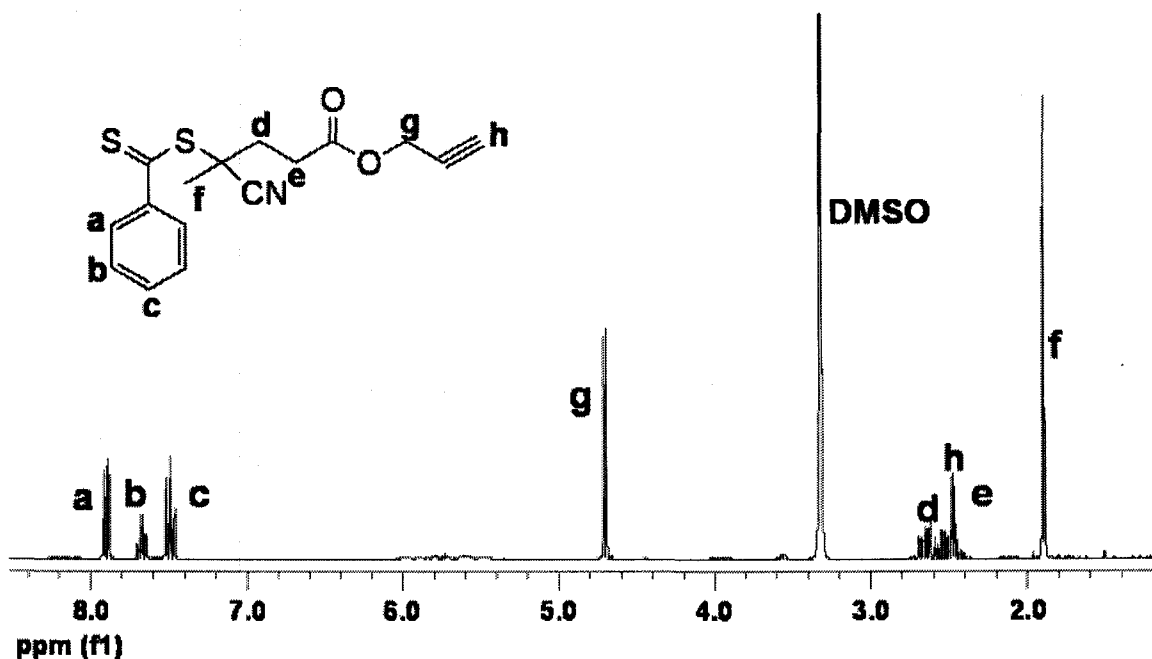
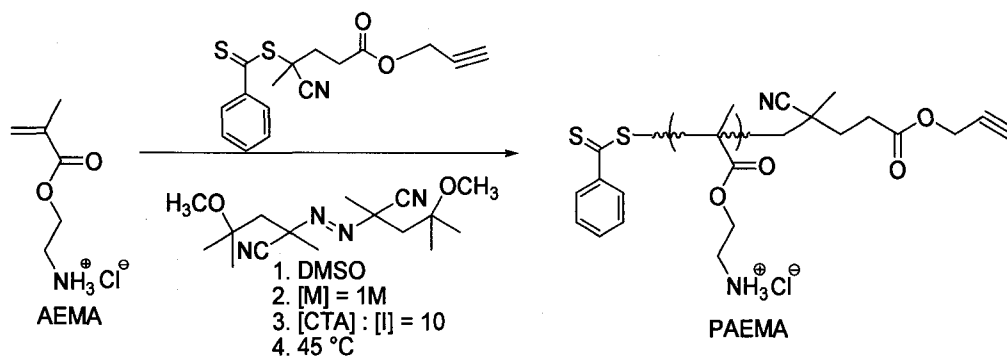
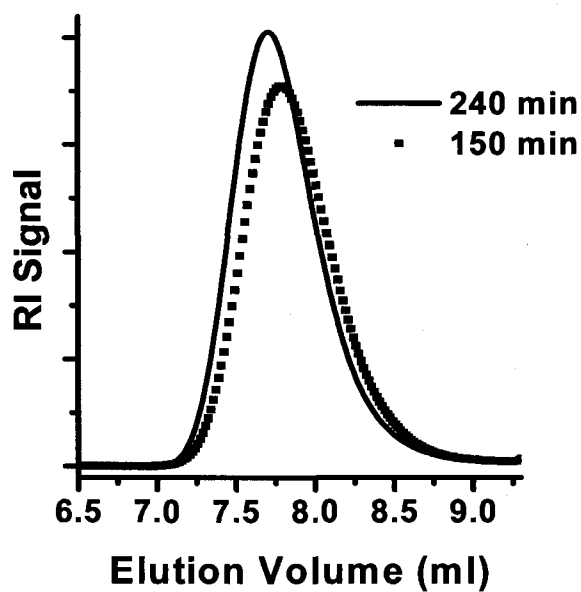


Figure V-1.  $^1\text{H}$  NMR spectrum of  $\alpha$ -alkynyl functionalized PAEMA (**26**).

CTP (**14**) was chosen based on results reported by our research group for the synthesis of well-defined, narrowly dispersed homopolymer and diblock copolymers of AEMA (**6**) *via* aqueous RAFT polymerization. Specifically, AEMA (**6**) monomer was homopolymerized directly in aqueous solution at 50 °C with PDIs below 1.2 and conversions up to 95%. We also determined that the controlled polymerization of AEMA (**6**) depends on polymerization temperature. AEMA (**6**) polymerization performed at 70 °C resulted in loss of CTP (**14**) within 45 minutes leading to an increase in polydispersity. Our results suggested that the relatively high PDI's reported by previous groups<sup>67</sup> are due to the high polymerization temperature, which results in various side reactions that lead to broadened molecular weight distributions.



**Scheme V-2.** Preparation  $\alpha$ -alkynyl-functionalized PAEMA (**26**) via RAFT polymerization at 45 °C.



**Figure V-2.** ASEC chromatograms for  $\alpha$ -alkynyl functionalized PAEMA (**26**) prepared at 45 °C in DMSO.

**Table V-1.** Preparation of  $\alpha$ -Alkynyl-Functionalized PAEMA (**26**) at 45 °C.

Time (min)	$M_n^1$	$M_n^2$	$M_n^3$	PDI <sup>1</sup>	Conv. <sup>1</sup> (%)
150	29000	27000	26000	1.12	42
240	35000	32000	33000	1.13	50

1. Calculated by ASEC-MALLS.

2. Calculated through <sup>1</sup>H NMR.

3. Theoretical molecular weight.

4. [M]:[CTA]:[I] = 400:1:0.1

Regarding the above issues, AEMA (**6**) polymerizations were carried out at 45 °C using V-70 (**27**) as the radical source and  $\alpha$ -alkynyl-functionalized (**25**) as the CTA in DMSO (Scheme V-2). For the polymerizations, an initial ratio of [M]<sub>0</sub> to [CTA]<sub>0</sub> of 400/1 and a [CTA]<sub>0</sub>/[I]<sub>0</sub> ratio of 10/1 were used. Molecular weights, polydispersities and conversion data are shown in Table V-1. ASEC-MALLS traces show unimodal distribution with PDIs below 1.2 and are free from high molecular weight termination products (Figure V-2). In addition, the degree of polymerization and thus the molecular weight were determined *via* <sup>1</sup>H NMR through integration of the relative intensities of methylene-protons resonance at 3.31 ppm and phenyl-protons of CTP (**14**) between 7.51 and 7.89 ppm (Figure V-3). The measured molecular weights by ASEC are in close agreement with the theoretical molecular weights and the molecular weights calculated through <sup>1</sup>H NMR. The existence of the alkyne group at the end of PAEMA (**16**) chains was evidenced *via* <sup>1</sup>H NMR, which displays a peak at 2.85 ppm (Figure V-3).

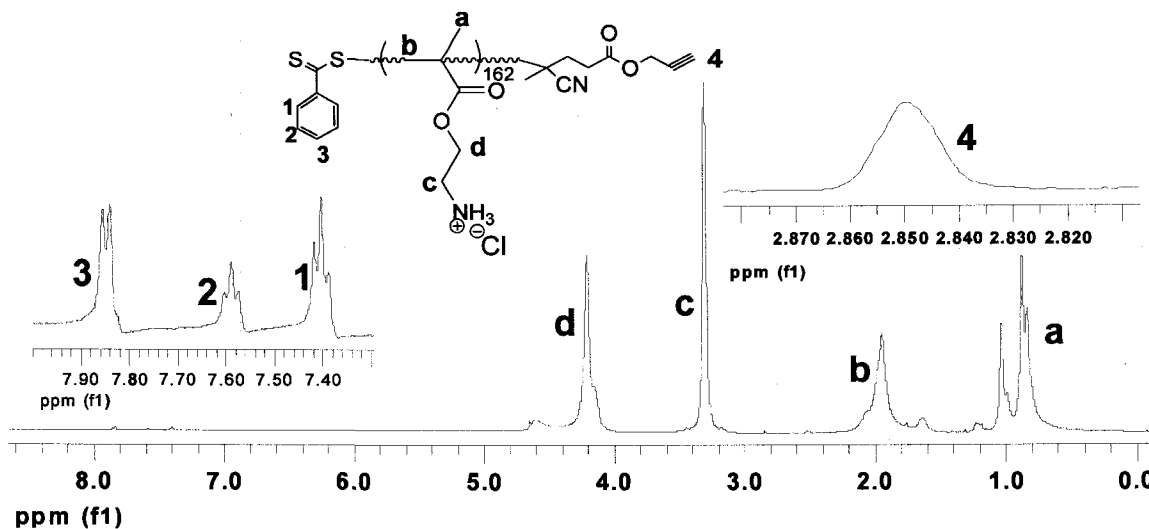


**Figure V-3.**  $^1\text{H}$  NMR spectrum of  $\alpha$ -alkynyl functionalized PAEMA (**26**).

**Table V-2.** Preparation of  $\alpha$ -Alkynyl-Functionalized PAEMA (**26**) at 45 °C.

<i>Samples</i>	Surface Thickness <sup>1</sup> (nm)	Static Contact Angle <sup>2</sup> (°)	RMS Surface Rroughness <sup>3</sup> (nm)
<i>Neat Silicon Wafer (SW)</i>	2.1 ± 0.06	22 ± 0.3	0.02
<i>Bromide Functionalized SW</i>	6.3 ± 0.4	77 ± 0.4	0.60
<i>Azide Functionalized SW</i>	6.5 ± 0.4	80 ± 0.3	0.70
<i>Polymer Modified SW</i>	17.1 ± 2.7	55 ± 0.3	9.10

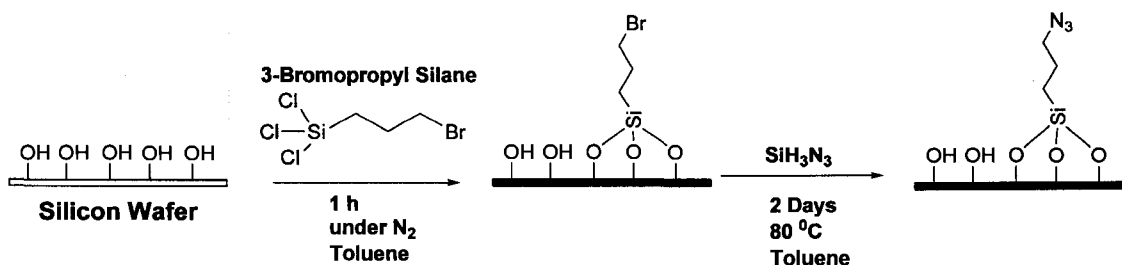
1. Calculated through ellipsometry.

2. Calculated through goniometer.

3. Calculated through AFM.

*Azide Modification of Silicon Wafers.* Silicon wafers were functionalized with azide groups using a two step reaction procedure (Scheme V-3). In the first step, 3-bromotrichlorosilane was used to introduce a bromide group on the surface of the silicon wafer. Confirmation of the deposition of 3-bromotrichlorosilane was achieved by ellipsometry (Table V-2), contact angle goniometer (Table V-2), and AFM (Table V-2)

and Figure V-4). Ellipsometry data for bromide modified silicon wafer showed a thickness change of 4 nm. This thickness indicates that multilayers were obtained, which may be due to the extended reaction time or the trichlorosilane anchoring group having a tendency to undergo some degree of surface cross-linking.<sup>235</sup> The resulting bromide functionalized silicon wafer was observed to have a contact angle of 77°, which is close to previously reported values.<sup>236</sup> Tapping mode AFM images of neat silicon wafer and bromide modified silicon wafer are shown in Figure V-4A and Figure V-4B. The neat silicon wafer displays a smooth surface topography with root mean square (RMS) roughness value of 0.02 nm (Table V-2). Although a morphology change is observed for the bromide modified silicon wafer surface, the appearance of large bright spots indicate a high surface thickness, which may be attributed to dust or multilayer formation on the silicon wafer surface (Figure V-4B).



**Scheme V-3.** Synthesis of Azide modified silicon wafer.

It was attempted to convert the bromide functionality to azide through reaction with  $\text{Si}(\text{CH}_3)_3\text{N}_3$ . In general, this substitution reaction is conducted by using sodium azide. However, we found that the limited solubility of sodium azide in DMF, giving a heterogeneous solution, leads to a low yield of substitution on the wafers. For this

reason,  $\text{Si}(\text{CH}_3)_3\text{N}_3$  was used for the substitution reaction, which gives a homogeneous solution in toluene. Surfaces were analyzed through ellipsometry (Table V-2), goniometer (Table V-2), and AFM (Table V-2 and Figure V-4). As expected, there is virtually no change in thickness, contact angle or RMS roughness after azide substitution. However, AFM images indicated unexpected changes in the morphology of the azide functionalized silicon wafer in the comparison to the bromide functionalized silicon wafer, that are not easily explained. To verify substitution, XPS (x-ray photoelectron spectroscopy) and further AFM studies should be performed.

*Click” reaction between azide functionalized silicon wafer and  $\alpha$ -alkynyl-functionalized PAEMA (26).* The Cu(I)-catalyzed reaction of the Huisgen 1,3-dipolar cycloaddition of azides and alkynes to afford 1,2,3-triazoles (Scheme V-4) is commonly referred to as a “click” reaction..<sup>237</sup> Although 1,3-dipolar cycloaddition reactions are often performed in water for faster reaction times, the reaction was conducted directly in DMSO to avoid any possible rearrangement reactions of PAEMA (16) at high temperatures. The grafting of  $\alpha$ -alkynyl-functionalized PAEMA (16) on azide functionalized silicon wafer was evaluated through ellipsometry (Table V-2), goniometer (Table V-2), ATR-FTIR (Figure V-5) and AFM (Table V-2 and Figure V-3).

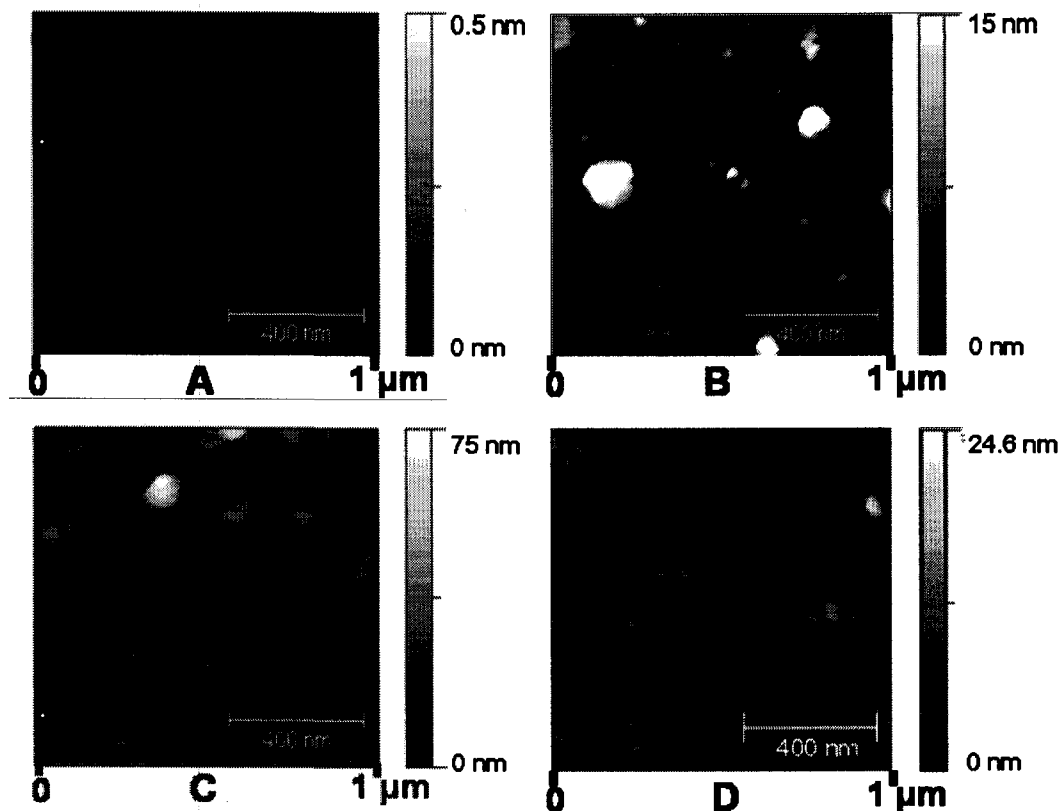
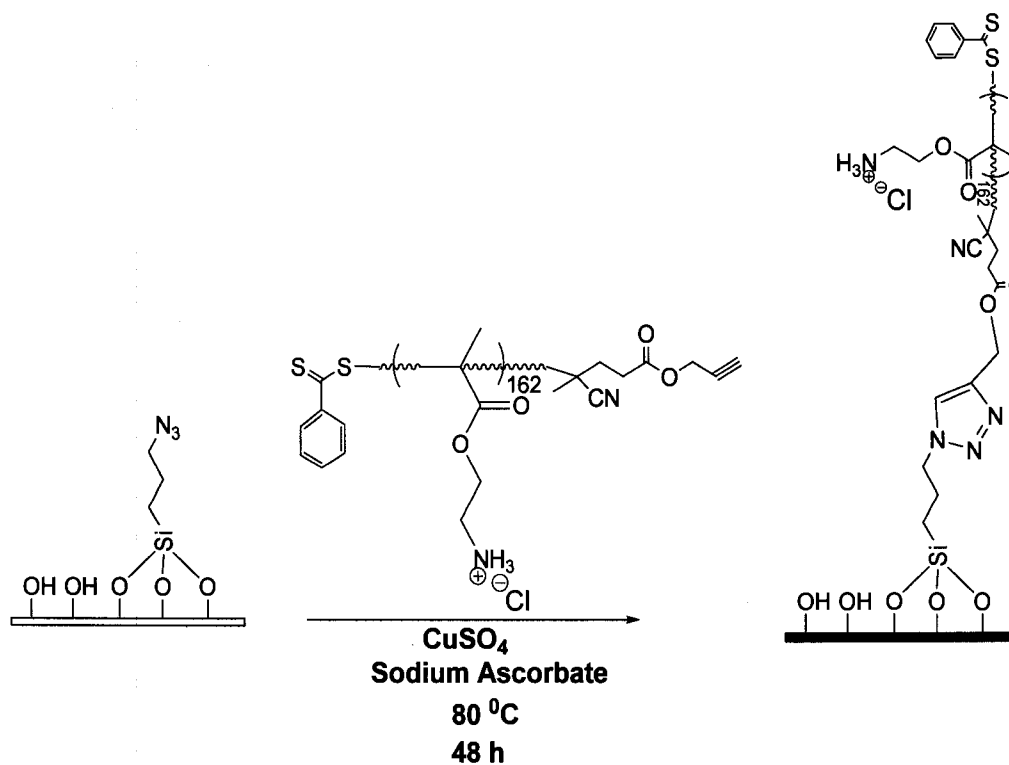


**Figure V-4.** Tapping mode AFM images of A. Neat silicon wafer; B. Bromide functionalized silicon wafer; C. Azide functionalized silicon wafer; D. PAEMA (**26**) modified silicon wafer.

The successful modification is evidenced by the appearance of a carbonyl peak at  $1720\text{ cm}^{-1}$ , associated with the carbonyl stretch, indicating the existence of the ester group of  $\alpha$ -alkynyl-functionalized PAEMA (**26**). Ellipsometry demonstrated a surface thickness increase of 11.1 nm. Water contact angle measurements of  $\alpha$ -alkynyl-functionalized PAEMA (**26**) modified silicon wafer showed a static contact angle of  $55^\circ$  which indicates a decrease of  $25^\circ$  in contact angle when compared to azide functionalized silicon wafers (Table V-2). The tapping mode AFM image of  $\alpha$ -alkynyl-functionalized PAEMA (**26**) modified silicon wafer shows granular features with an increase of surface RMS roughness to 9.10 nm (Figure V-4D). Furthermore, three dimensional (3D) surface



topography images of neat silicon wafers and  $\alpha$ -alkynyl-functionalized PAEMA (**26**) modified silicon wafer are shown in Figure V-6. A clear surface topography change is observed, indicating the successful surface modification of  $\alpha$ -alkynyl-functionalized PAEMA (**26**) via “click” chemistry. However, 3D surface topography of  $\alpha$ -alkynyl-functionalized PAEMA (**26**) modified silicon wafers demonstrates a non-uniform tethered polymer layer.



**Scheme V-4.** Surface attachment of  $\alpha$ -alkynyl-functionalized poly(AEMA) (**26**) on azide functionalized silicon wafer through click chemistry.

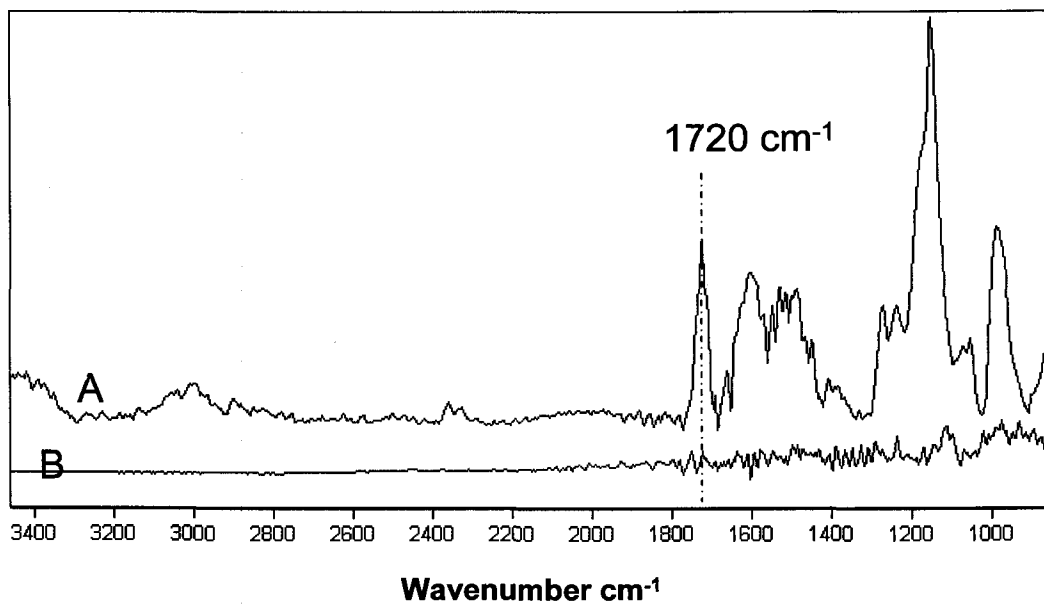


**Figure V-5.** ATR-FTIR spectra of A. PAEMA (6) modified silicon wafer; B. Neat silicon wafer.

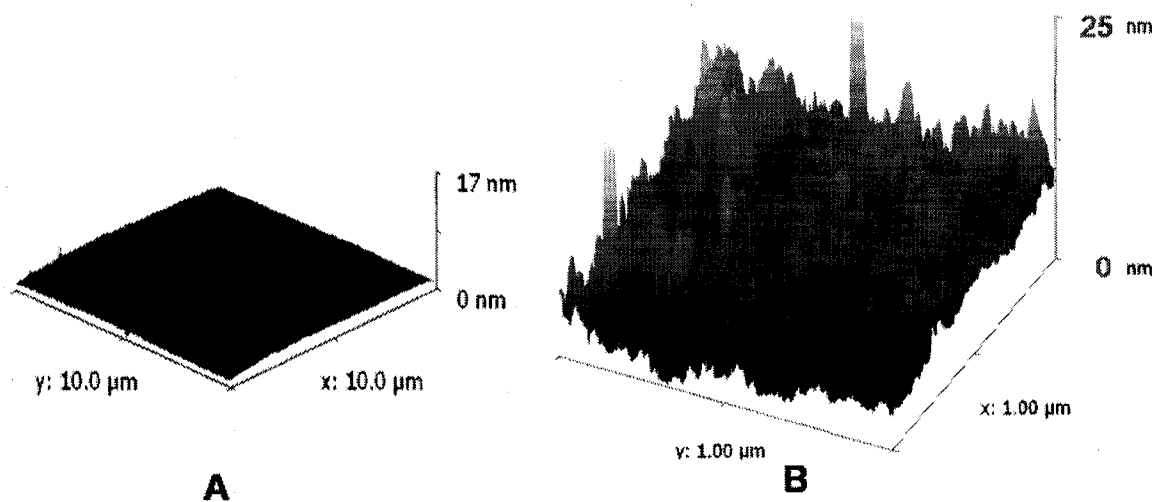


**Figure V-6.** 3D surface topography of A. Neat silicon wafer; B. PAEMA (16) modified silicon wafer.

This may be related to the “grafting to” approach. Even though this approach is experimentally simple and functionalized polymers are synthesized in solution providing better control, it usually suffers from a lower grafting density because of the steric hindrance imposed by grafted chains. This may result in non-uniform polymer layers on silicon wafers. However, Brittain’s research group has recently reported that a relatively high grafting density, comparable with the “grafting from” approach, was obtained via a “click” reaction, indicating the efficiency of surface modification through “click” chemistry.<sup>112</sup> To understand our coupling efficiency on the silicon wafer, an estimated grafting density ( $\sigma$ ) can be calculated through the following equation (1);

$$\sigma = \Gamma N_A \times 10^{-21} / M = (6.023 \Gamma \times 100) / M_n \quad (1)$$

where  $\Gamma$  is the surface coverage (absorbed amount,  $\text{mg}/\text{m}^2$ ),  $M$  ( $\text{g}/\text{mol}$ ) is the molar mass of the attached molecule and  $N_A$  is Avogadro’s number.  $\Gamma$  is calculated according to equation (2);

$$\Gamma = h\rho \quad (2)$$

where  $\rho$  is the bulk density of the attached molecule ( $\text{g}/\text{cm}^3$ ) and  $h$  is thickness of the tethered polymer layer calculated through ellipsometry. A grafting density of 0.39 chains/ $\text{nm}^2$  was obtained. This grafting density is relatively high for a “grafting to” approach. However, Brittain and coworkers performed the same technique with different polymers for the modification of silica nanoparticles and estimated a similar grafting density value. This high grafting density was attributed to the excellent efficiency of “click” chemistry.<sup>187</sup> It should be noted that an average thickness is utilized in the calculation, and the AFM analysis indicates variable thickness of the polymer layer.

## Conclusions

In this chapter, we report the synthesis of well-defined, narrowly dispersed  $\alpha$ -alkynyl-functionalized homopolymer of AEMA (**6**) via RAFT polymerization. Specifically, AEMA (**6**) monomer has been homopolymerized directly in DMSO with PDIs below 1.2 using  $\alpha$ -alkynyl CTP (**25**) as the CTA. The resulting  $\alpha$ -alkynyl-functionalized PAEMA (**26**) was also tethered to azide functionalized silicon wafers through a “grafting to” method using a “click” chemistry approach to produce a well-defined primary amine functionalized surface. The successful surface modification is evidenced through ellipsometry, water contact angle, ATR-FTIR and AFM analysis. An estimated grafting density of  $0.39 \text{ chains.nm}^{-2}$  is calculated, indicating an excellent grafting density for “grafting to” method. However, 3D AFM surface topography image demonstrates a non-uniform surface feature. This may be related to “grafting to” approach. Since primary amine groups are amenable to a wide range of post-polymerization chemistries, such as rapid formation of amides and imines, ring-opening of epoxy groups and Micheal addition, we believe that this study will enable developments in surface modification of bio-related materials such as sugars, carbohydrates, peptides and proteins to study bio-lubricity, surface drug-delivery, and protein-carbohydrate interactions. Further research in bio-functionalization of these PAEMA (**16**) modified surfaces is underway.

CHAPTER VI  
COPOLYMERIZATION OF SEC-BUTENYL ACETATE WITH STYRENE VIA  
EMULSION POLYMERIZATION

Introduction

Allylic monomers typically exhibit chain transfer to monomer via facile hydrogen atom abstraction from the allylic methylene group during free radical homopolymerization, resulting in a dead chain and stable allylic radicals.<sup>238,239,240,241</sup> The degradative chain transfer effects a slow homopolymerization rate and a diminished average kinetic chain length.<sup>242,243,244,245</sup> Moreover, the overall degree of polymerization (DP) is reduced because of the allylic radical's characteristic slow homopolymerization and re-initiation rates.<sup>246,247</sup> Despite these restrictions, allylic monomers are commonly used in thermosetting resins.<sup>248,249,250,251</sup> They are used at low levels in free-radical copolymerizations to improve chemical, electrical, and storage properties of polymers,<sup>252,253</sup> and in emulsion copolymerizations for coatings and adhesive applications.<sup>254</sup> The copolymerization behavior of allylic acetate with a variety of vinyl monomers has been reported.<sup>255</sup> Shigetomi et al. studied the copolymerization behavior of various allyl esters, such as allyl propionate, allyl butyrate, allyl isobutyrate, allyl valerate and allyl trimethylacetate, with vinyl acetate, and determined reactivity ratios using the Kelen-Tudos method.<sup>256</sup> The reactivity ratios of comonomers reported were: allyl propionate (M<sub>1</sub>)-vinyl acetate (M<sub>2</sub>): ( $r_1 = 0.42$  and  $r_2 = 1.29$ ), allyl butyrate (M<sub>1</sub>)-vinyl acetate (M<sub>2</sub>): ( $r_1 = 0.64$  and  $r_2 = 0.97$ ), allyl isobutyrate (M<sub>1</sub>)-vinyl acetate (M<sub>2</sub>): ( $r_1 = 0.51$  and  $r_2 = 1.04$ ), allyl valerate (M<sub>1</sub>)-vinyl acetate (M<sub>2</sub>): ( $r_1 = 0.58$  and  $r_2 = 1.07$ ) and allyl butyrate (M<sub>1</sub>)-vinyl acetate (M<sub>2</sub>): ( $r_1 = 0.34$  and  $r_2 = 1.15$ ). The relatively low

reactivity ratios for the allyl monomers in comparison with those for the comonomers in each pair indicate the allyl monomer's reduced tendency to incorporate into the polymer chain. The authors also reported that as the feed ratio of allyl esters increases, molecular weight and reaction rate decrease. McDonald et al. studied the free radical copolymerization of allyl acetate with methyl methacrylate, n-butyl acrylate and styrene **(15)**, and determined reactivity ratios from dyad fractions determined by proton ( $^1\text{H}$ ) and carbon ( $^{13}\text{C}$ ) NMR spectroscopy.<sup>257</sup> The comonomer reactivity ratios reported were: allylic acetate ( $\text{M}_1$ )-methyl methacrylate ( $\text{M}_2$ ): ( $r_1 = 0.024$  and  $r_2 = 41$ ), allylic acetate ( $\text{M}_1$ )-n-butyl acrylate ( $\text{M}_2$ ): ( $r_1 = 0.04$  and  $r_2 = 11.7$ ) and allylic acetate ( $\text{M}_1$ )-styrene **(15)** ( $\text{M}_2$ ): ( $r_1 = 0.021$  and  $r_2 = 66$ ). The very large difference in reactivity ratios for allylic acetate in comparison to those of styrene **(15)** and acrylate comonomers indicates the low reactivity of allylic acetate with itself and its low propensity to incorporate in the copolymer due to the production of a stable allylic radical after allylic hydrogen abstraction.<sup>246,247</sup> Pomery et al. studied free radical bulk polymerization of methyl methacrylate and allyl acetate using electron spin resonance and Fourier transform near infrared spectroscopy.<sup>258,259</sup> It was reported that allylic acetate delays the Trommsdorff effect and increases the percentage of total conversion at which the onset of the Trommsdorff effect occurs. Moreover, allylic acetate dominates the copolymerization behavior by altering the molecular weight distribution as well as the glass transition temperature.

Emulsion polymerization is employed in the production of a wide range of specialty polymers including adhesives, coatings, binders for nonwoven fabrics, additives for paper, textiles and construction materials, impact modifiers for plastic matrices and polymeric drug-delivery systems.<sup>260,261,262,263,264,265,266,267,268,269,270</sup> Incorporation of a comonomer is commonly desirable to obtain specific polymer properties. In a batch emulsion copolymerization, the comonomers are added at a given ratio at the start of the reaction. Incorporation of the comonomers into the polymer is governed by the reactivity ratios, the relative solubility and the partitioning of the monomers into the aqueous and organic phases. Differences in reactivity ratios and partitioning result in compositional drift during copolymerization and chemically heterogeneous copolymers.<sup>271</sup> Semicontinuous emulsion polymerization offers a way to control compositional drift, and also provides greater control of particle size distribution.<sup>272</sup> Addition strategies used in semicontinuous emulsion polymerization include the constant addition of a given monomer mixture at a rate lower than the polymerization rate (starved conditions), and the addition of monomers at rates higher than the polymerization rate (flood conditions).<sup>273,274,275</sup> In starved conditions, the consumption rate generally is equal to the feeding rate, so the copolymer composition is equal to the monomer feed ratio at any given time.<sup>276</sup> For systems in which at least one of the monomers has a relatively high water solubility, the situation is more complex.<sup>276</sup> In this case, some of the monomer is present in the aqueous phase and not in the polymer particle where polymerization takes place.<sup>277</sup> Thus, the comonomer ratio and monomer concentration are affected, which influence the copolymer composition. In these systems it is important to control the

monomer to water ratio in addition to the monomer feed ratio to achieve the desired copolymer composition.<sup>276</sup>

The allylic monomer sec-butenyl acetate **(28)** (SBA, **Scheme VI-1**) is produced as a by-product of a recently reported direct addition process for production of butyl acetate,<sup>278</sup> and thus has potential availability as a low-cost comonomer and polymerization additive. Gaylord et al. studied the homopolymerization behavior of SBA **(28)** in bulk.<sup>279,280</sup> They report an average DP of 2.8, with a high degree of effective chain transfer in addition to degradative chain transfer. The SBA **(28)** oligomers produced displayed on average one double bond for every three SBA **(28)** repeat units, indicating that the relatively stable radical produced via hydrogen abstraction from the SBA **(28)** monomer was able to react with the double bond of a second SBA **(28)** monomer. The authors suggest that the SBA **(28)**, due to the electron donating nature of the methyl substituent on the allylic carbon, exhibits higher levels of hydrogen abstraction in comparison to the unsubstituted allyl acetate. However, the resulting radical is more reactive in the substituted form due to differences in the resonance stabilized structures of the radicals. These results indicate that SBA **(28)** is an effective chain transfer agent with potential for use in copolymerization reactions to control molecular weight and produce copolymers of desired composition.

To our knowledge, the copolymerization behavior of SBA **(28)** has not been reported, nor has its behavior in emulsion polymerization. We report the copolymerization of SBA **(28)** with styrene (STY) **(15)** at varying comonomer feed ratios via semicontinuous emulsion polymerization. Copolymer analysis was performed using NMR, gel permeation chromatography (GPC), differential scanning calorimetry (DSC),



gas chromatography with flame ionization detection (GC-FID), dynamic light scattering and atomic force microscopy (AFM). Additionally, a kinetic study of the styrene (**15**)-SBA (**28**) copolymerization conversion behavior in batch emulsion polymerization was performed.

## Experimental

*Materials.* All reagents were used without further purification unless otherwise noted. 3-Butene-2-ol (97%), acetic anhydride (99%), ammonium persulfate ((NH<sub>4</sub>)<sub>2</sub>S<sub>2</sub>O<sub>8</sub>) (98%) and Amberlyst1 15 (dry) ionexchange resin were purchased from Acros Organics. Styrene (STY) (**15**) (99%) and t-butyl hydroperoxide (TBHP) (70% in water) were purchased from Sigma. Sodium bicarbonate (NaHCO<sub>3</sub>) (99%) and magnesium sulfate (MgSO<sub>4</sub>) (99%) were purchased from Fisher Scientific. Sulfated ethoxylated nonyl ammonium salt (Rhodapex1 CO-436) and polyoxyethylene nonylphenyl ether (Igepal1 CO-887) were obtained from Rhodia Co. Bruggolite1 FF6 was obtained from Bruggemann Chemicals and dioctyl sodium sulfosuccinate (Aerosol1 OT (75%)) was obtained from Cytec.

*<sup>1</sup>H-NMR Measurement.* A Varian 200 MHz NMR equipped with a standard 5 mm <sup>1</sup>H/<sup>13</sup>C probe was utilized to identify the structure of the SBA monomer. The copolymer structure and composition were identified via <sup>1</sup>H-NMR. Samples were prepared at 5 wt % in deuterated chloroform (CDCl<sub>3</sub>) containing 0.03 vol % tetramethylsilane (TMS) as an internal standard. <sup>1</sup>H-NMR spectra of monomers and other small molecules were obtained from 256 scans with a relaxation delay of 1 s and a pulse angle of 45 degrees.

*Particle Size Determination by Dynamic Light scattering Technique.* The latex particle size was measured via dynamic light scattering using a Microtrac1 UPA 250 Particle size Analyzer. The Microtrac1 software was employed to determine particle sizes and particle size distributions. Samples were prepared in glass scintillation vials via diluting a few droplets of latex with deionized (DI) water until a concentration of approximately 1% (w/w) concentration as reached. Two scans were averaged (*via* the instrumentation software) to determine the average article diameter.

*Residual Monomer Determination through Gas-Chromatography Flame Ionization Detection (GC-FID).* Residual monomer content was measured using a ThermoQuest Trace GC 2000 Gas Chromatograph (GC) and Flame Ionization Detector (FID) with an AS 2000 Autosampler. The GC column was an Agilent DB-1 capillary column measuring 30 m in length and 0.35 mm inner diameter with helium as the carrier gas at a flow rate of 5.0 mL/min. Samples were prepared by dissolving 1 g of wet latex in 10 g acetone. A 1  $\mu$ L aliquot was then removed for analysis. The injection port temperature was maintained at 200 °C and the FID temperature was maintained at 250 °C. The temperature program utilized was 40 °C for 3 min, followed by ramping at 10 °C/min to 220 °C and holding for 30 s before again ramping 30 °C/min to 250 °C and holding for 3 min. Results were analyzed using ChromQuest software and were reported in parts per million (ppm).

*Reverse Phase High Performance Liquid Chromatography (RP-HPLC).* A Waters 1525 binary HPLC pump equipped with two 250 mm  $\times$  4.6 mm Hypersil ODS (C-18) 5  $\mu$ m columns and a Waters 2414 RI detector was utilized to characterize reagents according to polarity. The columns were maintained at ambient temperature. Dimethylformamide (DMF) was used as a mobile phase at a flow rate of 1 mL/min.

*Molecular Weight Determination through Gel Permeation Chromatography (GPC).* Polymer molecular weight was determined via a GPC equipped with a Waters 515 HPLC pump and two 300 mm  $\times$  7.5 mm PL-Gel 5  $\mu$ m Mixed-C columns maintained at 40  $^{\circ}$ C. A Polymer Laboratories ELSD 1000 refractive index detector calibrated with poly(methyl methacrylate) standards was utilized to identify the molecular weights. A tetrahydrofuran (THF) mobile phase was utilized at a rate of 1 mL/min. Samples were prepared at a concentration of 20 mg/mL. Results were analyzed using Millennium 1-4.0 software.

*Thermal Analysis through Differential Scanning Calorimetry (DSC).* A TA Q-1000 Series DSC was utilized to identify the glass transition temperature ( $T_g$ ) of the latex polymer and provide evidence for the copolymerization of SBA **(28)** with styrene **(15)**. Measurements were performed under nitrogen purge. Samples (9–15 mg) were first heated to 150  $^{\circ}$ C, and then cooled at a rate of 25  $^{\circ}$ C at 20  $^{\circ}$ C/min to erase effects of thermal history. Polymer  $T_g$  was then determined from a second scan performed at a heating rate of 10 $^{\circ}$ C/min from 25  $^{\circ}$ C to 150  $^{\circ}$ C. The inflection point of the resultant curve was reported as the  $T_g$ . Results were analyzed using TA Instruments Universal Analysis software.

*Latex Solids and Percent Conversion.* Percent conversion was calculated gravimetrically from the actual percent solids and the theoretical percent solids. The actual percent solids was determined by adding approximately 1.0–1.5 g of latex to an aluminum pan of known weight and drying the sample in a 100 °C oven for 1 h. The actual percent solids were then calculated by dividing the weight of the dried sample by the weight of the wet sample. The percent conversion was determined by dividing the actual percent solids by the theoretical percent solids.

*Gel Content Analysis.* A polymer sample weighed to the nearest 0.5 g (D) was added to a scintillation vial as a dried polymer film. 10 mL of methyl ethyl ketone (MEK) was added, and the vial was sealed and placed in a 60 °C oven. After 1 h, the sample was removed and placed on a Vortex shaker for 30 min. The solution was filtered through a preweighed 400 mesh screen (E), dried, and reweighed to obtain the dry screen plus gel weight (F). The percent gel was then calculated from equation 1. Samples were tested in triplicate and the averaged results were reported.

$$\% \text{Gel} = \frac{F - E}{D} \times 100 \quad (1)$$

*Atomic Force Microscopy (AFM).* AFM was utilized to identify latex film morphology and the extent of film formation. Samples were prepared by spin casting films from latex on freshly cleaved mica at 1800 rpm for 15 s. A Digital Instruments Nanoscope IIIa AFM equipped with etched silicon probes, 125 μm long with a resonance frequency of 175 kHz, nominal force constant of 40 N/m and a nominal tip radius of 10 nm was utilized in tapping mode to image the dried film surface. Height and phase

images were recorded on 1  $\mu\text{m}$  - 1  $\mu\text{m}$  scan size with an image resolution of 256–256 pixels at a scan rate of 1 Hz. Image analysis was performed using Nanoscope version 5.30 r2 image analysis software.

*Monomer Synthesis.* Prior to synthesis, Amberlyst 15 (dry) ion exchange resin was washed with methanol for six hours and dried under vacuum. 3-Butene-2-ol (1 mol) was added very slowly into a mixture of acetic anhydride (1.05 mol) and Amberlyst 15 (dry) ion exchange resin (2% by weight of acetic anhydride). After addition, the solution was stirred for 30 min and the product mixture was added through an addition funnel to a sodium bicarbonate solution (1 M) while stirring. Three consecutive extractions were performed in a separatory funnel using sodium bicarbonate solution washes. The organic phase was dried over magnesium sulfate. The resulting organic phase was filtered into a completely dried flask and the resulting organic solution was vacuum distilled for further purification. A yield of 65% was calculated based on the moles of resulting product after purification versus the initial moles of 3-butene-2-ol. The boiling point of SBA (**28**) was determined to be 114 °C, which is consistent with previously reported values.<sup>281</sup>

The structure was confirmed through <sup>1</sup>H-NMR (Figure VI-1) and <sup>13</sup>C-NMR (Figure VI-2) analysis. Proton NMR signals are assigned as shown in Figure V-1, with SBA double bond protons **a** (5.1 ppm), **b** (5.2 ppm), and **c** (5.8 ppm), allylic proton **d** (5.0 ppm), doublet -CH<sub>3</sub> protons **e** (1.2 ppm) and singlet -CH<sub>3</sub> protons **f** (1.9 ppm). Additional resonances are also observed, which are attributed to the presence of crotyl acetate, and are assigned as double bond protons **h** (5.7 ppm) and **i** (5.6 ppm), secondary allylic protons **j** (4.3 ppm), multiplet -CH<sub>3</sub> protons **g** (1.6 ppm) and singlet -CH<sub>3</sub> protons **k** (2.2 ppm). Crotyl acetate formation presumably results from rearrangement of the double

bond. Integration and comparison of characteristic resonances attributed to crotyl acetate (**29**) (j, 4.3 ppm) and SBA (f, 1.9 ppm) provide an estimate of the relative concentrations of the two species. Vacuum distillation increases the SBA (**28**) purity from 88 to 97%.

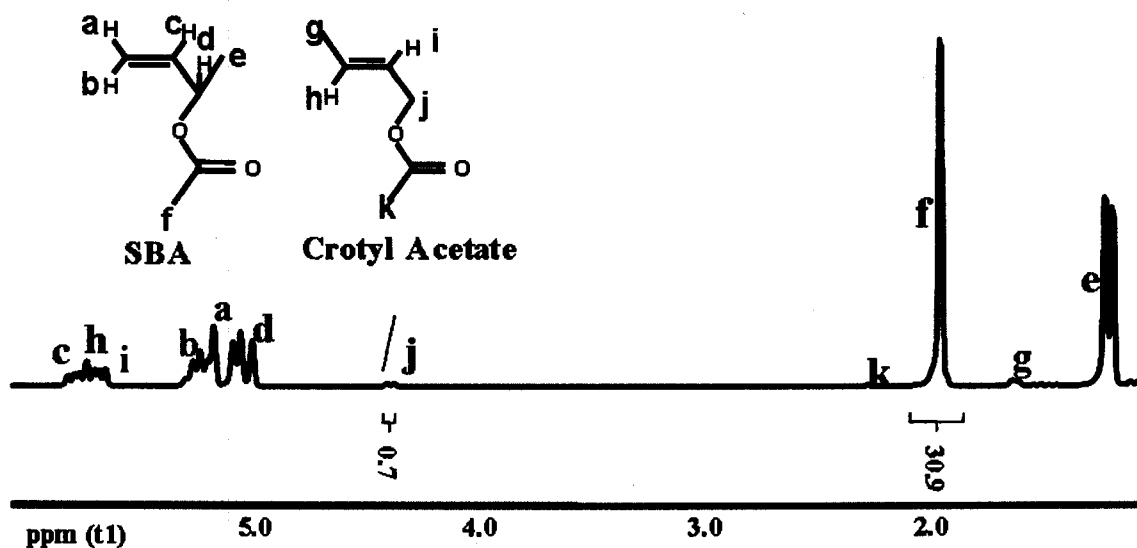


**Figure VI-1.**  $^1\text{H}$  NMR spectrum of SBA (**28**) after purification by vacuum distillation.

The  $^{13}\text{C}$ -NMR spectrum of purified SBA (**28**) is depicted in Figure VI-2, with signals assigned as: carbonyl carbon e (168 ppm), double bond carbons a (113 ppm) and b (135 ppm), allylic carbon c (68 ppm),  $-\text{CH}_3$  carbon at allylic position d (17 ppm) and  $-\text{CH}_3$  carbon next to carbonyl group f (19 ppm). Additional faint resonances are observed that are attributed to crotyl acetate (**29**) and are assigned as: carbon k (167 ppm), double bond carbons h (123 ppm) and i (129 ppm), secondary allylic carbon j (63 ppm),  $-\text{CH}_3$  carbon next to double bond g (15 ppm) and  $-\text{CH}_3$  carbon next to carbonyl group l (19 ppm).

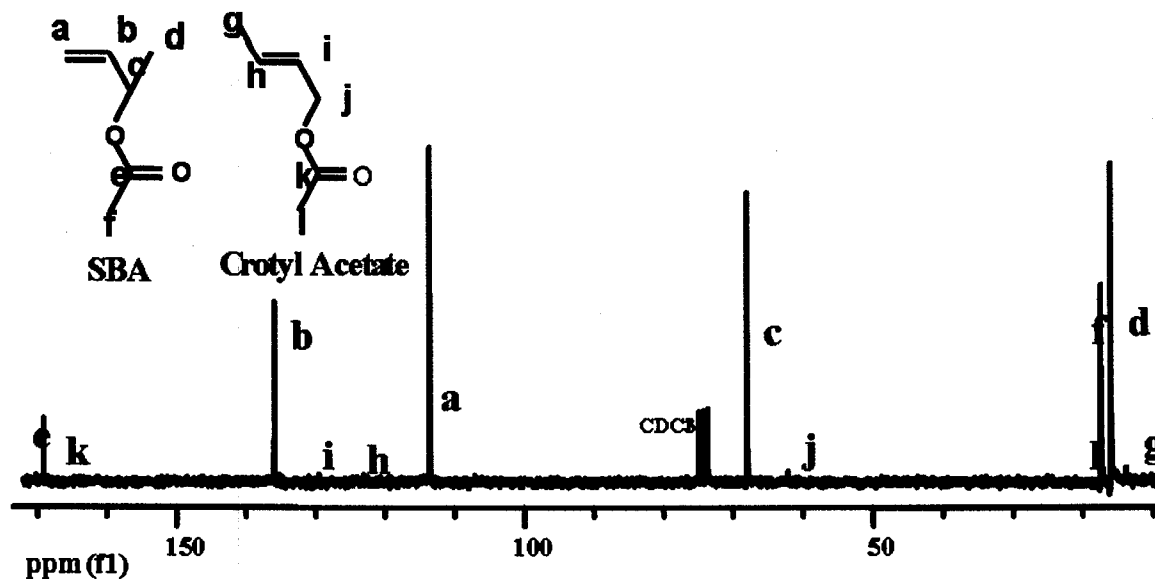


**Figure VI-2.**  $^{13}\text{C}$  NMR spectrum of SBA (**28**) after purification by vacuum distillation.

*Latex Synthesis through Semicontinuous Emulsion Polymerization.* Latices (STY-SBA (**30**)) were synthesized using a semicontinuous process in which both pre-emulsion and initiator were introduced into the reactor over time at a controlled rate. A Camile1 2000 automated data acquisition and control system was utilized during latex synthesis to control monomer addition rates. Manually programmed syringe pumps were used to control initiator feed rate. Reaction temperature was controlled by submerging the reaction vessel in an immersion circulator water bath maintained at 70 °C. The water bath and reaction temperatures were monitored and recorded by Camile1 controlled thermocouples.

Emulsion polymerizations were conducted in 100 mL glass reactors, according to the recipe given in Table VI-1A. Agitation was achieved with a mechanical stirrer fitted through the center opening of the reactor lid. A Claisen adapter was utilized to mount a nitrogen inlet and a condenser. The remaining reactor lid openings were sealed with

rubber septa. Initiator solutions and monomers were introduced into the reactor through needles placed in the septa, taking care to keep the needle tips separated. A water and surfactant mixture was then introduced into the reactor and purged with nitrogen for 10 min. The pre-emulsion was sheared at 1800 rpm for 20 min. Initiator solutions (7.24 mL/h) and pre-emulsion (0.015 mL/min) were introduced into the reactor using the Masterflex console drive. Copolymerization reactions were performed with different comonomer feeds, 100% STY-0% SBA (**31**), 93.9% STY-6.1% SBA (STY-SBA 6.1) (**30**), 87.5% STY-12.5% SBA (STY-SBA 12.5) (**30**) and 75% STY-25% SBA (STY-SBA 25) (**30**), at 70 °C for 90 min. The reactor was then removed from the water bath and cooled to ambient temperature before characterization. For proton NMR analysis, latices were washed with sodium chloride salt solution and then acidic solution to separate the emulsifier from the copolymer. Precipitated copolymers were then washed with water and dried under vacuum.

*Kinetic Study in Batch Emulsion Polymerization.* Kinetic studies were performed in batch emulsion polymerization reactions. Reactor charge, initiator, and preemulsion were prepared according to the recipe given in Table VI-1B, and added simultaneously to a 100 mL reactor. The solution was then stirred at 1800 rpm for 50 min. The reactor was then placed in a water bath adjusted to 70 °C and agitated with a mechanical stirrer fitted through the center opening of the reactor lid. A Claisen adapter was utilized to mount a nitrogen inlet and a condenser. Total reaction time was 225 min. Aliquots were taken at 15 min intervals and quenched in liquid nitrogen for solid content. Conversion was calculated based on solid content results of each aliquot by dividing the actual percent solids by theoretical percent solids.

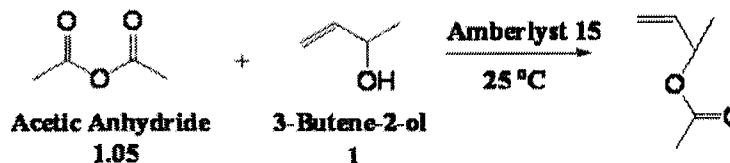


**Table VI-1.** A) Latex Recipe for Semi-Continuous Batch Process (93.9% STY-6.1% SBA) (**30**); B) Recipe for Batch process (93.9% STY-6.1% SBA) (**30**).

A		B	
Reactor Charge	Amount (g)	Reactor Charge	Amount (g)
DI water	15	DI Water	25
Rhodapex CO 436	1	Rhodapex CO 436	1
Preemulsion	Amount (g)	Preemulsion	Amount (g)
DI water	25	DI water	35
NaHCO <sub>3</sub>	1.25	NaHCO <sub>3</sub>	1.25
Rhodapex CO 436	2	Rhodapex CO 436	3.5
Igepal CO 887	2	SBA	2.1
Aerosol OT	1	Styrene	31.9
SBA	2.13		
Styrene	32.7		
Initiator	Amount (g)	Initiator	Amount (g)
(NH <sub>4</sub> ) <sub>2</sub> S <sub>2</sub> O <sub>8</sub>	0.44	(NH <sub>4</sub> ) <sub>2</sub> S <sub>2</sub> O <sub>8</sub>	1.35
TBHP	0.89	DI water	5
DI water	8		
FF6	0.77		
DI water	8		

## Results and Discussion

*Synthesis of sec-Butenyl Acetate.* The allylic monomer sec-butenyl acetate (SBA) (**28**) was synthesized through the esterification reaction of 3-butene-2-ol with acetic anhydride in the presence of Amberlyst 15 ion exchange catalyst at room temperature (Scheme VI-1). The resulting product was colorless, with a yield of 65%. NMR analysis indicated the presence of crotyl acetate (**29**) in addition to the SBA (**28**) (see experimental section and figures in appendix). Crotyl acetate (**29**) formation presumably results from rearrangement of the double bond.<sup>277</sup> After vacuum distillation the SBA (**28**) purity is 97%.



**Scheme VI-1.** SBA (**28**) Synthesis.

*Emulsion Copolymerization of SBA (**28**) with Styrene (**15**) (STY-SBA).*

Copolymerization reactions were performed using purified SBA (**28**) with styrene (STY) (**15**). Latices were synthesized using a semicontinuous emulsion process to control latex properties (homogeneity, rate of polymerization, particle size, and particle size distribution) in light of the following potential problems: degradative chain transfer arising from SBA, large differences in reactivity ratios for SBA (**28**) and STY (**15**), solubility differences of the monomers and monomer partitioning. A single latex recipe was used for copolymerization of SBA (**28**) with a range of comonomers, including STY (**15**), acrylate family monomers (methyl methacrylate and butyl acrylate) and vinyl acetate, but only STY-SBA (**30**) copolymer results are presented in this paper. A surfactant combination (5% (w/w) in 100 g emulsion formulation) of two anionic surfactants, Rhodapex CO-436 and Aerosol OT 75, and a nonionic surfactant, Igepal CO-887, were used in the pre-emulsion preparation. Rhodapex CO-436 belongs to the sulfate family of anionic surfactants, which are most commonly applied in emulsion polymerization of the acrylate family and convenient for polymerization in an acidic medium.<sup>261</sup> Igepal CO-887 nonionic surfactant was employed in conjunction with Rhodapex CO-436 anionic surfactant to help control particle size and size distribution.<sup>241,253</sup> Additionally, this combination produces a final polymer latex that is insensitive to changes in pH over a wide range.<sup>241</sup> Aerosol OT 75 is

an efficient wetting agent and emulsifier, characterized by its quick migration to the interface.<sup>282</sup> It can be used as the primary or coemulsifier for the synthesis of a wide variety of latex types such as styrene-butadiene, styrene-acrylic, vinyl acrylic and vinyl acetate and is a good emulsifier for hydrophobic resins as well as polar monomers like vinyl acetate.<sup>282</sup> It thus helps ensure the stability of the STY-SBA (**30**) pre-emulsions, where the monomers exhibit large polarity differences and the growing polymer chains demonstrate increase in hydrophobic character.

In heterogeneous polymerization systems such as emulsions, the type of initiator directly influences the residual monomer content.<sup>283</sup> Residual monomer will reside primarily in the organic or the water phase, depending on its solubility. Therefore, in choosing an initiator, it is important to consider its solubility in both phases. The copolymerization was initiated through a redox initiator system (1.3%) including water-soluble ammonium persulfate ( $(\text{NH}_4)_2\text{S}_2\text{O}_8$ ) and oil-soluble *t*-butyl hydroperoxide (TBHP) as oxidizing agents. Bruggolite FF6, which is a formaldehyde-free reducing agent based on a sulfinic acid derivative, was used as a reducing agent. This initiator system was used to accommodate the polarity difference between SBA (**28**) and STY (**15**) and the high possibility of chain termination reactions due to the allylic hydrogen abstractions of SBA. Moreover, such redox systems also allow polymerization over a wide temperature range. Persulfate initiators form acidic byproducts as they are consumed during polymerization, which lowers the pH as the reaction proceeds. The acid catalyzes the hydrolysis of esters (main chain) of vinyl acetate and acrylate family monomers.<sup>284</sup> Thus,  $\text{NaHCO}_3$  (1.2%) was employed as a buffer in the pre-emulsion recipe to avoid possible hydrolysis during copolymerization.

Comparative water solubility of SBA was evaluated by RP-HPLC, by comparing retention time with common commercial monomers used in emulsion polymerization based on their polarity.<sup>285</sup> RP-HPLC is not a quantitative technique but does offer useful qualitative information. Polar monomers are attracted to the polar mobile phase used for RP-HPLC, resulting in shorter retention times. Longer retention times are characteristic of nonpolar compounds that are more attracted to the stationary nonpolar column.<sup>286</sup> Table VI-2 gives retention times for 2-hydroxyethyl acrylate (2-HEA), hydroxyethyl methacrylate (HEMA), vinyl acetate (VA), methyl methacrylate (MMA), butyl acrylate (BA), styrene (STY) (**15**), 2-ethylhexyl acrylate (2-EHA), and SBA (**15**). The results indicate that hydrophobicity and polarity properties of SBA are very similar to those of MMA (retention time 5.7 min). Styrene (**15**) monomer, however, displays substantially reduced polarity and increased hydrophobicity (retention time at 6.6 min), as is expected from the structure of the monomers.

**Table VI-2.** Retention time of SBA and common commercial monomers characterized through RP-HPLC.

Monomers	Retention Time (min)
2-Hydroxyethyl Acrylate	5
2-Hydroxyethyl Methacrylate	5.2
Vinyl acetate	5.1
Methyl Methacrylate	5.7
SBA ( <b>28</b> )	5.7
Butyl Acrylate	6.3
Styrene	6.5
2-Ethylhexyl Acrylate	8.7

The emulsion system employed resulted in successful copolymerization of SBA **(28)** with STY **(15)**, as validated by  $^1\text{H-NMR}$ , GPC and DSC analysis. Proton NMR spectra for the copolymers are shown in Figure VI-3. Incorporation of SBA into the copolymer is indicated by the appearance of the characteristic SBA **(28)** allylic proton signal at 3.6 ppm. Moreover, the area under this peak increases with increasing SBA feed ratio. Integration and comparison of the peaks attributed to styrene **(15)** (phenyl protons – 7 ppm) and SBA (allylic proton 3.6 ppm) yield values of 6% SBA incorporation for the STY-SBA 6.1% **(30)** latex, 13% SBA incorporation for the STY-SBA 12.5% **(30)** latex and 22.6% SBA incorporation for the STY-SBA 25% latex **(30)**. Thus, SBA is incorporated at a high level into the copolymer at all feed ratios evaluated, even though a slight drop in SBA content is observed for the highest feed ratio. The level of allylic monomer incorporation observed for the SBA-STY **(30)** system is significantly higher than that generally reported for other allylic systems,<sup>256,257</sup> indicating that the chosen emulsion polymerization system allows increased incorporation of the allylic monomer. No signals are observed in the double bond region (~5–6 ppm), thus there is no indication of residual vinyl groups in the copolymer via proton NMR. Thus, in contrast to the bulk homopolymerization study of Gaylord et al.,<sup>279,280</sup> the SBA vinyl groups appear to be fully reacted in the emulsion copolymerization. The signal at 1.6 in the STY-SBA 6.1% **(30)** copolymer spectrum is most likely due to residual water. In the STY-SBA 25% **(30)** copolymer spectrum, additional signals are observed in the 0.7–2.2 ppm region that are indicative of increasing SBA **(28)** incorporation. The signal at 2.2 ppm is assigned as a -CH group of SBA. The signals at ~1.4 ppm (at the pendant group) and at 0.8 ppm (at the chain ends) are both attributed to separate -CH<sub>3</sub> protons.

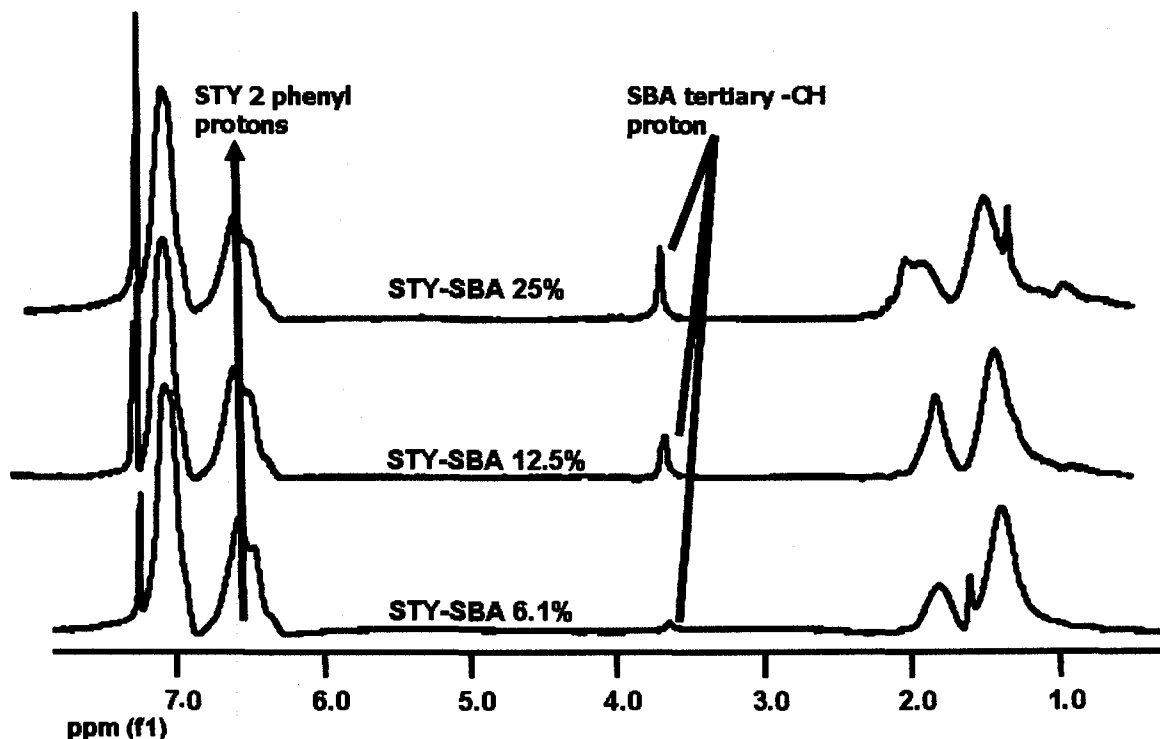


**Figure VI-3.**  $^1\text{H}$  NMR spectra of STY-SBA 6.1% (**30**), STY-SBA 12.5% (**30**) and STY-SBA 25% (**30**) copolymers showing increase in SBA tertiary allylic proton signal (3.6 ppm) with increasing SBA feed content.

Further evidence of copolymer production is observed in GPC analysis.

Unimodal, broad distribution traces are observed for the styrene (**15**) homopolymer and STY-SBA copolymers (Figure VI-4), with general shifts to lower molecular weight with increasing SBA feed ratio. The unimodal curves indicate that broad molecular weight distribution copolymers were produced, with no evidence of simultaneous production of styrene (**15**) homopolymer. Molecular weight data for the copolymers is given in Table VI-3. Molecular weight decreases with increasing SBA content. Measured polydispersity indices (PDI) for the styrene (**15**) homopolymer and copolymers with 6.1% and 12.5% SBA feed ratios are high (2.9–3.3), but PDI is dramatically reduced (2.1) when SBA monomer feed ratio is increased to 25%. Chain transfer reactions produce dead polymer

chains and stable radicals, and chain transfer to monomer is known to affect the molecular weight distribution, particularly at high conversion.<sup>284,287</sup> In the present copolymerization reactions,  $M_n$  and  $M_w$  decrease at a similar rate for low SBA feed ratios. When the SBA feed is increased to 25%,  $M_w$  drops faster than  $M_n$ , leading to reduced polydispersity.

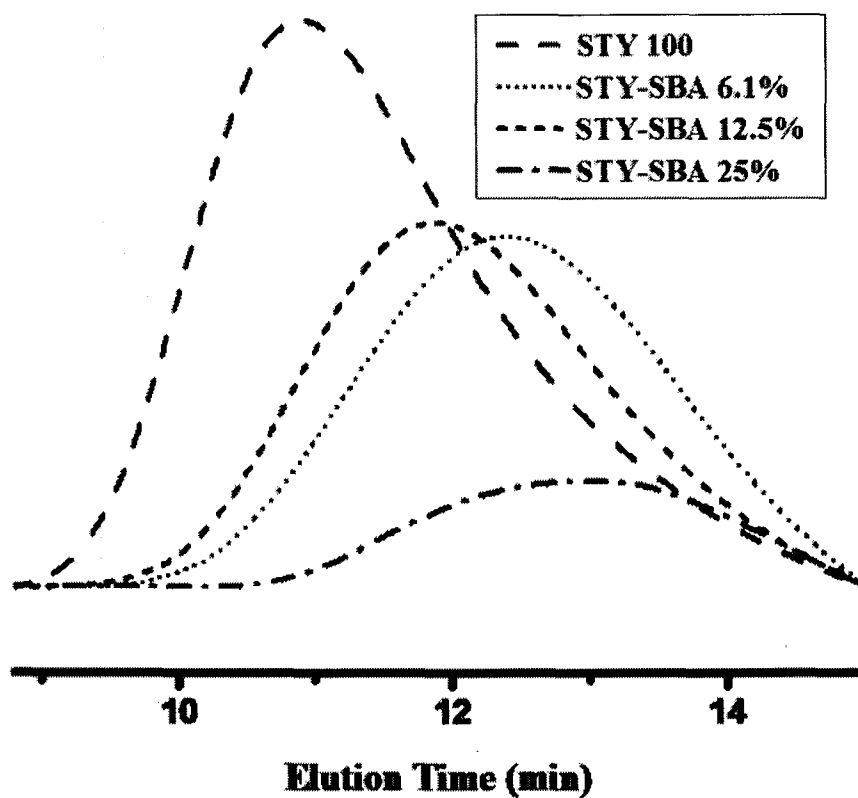


**Figure VI-4.** GPC traces of STY 100 (30), STY-SBA 6.1% (30), STY-SBA 12.5% (30) and STY-SBA 25% (30) copolymers.

**Table VI-3.** Molecular weight, polydispersity index (PDI) and glass transition temperature ( $T_g$ ) for copolymer systems.

Latex	$M_n \times 10^4$ <sup>a</sup>	$M_w \times 10^4$ <sup>a</sup>	PDI <sup>a</sup>	$T_g$ <sup>b</sup> (°C)
STY 100	7.2	21.2	2.9	104
STY-SBA 6.1%	3.2	10.7	3.3	90
STY-SBA 12.5%	3.0	8.9	3.0	82
STY-SBA 25%	2.3	4.7	2.1	75

<sup>a</sup> Determined by GPC.

<sup>b</sup> Determined by DSC.

DSC traces exhibit a single  $T_g$ , with shifts to lower values as a function of increasing SBA feed ratio (Table VI-3), providing further evidence for copolymer production. The reduced  $T_g$  is explained by the lower expected  $T_g$  of the acetate homopolymer relative to polystyrene (**31**), and also in part due to the lower molecular weight of the copolymers in comparison to the homopolystyrene (**31**). Appearance of a single  $T_g$  indicates copolymer formation. Films formed from the homopolystyrene (**31**) latex were friable, even when dried at elevated temperatures. In general, styrene (**15**) must be copolymerized with a lower  $T_g$  comonomer to produce continuous films. The incorporation of SBA monomer in the polystyrene (**15**) chain results in a more flexible, lower  $T_g$  copolymer, which is desirable for film applications requiring higher ductility.

The semicontinuous emulsion process employed yielded relatively small latex particles with monomodal particle size distributions, indicating the synthesis of a homogeneous product. Dynamic light scattering traces for two representative copolymers systems are shown in Figure VI-5. Similar unimodal traces were obtained for all of the systems (as produced by the light scattering software). There is no evident trend in



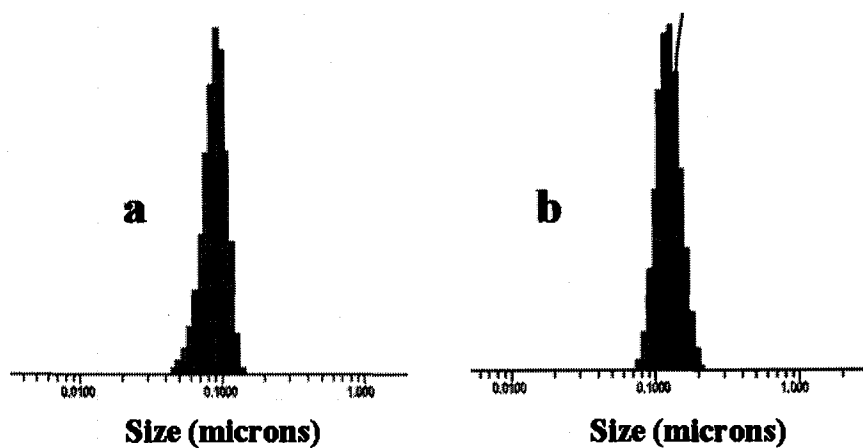


**Figure VI-5.** Dynamic light scattering traces for a) 6.1% SBA and b) 25% SBA.

particle size as a function of SBA feed content (Table VI-4), and the latex particle sizes are desirably small and consistent for all copolymers. Copolymerizations were repeated three times for the STY-SBA 6.1% (**30**) and STY-SBA 12.5% (**30**) samples to evaluate the reproducibility of particle size and particle size distributions of the latex produced from the semicontinuous emulsion polymerization system. Each repetition produced a unimodal distribution with minimal differences between batches (within experimental error). Tapping mode AFM images of spin coated films prepared from the copolymer latices are shown in Figure VI-6. The films appear well coalesced. The measured diameters of the coalesced particles in the dried films are consistent with the latex particle sizes determined by light scattering (within statistical variation) (Table VI-4). The homopolystyrene (**31**) latex, on the other hand, yielded poorly coalesced, friable films which were not imaged. Residual (unreacted) monomer levels were determined via GC-FID for each latex at the end of the ninety-minute polymerization cycle (Table VI-5).

**Table VI-4.** Number average particle size of latex (via dynamic light scattering (DLS)) and of film (via AFM).

Latex	Particle size by (DLS) <sup>a</sup> <i>run 1</i> (nm)	Particle size by (DLS) <sup>a</sup> <i>run 2</i> (nm)	Particle size by (DLS) <sup>a</sup> <i>run 3</i> (nm)	Particle size by (AFM) <sup>b</sup> (nm)
STY 100%	89±17	-----	-----	-----
STY-SBA 6.1%	151±29	114±20	121±18	147±30
STY-SBA 12.5%	91±18	134±27	113±19	108±21
STY-SBA 25%	103±18	-----	-----	112±22

<sup>a</sup> DLS error represents range from 2 scans.

<sup>b</sup> AFM error represents one standard deviation.

Residual monomer levels increase as a function of SBA feed ratio. This increase is due to both the high difference in the reactivity ratios of the comonomers and to the chain transfer to allylic monomer. As reported for the copolymerization of vinyl acetate with butyl methacrylate,<sup>281</sup> a high reactivity ratio difference causes a near cessation of polymerization, with resultant increase in the levels of unreacted monomer. Although residual levels of both STY and SBA monomers increase with increasing SBA feed ratios, there are lower levels of unreacted STY (**25**) than SBA (**28**) for all latices. It is likely that copolymer chains initially grow through STY (**15**) polymerization prior to SBA (**28**) copolymerization. Copolymer chains are terminated with SBA(**28**) monomer via chain transfer. Higher SBA feed concentrations effect greater chain transfer, as expected.

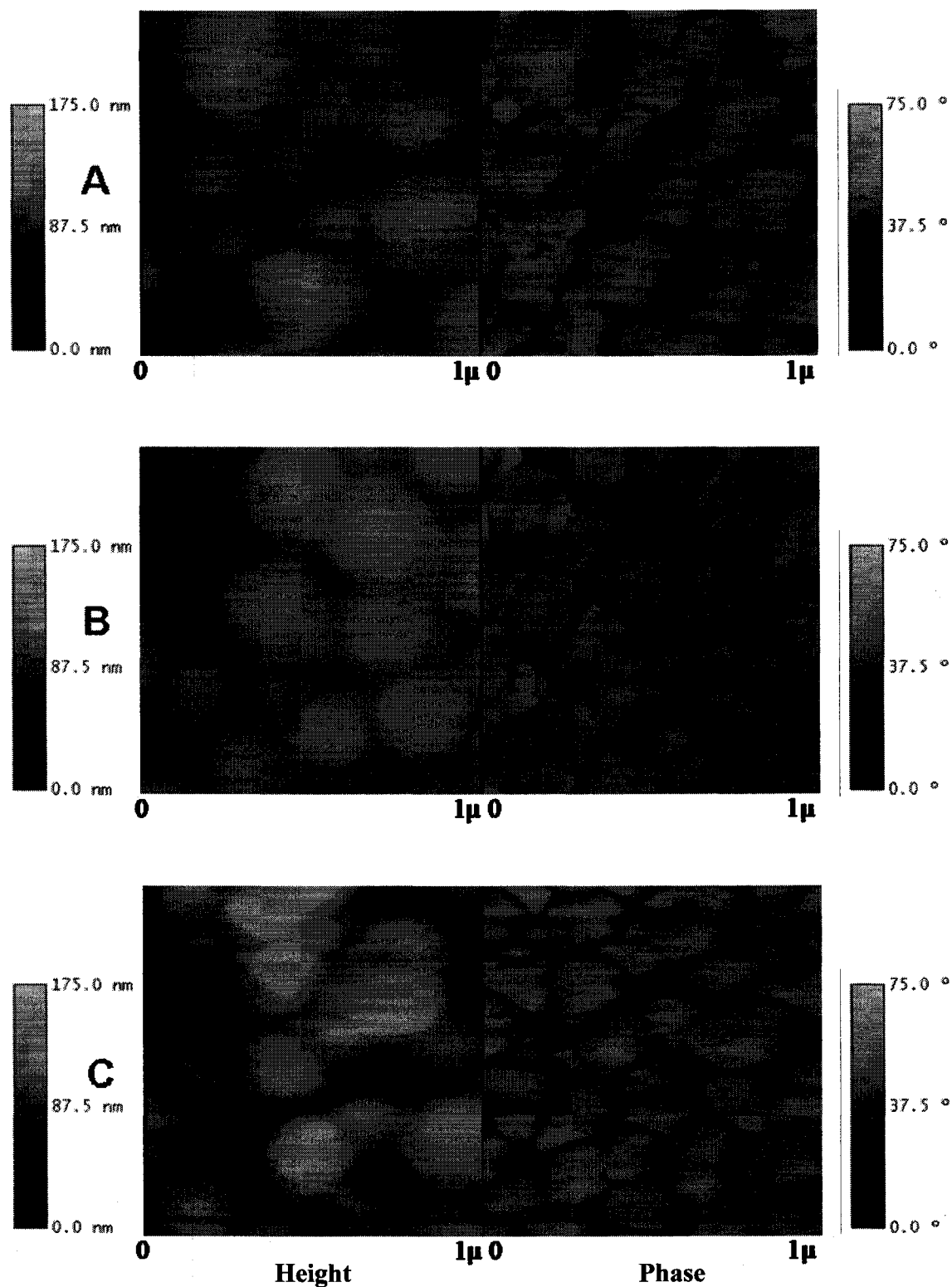


**Figure VI-6.** AFM tapping mode height and phase images of spin coated films prepared from A) STY-SBA 6.1% (30), B) STY-SBA 12.5% (30) and C) STY-SBA 25% (30) latexes.

**Table VI-5.** Solids, gel content, residual monomer and conversion results for semi-continuous emulsion copolymerization reactions.

<b>Latex</b>	<b>Solid (%)</b>	<b>Gel Content (%)</b>	<b>SBA Residual Monomer<sup>a</sup> (%)</b>	<b>Styrene Residual Monomer<sup>a</sup> (%)</b>	<b>Conversion (%)<sup>b</sup></b>
<b>STY 100%</b>	41	1.5	0	0.4	99
<b>STY-SBA 6.1%</b>	41	2.3	0.75	0.75	98
<b>STY-SBA 12.5%</b>	39	1.3	2.22	1.04	93
<b>STY-SBA 25%</b>	26	1.7	2.53	1.33	62

<sup>a</sup> Determined by GC-FID.

<sup>b</sup> Determined from percent solids.

Solid content analysis of the latex indicates the amount of polymer produced. Relatively high solid contents of approximately 40% are achieved for the homopolymer styrene **(15)**, STY-SBA 6.1% **(30)**, and STY-SBA 12.5% **(30)** polymerizations (Table VI-5). A sharp reduction in the solid content to 26% is observed for the STY-SBA 25% **(30)** latex, attributed to high levels of chain transfer to monomer with concomitant decrease in monomer conversion. Monomer conversions calculated from solid content values indicate 98% conversion for the STYSBA 6.1% latex **(30)**, 93% for the STY-SBA **(30)** 12.5% latex and only 62% conversion for the STY-SBA 25% latex **(30)**. Conversions calculated from residual monomer, however, estimate much higher levels, with 97% conversion for the STY-SBA 12.5% **(30)** latex and 96% conversion for the STY-SBA 25% **(30)** latex. It is likely that low molecular weight oligomers are produced as a result of chain transfer reactions, and that their production levels increase with increasing SBA content in the monomer feed. Volatile oligomers evaporate during the solid content evaluation at 100 °C after 1 h, and thus these low molecular weight species are not included in the monomer conversion calculated from solid content. At the same time, residual monomer levels are reduced when the oligomers are formed, so conversion

calculated from residual monomer data appears higher than that calculated from solid content levels. Additional low level peaks were observed in the GC-FID chromatogram that may indicate the presence of the oligomers; however, these peaks were not specifically identified. There is no evident trend in gel content for the copolymers (Table VI-5).

*Kinetic Study using Batch Emulsion Polymerization.* The effects of degradative chain transfer are further exhibited in studies of conversion as a function of reaction time in a batch emulsion polymerization. In this study, overall conversion of both monomers was determined (based on solid content) to observe the effects of chain transfer reactions in the case where feed ratio is not controlled over time (Figure VI-7). For the lowest monomer feed ratio, STY-SBA 6.1% (**30**), conversion increases steadily over a period of three hours until almost 100% conversion is achieved. For the higher SBA (**28**) feed ratios, conversion rate decreases. After 200 min, only 60% conversion is achieved for the STY-SBA 12.5% (**30**) copolymer and 40% conversion is obtained for the STY-SBA 25% (**30**) copolymer. Chain transfer increases with increasing SBA (**28**) content, producing unreactive polymer chains due to the high amount of allylic hydrogen abstraction and formation of stable radicals, thereby decreasing rate of copolymerization and conversion. However, these effects are minimal at low concentrations of SBA (**28**) in the latex. At low SBA (**28**) concentrations, high conversions and high levels of incorporation of allylic monomer into the copolymer are easily achieved.

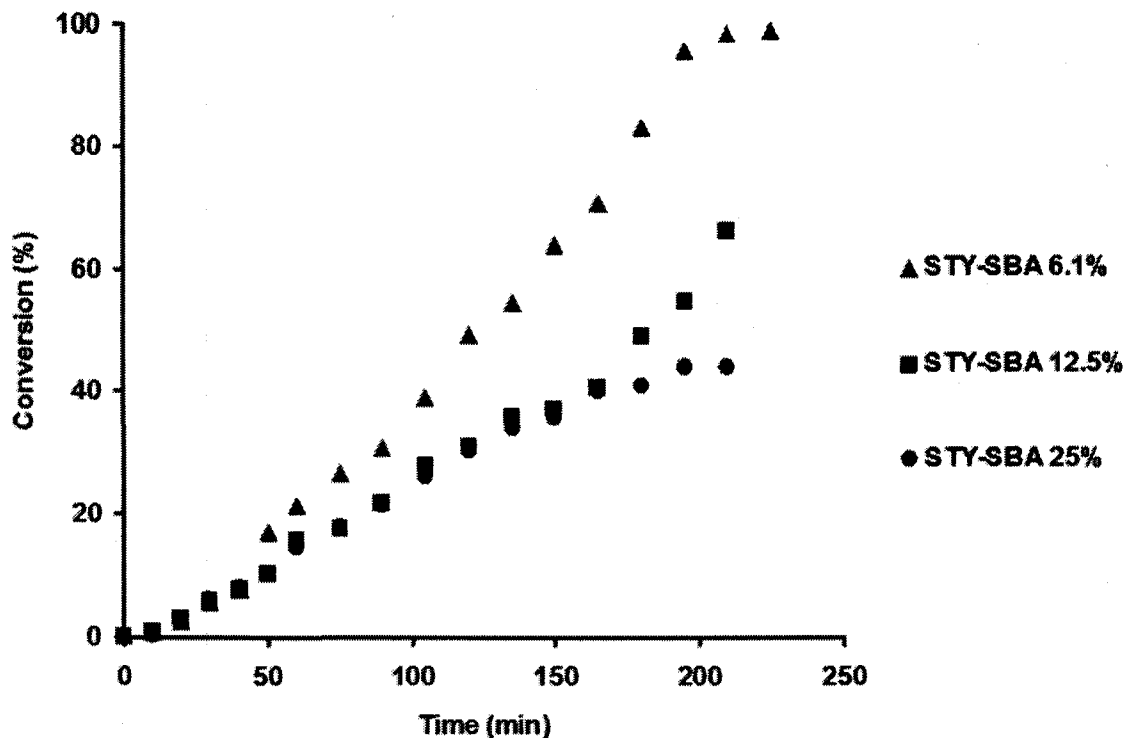


**Figure VI-7.** Conversion as a function of time for STY-SBA 6.1% (**30**), STY-SBA 12.5% (**30**) and STY-SBA 25% (**30**) copolymers performed in batch process.

### Conclusions

Copolymers of the allylic monomer sec-butenyl acetate (**28**) with styrene (**15**) were successfully produced via semicontinuous emulsion polymerization, as evidenced by  $^1\text{H-NMR}$ , GPC, and DSC analysis. Latices produced exhibited unimodal particle size distributions. Copolymers exhibiting a single  $T_g$ , with unimodal molecular weight distribution, were obtained for monomer feed ratios up to 25% SBA(**28**). At low concentrations of SBA (**28**) in the latex (up to 6%) conversion of 98% was readily achieved, with over 99% incorporation of the allylic monomer into the resultant copolymer. At higher SBA (**28**) feed concentrations, conversion and comonomer incorporation into the copolymer were reduced, especially at the 25% SBA (**28**) level,

because of degradative chain transfer. Copolymer molecular weights and  $T_g$ s are decreased with increasing SBA (**15**) incorporation. These studies indicate the potential utility of sec-butenyl acetate, especially at low concentration levels, as an effective chain transfer agent to control molecular weight of styrene polymers, while providing high conversions,  $T_g$  modification and enhanced film formation properties. This allylic monomer was readily copolymerized with styrene via emulsion polymerization, despite large differences in polarity and reactivity ratio of the two monomers, and is thus expected to prove useful in a wide range of vinyl polymerizations.

## CHAPTER VII

## CONCLUSIONS

This research specifically focused on the synthesis of well-defined, carboxylic acid functionalized glycopolymers through high yield post-polymerization reactions between well-defined primary amine functionalized polymers and carboxylic acid functionalized sugars. The surface modification of silicon wafers with PAEMA (**16**) was also studied using “click” chemistry. The resulting surface presented a non-uniform, high grafting density polymer brush layer.

The first step of this research was to overcome the current challenges of polymerizing AEMA (**6**) through CRP techniques, which include the loss of polymerization control, high polydispersity and slow polymerization rate. For this purpose, well-defined, narrowly dispersed homopolymer and diblock copolymers of AEMA have been synthesized *via* aqueous RAFT polymerization. Specifically, AEMA monomer has been homopolymerized directly in aqueous solution with PDIs below 1.2 and conversions up to 95%. To our knowledge, this is the first report of aqueous AEMA (**6**) RAFT polymerization with very low polydispersity and good control without the necessity of protecting group chemistry. The resulting PAEMA (**16**) was also chain extended with HPMA (**8**) to produce well defined diblock copolymers with high blocking efficiency and PDIs lower than 1.1. Building on our earlier work and recent literature reports, we show for the first time a series of novel, well-defined block copolymers of AEMA (**6**) and HPMA (**8**) with high conversion. Since primary amine groups are amenable to a wide range of post-polymerization chemistries, such as rapid formation of amides and imines, ring-opening of epoxy groups and Micheal addition, we believe that



this study will enable developments in several areas, including synthesis of controlled architecture, bio-inspired polymers through the conjugation of the primary amine pendant groups with targeted sugars, peptides or amino acids. Improved crosslinking strategies for shell cross-linked micelles, and robust surface functionalization for various surface chemistries are also possible. Diblock copolymers of AEMA (6) and HPMA (8) may prove useful as drug/gene delivery vehicles through electrostatic complexation of the positively charged AEMA (6) block with the negatively charged phosphate backbone of polynucleotides. In addition, the susceptibility of the AEMA (6) block to post-polymerization reactions facilitates the conjugation of this diblock copolymer with targeted drugs or bio-molecules.

The second part of the research demonstrates for the first time the synthesis of well-defined carboxylic acid functionalized glycopolymers *via* one step, high-yield post-polymerization modification approaches. Specifically, APMA (12) monomer was homopolymerized directly in aqueous solution with PDIs below 1.1 through aqueous RAFT polymerization. The well-defined, narrowly dispersed PAPMA (17) was bioconjugated with D-glucuronic acid sodium salt (5) *via* a reductive amination reaction pathway in alkaline medium to obtain well-defined glycopolymers with near quantitative substitution.

In addition, the bioconjugation of PAEMA (16) and PAEMA-*b*-PHPMA (18) with D-glucuronic acid sodium salt (5) was also demonstrated. Lower yields of bioconjugation were achieved, due to the possible degradation of PAEMA (16) in alkaline medium at high temperature. The resulting glycopolymers probably include inhomogeneous sequences within the chain.

Building on our earlier work and recent literature reports, this study shows the first example of well-defined carboxylic acid functionalized glycopolymers prepared via one step, high-yield post-polymerization modification. PAPMA is demonstrated to be a versatile primary amine functionalized polymer which readily undergoes reductive amination reactions with sugars with high yields. Therefore, this study will enable new capabilities in the synthesis of controlled architecture glycopolymers with multiple functionalities, without the need for stringent purification methods.

The third part of this research shows the preparation of the PAEMA (**16**) brushes on a silicon wafer via one step using a “click” chemistry approach. First, a well-defined,  $\alpha$ -alkynyl-functionalized homopolymer of AEMA (**26**) was synthesized via RAFT polymerization with PDIs below 1.2 using  $\alpha$ -alkynyl CTP (**25**) as the CTA. The resulting  $\alpha$ -alkynyl-functionalized PAEMA (**26**) was also tethered to azide functionalized silicon wafers through a “grafting to” method using a “click” chemistry approach. The preliminary results of ellipsometry, water contact angle, ATR-FTIR and AFM analysis demonstrated a non-uniform polymer brush layer with an estimated grafting density of  $0.39 \text{ chains/nm}^{-2}$ , indicating an excellent grafting density for the “grafting to” method. This study shows that “click” chemistry is a simple and effective method to obtain primary amine functionalized polymer brushes. These studies will potentially enable further developments in surface modification of bio-related materials such as sugars, carbohydrates, peptides and proteins to study biomaterials related processes including bio-lubricity, surface drug-delivery, and protein-carbohydrate interactions.

The primary contribution of this research is the demonstration of a simple and effective synthetic pathway to obtain carboxylic acid functionalized glycopolymers without the need for complex, time-consuming purification steps. The proposed objectives of this research included development of a direct synthetic pathway for production of well-defined primary amine functionalized polymers using aqueous RAFT polymerization techniques, followed by post-polymerization reactions involving reductive amination reaction between the well-defined amine functionalized polymers and D-glucuronic acid sodium salt (**5**) to form glycopolymers. The accomplishments in the first part of the research indicate that the aqueous RAFT polymerization is a convenient technique to achieve well-defined primary amine functionalized polymers without using protective group chemistry. The second part of the study validates the effectiveness of the reductive amination reaction in the synthesis of well-defined homogeneous carboxylic acid functionalized glycopolymers. This approach provides mild, effective post-polymerization reactions and facilitates the complex glycopolymer synthesis. These new synthetic charged glycopolymers can serve as synthetic analogues to HA (**1**) for evaluation of their utility in biomedical applications. The fifth chapter addresses the last objective, which was the evaluation of the effectiveness of “click” chemistry in the preparation of primary amine functionalized polymer brushes through the “grafting to” method. The preliminary results indicate that “click” chemistry is an effective method for attaining primary amine functionalized polymer brushes on the silicon wafer.

## RECOMMENDED FUTURE WORK

This dissertation demonstrates the successful controlled polymerization of primary amine functionalized vinyl monomers (AEMA **(6)** and APMA **(12)**) through aqueous RAFT polymerization and their bioconjugation with D-glucuronic acid sodium salt **(5)** through reductive amination. A quantitative conversion was achieved in the bioconjugation between PAPMA **(16)** and D-glucuronic acid sodium salt **(5)**. The resulting polymer presents the first example of a carboxylic acid functionalized glycopolymer. This glycopolymer may specifically be used for comparative evaluation with hyaluronic acid. Suggested further studies involving the glycopolymers include evaluation of nanotribological performance of thin films prepared from the glycopolymer, investigation of protein-glycopolymers interactions and development of stimuli-responsive films utilizing layer-by-layer assembly processes.

We also demonstrate the surface attachment of PAEMA **(16)** through “click” chemistry. However, there is still an incomplete understanding of the factors controlling the surface morphology observed for this system. Therefore, a detailed surface characterization using AFM and XPS spectroscopy is recommended to determine the extent of functionalization and coverage of the surfaces. Additionally, the synthesized alkynyl-functionalized CTP **(25)** can be attached to the azide functionalized surface to produce PAEMA **(16)** brushes through the “grafting from” technique. A comparison of the grafting density and surface morphology of systems prepared through “grafting to” and “grafting from” approaches is recommended. The resulting primary amine functionalized brushes can further be bioconjugated with D-glucuronic acid sodium salt **(5)** to yield carboxylic acid functionalized glycopolymer brushes.

## APPENDIX

### Introduction

Recently, much research has focused on the synthesis of polymer brushes through RAFT polymerization techniques. Researchers have used five different approaches to develop polymer brushes on both silica nanoparticles and silicon wafer. First, a conventional surface initiator was attached on the surface and then RAFT polymerization attempted upon addition to CTA.<sup>288,289</sup> Second, CTA was attached on the surface through the R group.<sup>290,291,292</sup> Third, the CTA was immobilized on the surface from the Z group.<sup>293,294,295</sup> Fourth, the functional polymer was first prepared through RAFT polymerization and attached on the surface through click chemistry or reacting with a surface double bond in the presence of excess radical initiator<sup>296</sup> Finally, the block copolymers carrying triethoxysilyl groups were synthesized and attached on the surface.<sup>297,298</sup> Among these methods, R group approach has attracted much attention due to its simple reaction conditions and having a potential to provide higher molecular grafted polymers and grafting density.

In this chapter, two attempted methods to attach the CTA on the silicon wafer using the R group approach are described. However, these two approaches failed, most likely due to side reactions. Additionally, an attempt to synthesize a conventional free radical initiator for the purpose of surface polymerization is described.

## Experimental

*Materials.* All reagents were used without further purification unless otherwise noted. Methacryloyl chloride (>97%), aminopropyltrimethoxysilane (98%) (APTMS), 9-Decen-1-ol (97%), allyl alcohol (99%), trichlorohydrosilane (99%), anhydrous tetrahydrofuran (THF), dichloroethane (CH<sub>2</sub>Cl<sub>2</sub>) and anhydrous toluene, were purchased from Aldrich. 4-Dimethylamino-pyridine (99%) (DMAP), 2-mercaptothiazoline (98%) and *N,N'*-dicyclohexyl-carbodiimide (99%) (DCC) were purchased from Acros Organics. Phenylmagnesium bromide solution (3M in diethyl ether), Karstedt catalyst were purchased from Fluka. 30% Hydrogen peroxide (H<sub>2</sub>O<sub>2</sub>), sulfuric acid (H<sub>2</sub>SO<sub>4</sub>), diethylether, ethylacetate, hexane, and hydrochloric acid were purchased from Fisher. 4,4'-azobis(4-cyanovaleric acid) (V-501) (**13**) was purchased from Wako Pure Products and recrystallized from methanol. Silicon wafers were purchased from Silicon Inc., and cut into 1 x 2 cm pieces using a diamond-tipped glass cutter. 4-Cyanodithiobenzoic acid (CTP) (**14**) was synthesized according to literature procedure.<sup>180</sup>

*The Synthesis of Dec-9-enyl 4-Cyano-4-(Phenylcarbonothioylthio)-Pentanoate (32).* In a 100 ml flask equipped with stir bar and an additional funnel, a solution of CTP (**14**) (1 g, 3.58 mmol), 9-Decen-1-ol (0.614 g, 3.94 mmol), 4-(dimethylamino)pyridine (DMAP) (40 mg, 0.317 mmol) in 30 ml of dichloromethane was cooled to 0 °C under nitrogen. DCC (0.812 g, 3.94 mmol) was dissolved in 5 ml of dichloromethane and added dropwise to the reaction flask under stirring. The reaction was stirred under room temperature for overnight. Dec-9-enyl 4-cyano-4-(phenylcarbonothioylthio)-pentanoate was purified via column chromatography using 2:1 hexane:ethyl acetate eluent mixture.

After removal of solvent, the red fraction gave 4-cyano-4-((thiobenzoyl)sulfanyl)-pentanoic acid as a red oil. The product solidified upon sitting at -20 °C.

$^1\text{H}$  NMR ( $\text{CDCl}_3$ )  $\delta$  (ppm): 1.95 (s, 3H,  $\text{CH}_3$ ); 2.40- 2.80 (m, 4H,  $\text{CH}_2\text{CH}_2$ ); 7.42 (m, 2H, *m*-ArH); 7.60 (m, 1H, *p*-ArH); 7.91 (m, 2H, *o*-ArH).

*Hydrosilylation of Dec-9-enyl 4-Cyano-4-(Phenylcarbonothioylthio)-Pentanoate.*

Hydrosilylation experiment was implemented for the addition of trichlorosilane on the double bond of dec-9-enyl 4-cyano-4-(phenylcarbonothioylthio)-pentanoate. In a glove box, to a dry flask were added 1.0 g of 1 and 15 ml of trichlorosilane, followed by the addition of 4  $\mu\text{l}$  of Karstedt catalyst. The mixture was stirred at room temperature within 5 h. The starting color of the mixture was dark pink and this was maintained during the reaction. After the reaction, reaction medium was filtered and excess trichlorosilane was removed under reduced pressure. The resulting product was red solid, which was dissolved in  $\text{CDCl}_3$  and characterized through  $^1\text{H}$  NMR.

*Activation of CTP (14).* CTP (**14**) (1.40 g, 5.00 mmol), 2-mercaptothiazoline (0.596 g, 5.00 mmol), and dicyclohexylcarbodiimide (DCC) (1.24 g, 6.00 mmol) were dissolved in 20 mL of dichloromethane. (Dimethylamino)pyridine (DMAP) (61 mg, 0.50 mmol) was added slowly to the solution, which was stirred at room temperature for 6 h. The solution was filtered to remove the salt. After removal of solvent and silica gel column chromatography (5:4 mixture of hexane and ethyl acetate), activated CPDB was obtained as a red oil (1.57 g, 83% yield).

$^1\text{H}$  NMR (300 MHz,  $\text{CDCl}_3$ ):  $\delta$  (ppm) 7.90 (d, 2H, ph); 7.56 (t, 1H, ph); 7.38 (t, 2H, ph); 4.58 (t, 2H,  $\text{NCH}_2\text{CH}_2\text{S}$ ); 3.60-3.66 (m, 2H,  $(\text{CN})\text{C}(\text{CH}_3)\text{-CH}_2\text{CH}_2\text{CON}$ ); 3.31 (t, 2H,  $\text{NCH}_2\text{CH}_2\text{S}$ ); 2.50-2.56 (m, 2H,  $(\text{CN})\text{C}(\text{CH}_3)\text{CH}_2\text{CH}_2\text{CON}$ ); 1.95 (s, 3H,  $(\text{CH}_3)\text{C}(\text{CN})\text{S}$ ).

*Functionalization of Silicon Wafers with CTP (14).* Pre-cut silicon wafers were rinsed with ethanol, acetone and then immersed in piranha solution (conc.  $\text{H}_2\text{SO}_4/\text{H}_2\text{O}_2$ ) for approximately 1 h. The silicon substrates were then washed thoroughly with deionized water. After a washing step with ethanol the wafers were blown dried and immediately immersed in a solution of aminopropyltrimethoxysilane (APTMS) (1 vol.-%) in toluene for 1 h. The samples were rinsed with toluene, acetone, and ethanol. After drying the silicon pieces were immersed in a solution of activated CTP (**14**) in dry toluene (5 vol.-%). The mixture was left to react overnight. The samples were then rinsed with toluene and ethanol.

*Synthesis of Asymmetric Azo-Initiator.* 4,4'-azobis(4-cyanovaleric acid) (**13**) (3.0 g, 11 mmol), dimethylaminopyridine (DMAP) (80 mg, 0.65 mmol) and butanol (0.815 g, 11 mmol) were dissolved in tetrahydrofuran (THF) (25 mL) in a 250 mL round bottom flask under an Ar atmosphere. The solution was cooled to 0 °C and dicyclohexylcarbodiimide (DCC) (2.2 g, 11 mmol) in 20 mL of THF was added dropwise with vigorous stirring. The reaction mixture was stirred at 0 °C for 5 min and then allowed to warm to room temperature overnight. Precipitated dicyclohexylurea (DCU) was removed by filtration and 100 mL of dichloromethane ( $\text{CH}_2\text{Cl}_2$ ) was added. The crude mixture was washed with water (25 mL x 2) and dried over magnesium the crude mixture, allyl alcohol (0.65 g, 11.2 mmol) and DMAP (80 mg, 0.65 mmol) were



dissolved in 25 mL of  $\text{CH}_2\text{Cl}_2$  and cooled to 0 °C. DCC (2.2 g, 11 mmol) in 25 mL of  $\text{CH}_2\text{Cl}_2$  was added dropwise via syringe. The reaction was kept at 0 °C for 5 minutes and then allowed to warm to room temperature overnight. The solids were removed by filtration and the filtrate was washed with saturated sodium bicarbonate (25 mL x 2), water (25 mL x 2) and dried over  $\text{MgSO}_4$ . The solids were removed by filtration and the solvent was removed by rotary evaporation. The residue was passed through a short plug of silica gel using  $\text{CH}_2\text{Cl}_2$  as an eluent. After removal of solvent, the final product was obtained as a yellow oil that solidified upon standing at -4 °C.

$^1\text{H}$  NMR (300 MHz,  $\text{CDCl}_3$ )  $\delta$ : 0.918 (t, 3H); 1.12-1.85 (m, 10H); 2.21-2.65 (m, 8H); 4.00-4.15 (m, 2H); 5.42-4.64 (m, 2H); 5.18-5.38 (m, 2H); 5.80-5.95 (m, 1H).

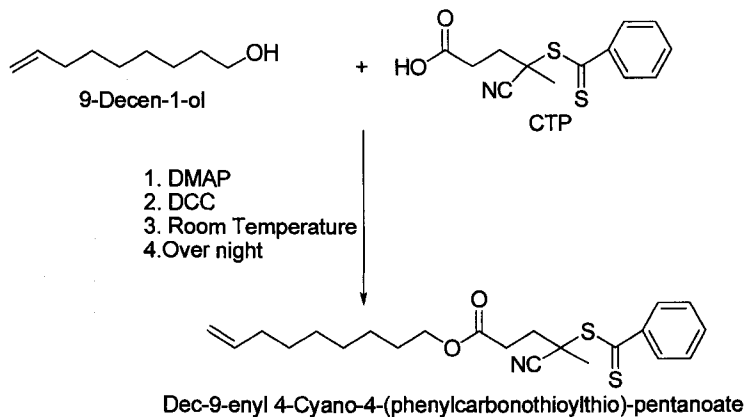
*Hydrosilylation of Asymmetric Azo-Initiator.* Hydrosilylation experiment was performed as described in the previous section.

## Results and Discussion

Initially, the synthesis of trichlorosilane functionalized CTP (**14**) was attempted. First CTP (**14**) carrying a double bond on the R group was synthesized (Scheme Appendix-1). CTP (**14**) was reacted with 9-decen-1-ol in the presence of DCC/DMAP coupling agents. The resulting product was verified through  $^1\text{H}$ -NMR (Figure Appendix-1).

It was attempted to attach the resulting product, 9-enyl 4-cyano-4-(phenylcarbanothioylthio)-pentanoate, to the silicon wafer surface using trichlorohydrosilane coupling agent in the presence of Karstedt catalyst. However, the

reaction appeared unsuccessful. The reason for this may be the potential complexation of the catalyst with the sulfur atoms of the CTP (**14**) double bond.



**Scheme Appendix-1.** Synthesis of 9-enyl 4-cyano-4-(phenylcarbonothioylthio)-pentanoate.

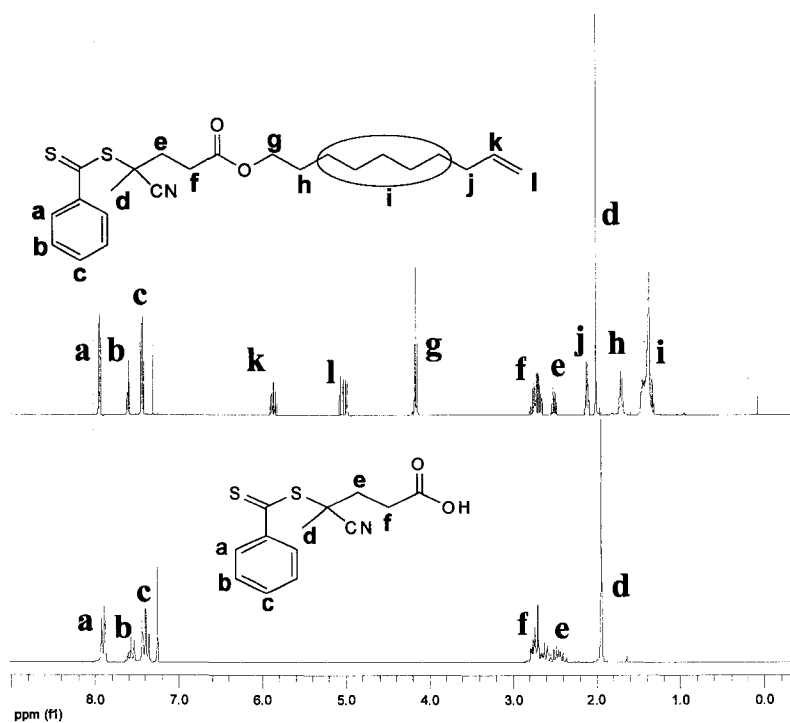
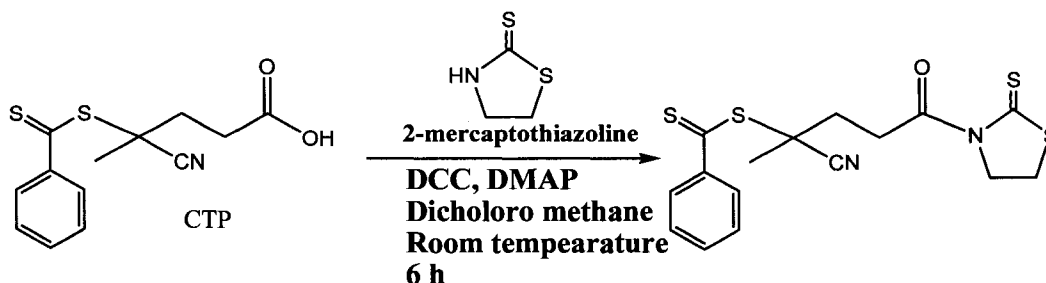


**Figure Appendix-1.**  $^1\text{H-NMR}$  of 9-enyl 4-cyano-4-(phenylcarbonothioylthio)-pentanoate.

Regarding the possible side reactions during the hydrosilylation reaction, it was decided to attempt to attach the CTP (**14**) directly to the amine functionalized silicon wafers through the R group. For this purpose, CTP (**14**) was first activated upon the reaction with 2-mercaptothiazoline in the presence of DCC/DMAP coupling agents (Scheme Appendix-2). The resulting product was characterized through  $^1\text{H-NMR}$  (Figure Appendix-2). The activated CTP (**14**) was reacted with amine functionalized silicon wafers overnight using toluene as solvent. However, a color transformation was observed in the solution from red to yellow, indicating the aminolysis reaction, where the free amine attacks to dithiocarbonyl group resulting in side products.



**Scheme Appendix-2.** CTP activation.

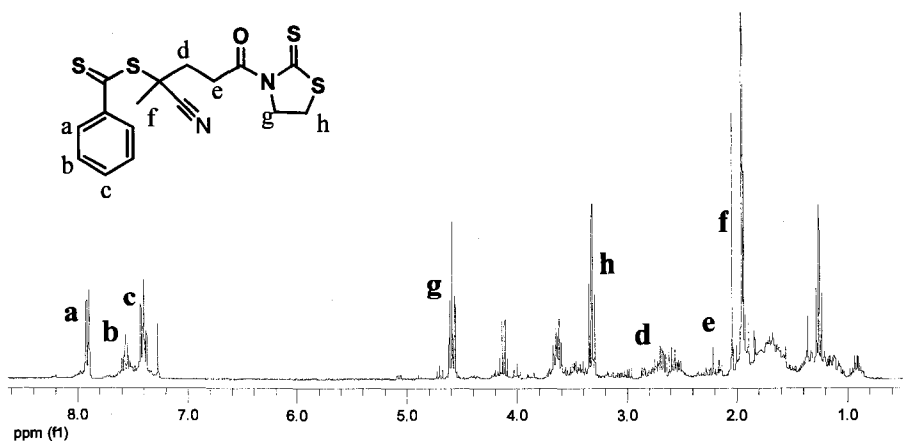
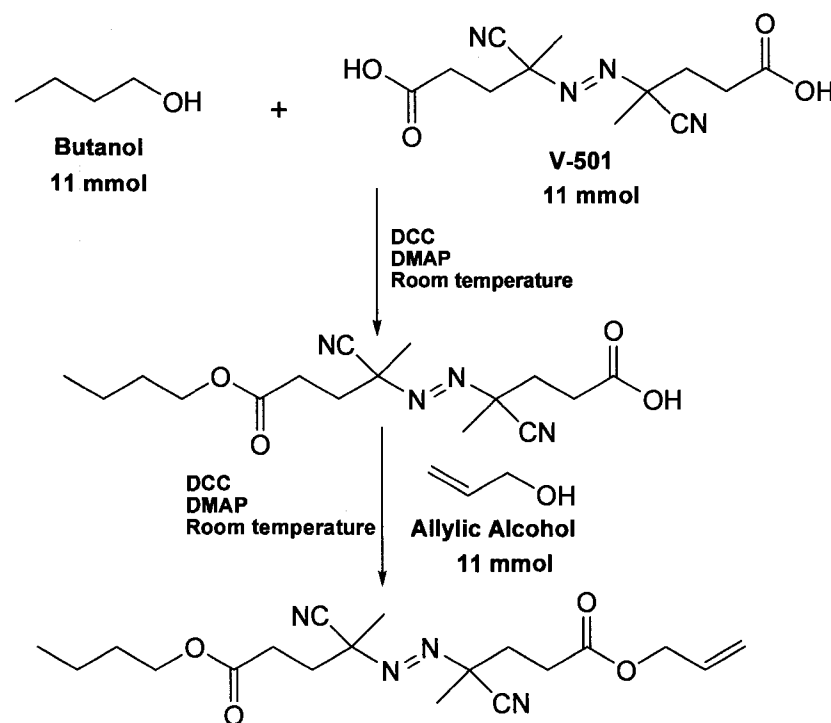


**Figure Appendix-2.**  $^1\text{H-NMR}$  of CTP activation.

Finally, it was attempted to synthesize trichlorosilane functionalized asymmetric diazoinitiator to use for the surface polymerization. 4,4'-azobis(4-cyanovaleric acid) (**13**) was first reacted with n-butanol in the presence of DCC/DMAP coupling agents and then the resulting product was reacted with allylic alcohol to yield double bond functionalized asymmetric diazoinitiator (Scheme Appendix-3). The resulting product was proved through  $^1\text{H-NMR}$  (Figure Appendix-3). However, the addition of trichlorohydro silane to the double bond did not occur. The reason of this might be incorrect choice of catalyst system.



**Scheme Appendix-3.** Synthesis of double bond functionalized asymmetric diazoinitiator.

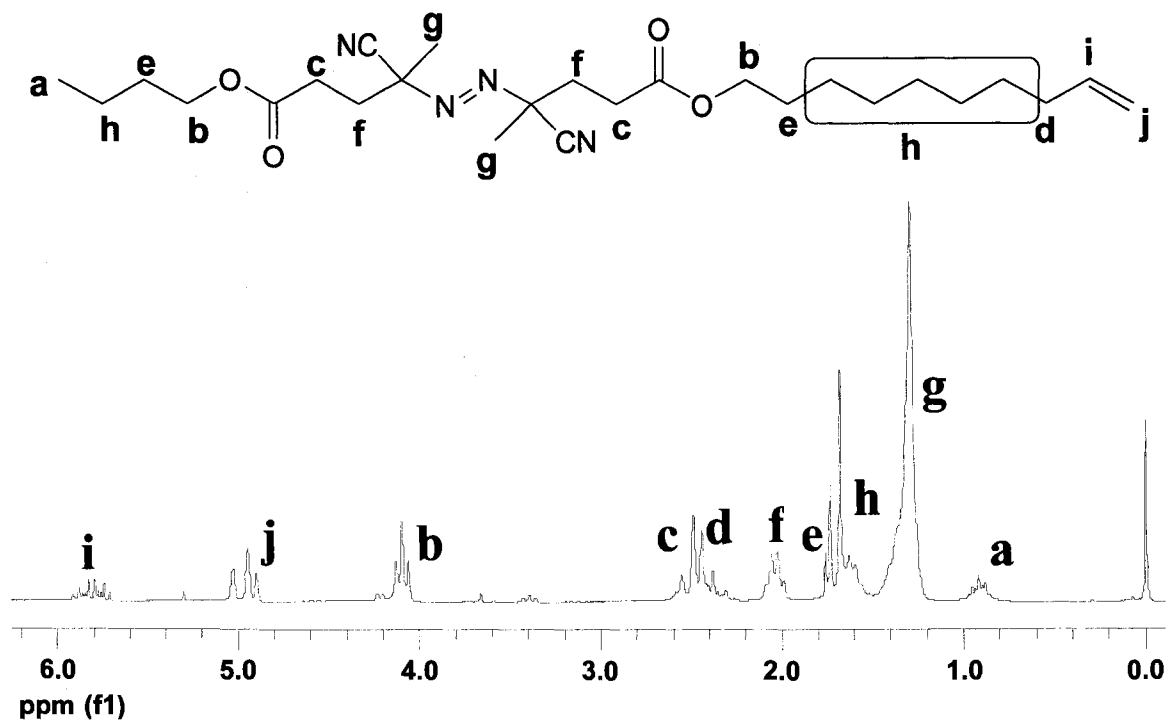


**Figure Appendix-3.** <sup>1</sup>H-NMR of the double bond functionalized asymmetric diazo initiator.

## Conclusion

In this part of the dissertation, it was attempted to synthesize a convenient surface CTA or initiator for RAFT polymerization from the surface. However, none of the approaches were successful. The main problem in the synthesis of surface CTA is the hydrosilylation step, where trichlorohydrosilane adds to the double bond in the presence of a specific catalyst system. The reactions were performed in the presence of the Karstedt catalyst, which is widely reported for hydrosilylation reactions of double bonds.<sup>299</sup> It is likely that both sulfur and nitrogen atoms form complexes with the catalyst. This decreases the catalysis activity during the reaction. In addition, although a strong activation agent was used to activate the carboxylic acid group of the CTP (**14**), the direct deposition of CTP (**14**) on the amine functionalized surface failed. The results prove that the aminolysis reaction can be avoided even in the presence of the strong activation agent.

## REFERENCES

- 
- (1) Abatangelo, G.; O'Reagan, J. *Eur. J. Rheumatol. Inflamm.* **1995**, *15*, 6.
  - (2) Schurtz, J. *Pure Applied Chemistry* **1996**, *A33*, 1249.
  - (3) Guerra, D.; Sbarbati, R.; Cascone, M. G.; Barbandi, N.; Lazzeri, L. *J. Mater Sci.: Mater Med* **1994**, *5*, 613.
  - (4) Weiss, C; The chemistry, Biology and Mediacal Applications of HA and Its Derivatives, Portland Press, **1998**.
  - (5) Crescenzi, V.; Tomasi, M.; Francescangeli, A.; *In New Frontiers in Medical Science*, Elsevier, **2000**.
  - (6) Benedetti, L.; Cortivo, R.; Berti, T.; Pea, F. *Biomaterials* **1993**, *14*, 1154.
  - (7) Okamoto, Y.; Minami, S.; Matuhasi, A.; *Elsevier Applied Science*, NewYork, **1992**.
  - (8) Chandy, T.; Sharma, C. P. *Biomater. Art Cells Art Org.* **1990**, *18*, 1.
  - (9) Akira, T.; Kaburaki, M.; Oka, Y.; Hyaluronic Acid, Polymer Science and Engineering Encyclopedia, 1996, CRC press, 3078.
  - (10) Tadmor, R.; Chen, N.; Isrealachvili, J. *J. Biomed. Mater. Res* **2002**, *61*, 514.
  - (11) Benz, M.; Chen, N.; Isrealachvili, J. *J. Biomed. Mater. Res.* **2004**, *71*, 6.
  - (12) Kim, S. A.; Huyn, D.; Moon, T. S.; Mitsumat, T.; Hong, J. S.; Ahn, K. H.; Lee, S. J. *Polymer* **2005**, *46*, 7156.
  - (13) Milas, M.; Rinaudo, M.; Roure, I.; Al-Assaf, S.; Phillips, G.O.; Williams, P.A *Biopolymers* **2001**, *59*, 191.
  - (14) Falcone, S. J.; Palmeri, D. M.; Berg, R. A. *J. of Biomed. Mater. Res. Part A* **2006**, *76A(4)*, 721.
  - (15) Choi, S.-K.; Mammen, M.; Whitesides, G. M. *J Am Chem Soc* **1997**, *119*, 4103.

- 
- (16) Gordon, E. J.; Strong, L. E.; Kiessling, L. L. *Bioorg Med Chem* **1998**, *6*, 1293.
- (17) Yoshida, T.; Akasaka, T.; Choi, Y.; Hattori, K.; Yu, B.; Mimura, T.; Kaneko, Y.; Nakashima, H.; Aragaki, E.; Premanathan, M.; Yamamoto, N.; Uryu, T. *J Polym Sci Part A: Polym Chem* **1999**, *37*, 789.
- (18) Roy, R.; Baek, M.-G. *Rev Mol Biotechnol* **2002**, *90*, 291.
- (19) Fleming, C.; Maldjian, A.; Costa, D. D.; Rullay, A. K.; Haddleton, D. M.; St. John, J.; Penny, P.; Noble, R. C.; Cameron, N. R.; Davis, B. G. *Nat Chem Biol* **2005**, *1*, 270.
- (20) Li, J.; Zacharek, S.; Chen, X.; Wang, J.; Zhang, W.; Janczuk, A.; Wang, P. G. *Bioorg Med Chem* **1999**, *7*, 1549.
- (21) Garcia-Martin, M. G.; Jimenez-Hidalgo, C.; Al-Kass, S. S. J.; Caraballo, I.; de Paz, M. V.; Galbis, J. A. *Polymer* **2000**, *41*, 821.
- (22) Roche, A. C.; Fajac, I.; Grosse, S.; Frison, N.; Rondanino, C.; Mayer, R.; Monsigny, M. *Cell Mol Life Sci* **2003**, *60*, 288.
- (23) Yun, Y. H.; Goetz, D. J.; Yellen, P.; Chen, W. *Biomaterials* **2004**, *25*, 147.
- (24) Novick, S. J.; Dordick, J. S. *Chem Mat* **1998**, *10*, 955.
- (25) Miyata, T.; Uragami, T.; Nakamae, K. *Adv DrugDeliv Rev* **2002**, *54*, 79.
- (26) Kim, S.-H.; Kim, J.-H.; Akaike, T. *FEBS Lett* **2003**, *553*, 433.
- (27) Karamuk, E.; Mayer, J.; Wintermantel, E.; Akaike, T. *Artif Organs* **1999**, *23*, 881.
- (28) Taguchi, T.; Kishida, A.; Sakamoto, N.; Akashi, M. *J Biomed Mater Res* **1998**, *41*, 386.
- (29) Liu, X.-C.; Dordick, J. S. *J Polym Sci Part A: Polym Chem* **1999**, *37*, 1665.
- (30) Wulff, G.; Zhu, L.; Schmidt, H. *Macromolecules* **1997**, *30*, 4533.



- 
- (31) Wulff, G.; Schmidt, H.; Zhu, L. *Macromol ChemPhys* **1999**, *200*, 774.
- (32) Ambrosi, M.; Cameron, N. R.; Davis, B. G.; Stolnik, S. *Org Biomol Chem* **2005**, *3*, 1476.
- (33) Lowe, A. B.; Wang, R. *Polymer* **2007**, *48*, 2221.
- (34) Ladmiral, V.; Mantovani, G.; Clarkson, G. J.; Cauet, S.; Irwin, J. L.; Haddleton, D. *M. J. Am. Chem. Soc.* **2006**, *128*, 4823.
- (35) Wu, P.; Malkoch, M.; Hunt, J. N.; Vesterberg, R.; Kaltgrad, E.; Finn, M. G.; Fokin, V. V.; Sharpless, K. B.; Hawker, C. J. *Chem Commun* **2005**, 5775.
- (36) Xue, C.; Donuru, V. R. R.; Liu, H. *Macromolecules* **2006**, *39*, 5747.
- (37) Anderson, M.; Oscarson, S.; *Bioconjug Chem* **1993**, *4*, 246.
- (38) Hu, Y.; Liu, Y.; Hong, C.; Pan, C. *J Appl Polym Sci* **2005**, *98*, 189.
- (39) O'Reilly, R. K.; Hawker, C. J.; Wooley, K. L. *Chem.Soc. Rev.* **2006**, *35*, 1068.
- (40) Read, E. S.; Armes, S. P. *Chem. Commun.* **2007**, DOI:10.1039/b701217a.
- (41) Deming, T. J. *Nature (London)* **1997**, *190*, 386.
- (42) Wong, M. S.; Cha, J. N.; Choi, K. S.; Deming, T. J.; Stucky, G. D. *Nano letter* **2002**, *2*, 583.
- (43) Halowaka, E. P.; Pochan, D. J.; Deming, T. J. *J. Am. Chem. Soc.* **2005**, *127*, 12423.
- (44) Yuan, J. -J.; Jin, R. -H *Langmuir* **2005**, *21*, 3136.
- (45) Jin, R.-R.; Yuan, J.-J. *Macromol. Chem. Phys.* **2005**, *206*, 2160.
- (46) Yuan, J.-J.; Mykhaylyk, O. O.; Ryan, A. J.; Armes, S. P. *J. Am. Chem. Soc.* **2007**, *129*, 1717.
- (47) Chen, X.; Armes, S. P. *Adv. Mater.* **2003**, *15*, 1558.
- (48) Chen, X.; Armes, S. P.; Greaves, S. J.; Watts, J. F. *Langmuir* **2004**, *20*, 587.

- 
- (49) Vo, C. D.; Schmid, A.; Armes, S. P. *J. Am. Chem. Soc.* **2007**, *23*, 408.
- (50) Duracher, D.; Sauzedde, F.; Elaissari, A.; Perrin, A.; Pichot, C. *Colloid and Polymer Science* **1998**, *276*, 219.
- (51) Nabzar, L.; Duracher, D.; Elaissari, A.; Chauveteau, G.; Pichot, C. *Langmuir* **1998**, *14*, 5062.
- (52) Prazeres, T. V. J.; Santos, A. M.; Martinho, J. M. G.; Elaissari, A.; Pichot, C. *Langmuir* **2004**, *20*, 6834.
- (53) Musyanovych, A.; Rossmann, R.; Tontsch, C.; Landfester, K. *Langmuir* **2007**, *23*, 5367.
- (54) Narrin, R.; Armes, S. P. *Biomacromolecules* **2003**, *4*, 1746.
- (55) Housni, A.; Cai, H.; Pun, S. H.; Narain, R. *Langmuir* **2007**, *23*, 5056.
- (56) Yang, Q.; Xu, Z.; Dai, Z.; Wang, J.; Ulbricht, M. *Chem. Mater.* **2005**, *17*, 3050.
- (57) Iwasaki, Y.; Takami, U.; Shinohara, Y.; Kurita, K.; Akiyoshi, K. *Biomacromolecules* **2007**, *8*, 2788.
- (58) Chang, Y.; Ahn, Y. S.; Hahn, T.; Chen, Y. *Langmuir* **2007**, *23*, 4112.
- (59) Kim, M. R.; Jeong, J. H.; Park, T. G. *Biotechnol. Prog.* **2002**, *18*, 495.
- (60) Kuroda, K.; DeGrado, W. F. *J. Am. Chem. Soc.* **2005**, *127*, 4128.
- (61) Dubruel, P.; Christiaens, B.; Rosseneu, M.; Vanderkerckhove, J.; Grooten, J.; Goossens, V.; Schacht, E. *Biomacromolecules* **2004**, 3791.
- (62) Van Dijk-Wolthuis, W.N.E.; van de Wetering, P.; Hinrichs, W. L. J.; Hofmeyer, L. J. F.; Liskamp, R. M. J.; Crommelin, D. J. A.; Hennink, W. E. *Bioconjugate Chem.* **1999**, *10*, 687.
- (63) Matyjaszewski, J. Xia, J. *Chem. Rev.* **2001**, *101*, 2921.

- 
- (64) Moad, G.; Rizzardo, E.; Tang, S. H. *Aust. J. Chem.* **2005**, *58*, 379.
- (65) McCormick, C. L.; Lowe, A. B. *ACC. Chem. Res.* **2004**, *37*, 312.
- (66) Dufresne, M. H.; Leroux, J. C. *Pharm. Res.* **2004**, *21*, 160.
- (67) He, L.; Read, E. S.; Armes, S. P.; Adams, D. J. *Macromolecules*, **2007**, *40*, 4429.
- (68) Scales, C. W.; Convertine, A. J.; McCormick, C. L. *Biomacromolecules* **2006**, *7*, 1389.
- (69) David, A.; Kopeckova, P.; Minko, T.; Rubinstein, A.; Kopecek, J. *Eur. J. Cancer* **2004**, *20*, 148.
- (70) Satch-Fainaro, R.; Hailu, H.; Davies, J. W.; Summerford, C.; Duncan, R. *Bioconjugate Chem.* **2003**, *14*, 1724.
- (71) Tang, A.; Kopeckova, P.; Kopecek, J. *Pharm. Res.* **2003**, *20*, 360.
- (72) Ulbrich, K.; Etrych, T.; Chytil, P.; Pechar, M.; Jelinkova, M.; Rihova, B. *Int. J. Pharm.* **2004**, *277*, 63.
- (73) Nori, A.; Kopecek, J. *Adv. Drug delivery Rev.* **2005**, *57*, 609.
- (74) Kovar, M.; Kovar, L.; Subr, V.; Etrych, T.; Ulbrich, K.; Mrkvan, T.; Louchka, J.; Rihova, B. *J. Controlled Release* **2004**, *99*, 301.
- (75) Jelinkova, M.; Strohalm, J.; Etrych, T.; Ulbrich, K.; Rihova, B. *Pharm. Res.* **2003**, *20*, 1558.
- (76) Etrych, T.; Jelinkova, M.; Rihova, B.; Ulrich, K.; *J. Controlled Release* **2001**, *73*, 89.
- (77) McCormick, C. L.; Kirkland, S. E.; York, A. W. *J. Macromol. Sci. Polym. Rev.* **2006**, *46*, 421.

- 
- (78) Scales, W. C.; Huang, F.; Li, N.; Vasilieva, Y. A.; Ray, J.; Convertine, A. J.; McCormick, C. L. *Macromolecules* **2006**, *39*, 6871.
- (79) Y. Li, B. S. Lokitz, C. L. McCormick *Angew. Chem. Int. Ed.*, **2006**, *45*, 5792.
- (80) Chiefari, J.; Chong, Y. K.; Ercole, F.; Krstina, J.; Jeffery, J.; Le, T. P. T.; Mayadunne, R. T. A.; Meijs, G. F.; Moad, C. L.; Moad, G.; Rizzardo, E.; Thang, S. H. *Macromolecules* **1998**, *31*, 5559.
- (81) Rizzardo, E.; Thang, S. H.; Moad, G.: PCT Int. Appl. WO 9905099, 1998.
- (82) Lokitz, B. S.; Ph. D. Thesis, University of Southern Mississippi: Hattiesburg, 2007.
- (83) Moad, G.; Soloman, D. G. *The Chem of Radical Polymerization 2nd Ed*, 2 ed.; Elsevier: Amsterdam, 2006.
- (84) Quinn, J. F.; Barner, L.; Barner-Kowollik, C.; Rizzardo, E.; Davis, T. P. *Macromolecules* **2002**, *35*, 7620.
- (85) You, Y. Z.; Hong, C. Y.; Bai, R. K.; Pan, C. Y.; Wang, J. S. *Macromol. Chem. Phys.* **2002**, *203*, 477.
- (86) Quinn, J. F.; Barner, L.; Davis, T. P.; Thang, S. H.; Rizzardo, E. *Macromol. Rapid Commun.* **2002**, *23*, 717.
- (87) Chen, G.; Zhu, X.; Zhu, J.; Cheng, Z. *Macromol. Rapid Commun.* **2004**, *25*.
- (88) Barner-Kowollik, C.; Buback, M.; Charleux, B.; Coote, M. L.; Drache, M.; Fukuda, T.; Goto, A.; Klumperman, B.; Lowe, A. B.; McCleary, J. B.; Moad, G.; Monteiro, M. J.; Sanderson, R. D.; Tonge, M. P.; Vana, P. *J. Polym. Sci., Part A: Polym. Chem.* **2006**, *44*, 5809.
- (89) Wang, A. R.; Zhu, S. *J. Polym. Sci., Polym. Chem.* **2003**, *41*, 1553.

- 
- (90) Thomas, D. B.; Convertine, A. J.; Myrick, L. J.; Scales, C. W.; Smith, A. E.; Lowe, A. B.; Vasilieva, Y. A.; Ayres, N.; McCormick, C. L. *Macromolecules* **2004**, *37*, 8941.
- (91) Moad, G.; Chiefari, J.; Chong, Y. K.; Krstina, J.; Mayadunne, R. T. A.; Postma, A.; Rizzardo, E.; Thang, S. H. *Polym. Int.* **2000**, *49*, 993.
- (92) Moad, G.; Rizzardo, E.; Thang, S. H. *Aust. J. Chem.* **2006**, *59*, 669.
- (93) Chiefari, J.; Mayadunne, R. T. A.; Moad, C. L.; Moad, G.; Rizzardo, E.; Postma, A.; Skidmore, M. A.; Thang, S. H. *Macromolecules* **2003**, *36*, 2273.
- (94) Stenzel, M. H.; Cummins, L.; Roberts, G. E.; Davis, T. P.; Vana, P.; Barner-Kowollik, C. *Macromol. Chem. Phys.* **2003**, *204*, 1160.
- (95) Destarac, M.; Charmot, D.; Franck, X.; Zard, S. Z. *Macromol. Rapid Commun.* **2001**, *21*, 1035.
- (96) Mayadunne, R. T. A.; Rizzardo, E.; Chiefari, J.; Chong, Y. K.; Moad, G.; Thang, S. H. *Macromolecules* **1999**, *32*, 6977.
- (97) Rizzardo, E.; Chiefari, J.; Mayadunne, R. T. A.; Moad, G.; Thang, S. H. *ACS Symp. Ser.* **2000**, *768*, 278.
- (98) Kwak, Y.; Goto, A.; Tsujii, Y.; Murata, Y.; Komatsi, K.; Fukuda, T. *Macromolecules* **2002**, *35*, 3026.
- (99) Barner-Kowollik, C.; Quinn, J. F.; Nguyen, T. L. U.; Heuts, J. P. A.; Davis, T. P. *Macromolecules* **2001**, *34*, 7849.
- (100) Moad, G.; Chiefari, J.; Mayadunne, R. T. A.; Moad, C. L.; Postma, A.; Rizzardo, E.; Thang, S. H. *Macromol. Symp.* **2002**, *182*, 65.
- (101) Monteiro, M. J.; de Brouwer, H. *Macromolecules* **2001**, *34*, 349.

- 
- (102) Barner-Kowollik, C.; Quinn, J. F.; Morsley, D. R.; Davis, T. P. *J. Polym. Sci., Polym. Chem.* **2001**, *39*, 1353.
- (103) Thomas, D. B.; Sumerlin, B. S.; Lowe, A. B.; McCormick, C. L. *Macromolecules* **2003**, *36*, 1436.
- (104) Donovan, M. S.; Sumerlin, B. S.; Lowe, A. B.; McCormick, C. L. *Macromolecules* **2002**, *35*, 8663.
- (105) Schilli, C.; Lanzendoerfer, M. G.; Müller, A. H. E. *Macromolecules* **2002**, *35*, 6819.
- (106) Barner-Kowollik, C.; Vana, P.; Davis, T. P. In *Handbook of Radical Polymerization*; Matyjaszewski, K.; Davis, T. P., Eds.; Wiley: Hoboken, 2002; pp 187.
- (107) Vana, P.; Davis, T. P.; Barner-Kowollik, C. *Macromol. Theory Simul.* **2002**, *11*, 823.
- (108) Wang, A. R.; Zhu, S. *Macromol. Theory Simul.* **2003**, *12*, 663.
- (109) McLeary, J. B.; Calitz, F. M.; McKenzie, J. M.; Tonge, M. P.; Sanderson, R. D.; Klumperman, B. *Macromolecules* **2005**, *38*, 3151.
- (110) McLeary, J. B.; McKenzie, J. M.; Tonge, M. P.; Sanderson, R. D.; Klumperman, B. *Chem. Commun.* **2004**, 1950.
- (111) Fischer, H.; Radom, L. *Angew. Chem. Int. Ed.* **2001**, *40*, 1340.
- (112) Calitz, F. M.; Tonge, M. P.; Sanderson, R. D. *Macromolecules* **2003**, *36*, 5.
- (113) Ah Toy, A.; Vana, P.; Davis, T. P.; Barner-Kowollik, C. *Macromolecules* **2004**, *37*, 744.

- 
- (114) Barner-Kowollik, C.; Coote, M. L.; Davis, T. P.; Radom, L.; Vana, P. *J. Polym. Sci., Polym. Chem.* **2003**, *41*, 2828.
- (115) Perrier, S.; Barner-Kowollik, C.; Quinn, J. F.; Vana, P.; Davis, T. P. *Macromolecules* **2002**, *35*, 8300.
- (116) Zhang, M.; Ray, W. H. *Ind. Eng. Chem. Res.* **2001**, *40*, 4336.
- (117) Coote, M. L.; Radom, L. *J. Am. Chem. Soc.* **2003**, *125*, 1490.
- (118) Coote, M. L. *Macromolecules* **2004**, *37*, 5023.
- (119) Vana, P.; Quinn, J. F.; Davis, T. P.; Barner-Kowollik, C. *Aust. J. Chem.* **2002**, *55*, 425.
- (120) Monteiro, M. J.; Bussels, R.; Beuermann, S.; Buback, M. *Aust. J. Chem.* **2002**, *55*, 433.
- (121) Barner-Kowollik, C.; Vana, P.; Quinn, J. F.; Davis, T. P. *J. Polym. Sci., Polym. Chem.* **2002**, *40*, 1058.
- (122) Kwak, Y.; Goto, A.; Fukuda, T. *Macromolecules* **2004**, *37*, 1219.
- (123) Kwak, Y.; Goto, A.; Tsujii, Y.; Murata, Y.; Komatsu, K.; Fukuda, T. *Macromolecules* **2002**, *40*, 1058.
- (124) Kwak, Y.; Goto, A.; Komatsu, K.; Sugiura, Y.; Fukuda, T. *Macromolecules* **2004**, *37*, 4434.
- (125) Wang, A. R.; Zhu, S.; Kwak, Y.; Goto, A.; Fukuda, T.; Monteiro, M. J. *J. Polym. Sci., Polym. Chem.* **2003**, *41*, 2833.
- (126) Walbiner, M.; Wu, J. Q.; Fischer, H. *Helv. Chim. Acta* **1995**, *78*, 910.
- (127) Calitz, F. M.; McLeary, J. B.; McKenzie, J. M.; Tonge, M. P.; Klumperman, B.; Sanderson, R. D. *Macromolecules* **2003**, *36*, 9687.

- 
- (128) Plummer, R.; Goh, Y.; Whittaker, A. K.; Monteiro, M. J. *Macromolecules* **2005**, *38*, 5352.
- (129) Müller, A. H. E.; Zhuang, R.; Yan, D.; Litvenko, G. *Macromolecules* **1995**, *28*, 4326.
- (130) de Brouwer, H.; Ph. D. Thesis, Eindhoven University of Technology: Eindhoven, 2001.
- (131) Chong, B. Y. K.; Moad, G.; Rizzardo, E.; Skidmore, M. A.; Thang, S. H. In *27th Australian Polymer Symposium*, 2004.
- (132) Chong, Y. K.; Le, T. P. T.; Moad, G.; Rizzardo, E.; Thang, S. H. *Macromolecules* **1999**, *32*, 2071.
- (133) Li, Y.; Lokitz, B. S.; McCormick, C. L. *Macromolecules* **2006**, *39*, 81.
- (134) Mitsukami, Y.; Donovan, M. S.; Lowe, A. B.; McCormick, C. L. *Macromolecules* **2001**, *34*, 2248.
- (135) Sumerlin, B. S.; Donovan, M. S.; Mitsukami, Y.; Lowe, A. B.; McCormick, C. L. *Macromolecules* **2001**, *34*, 6561.
- (136) Sumerlin, B. S.; Lowe, A. B.; Thomas, D. B.; McCormick, C. L. *Macromolecules* **2003**, *36*, 5982.
- (137) Donovan, M. S.; Lowe, A. B.; Sanford, T. A.; McCormick, C. L. *J. Polym. Sci., Polym. Chem.* **2003**, *41*, 1262.
- (138) Thomas, D. B.; Convertine, A.; Hester, R. D.; Lowe, A. B.; McCormick, C. L. *Macromolecules* **2004**, *37*, 1735.
- (139) Convertine, A. J.; Lokitz, B. S.; Lowe, A. B.; Scales, C. W.; Myrick, L. J.; McCormick, C. L. *Macromol. Rapid Commun.* **2005**, *26*, 791.



- 
- (140) Convertine, A. J.; Ayres, N.; Scales, C. W.; Lowe, A. B.; McCormick, C. L. *Biomacromolecules* **2004**, *5*, 1177.
- (141) Convertine, A. J.; Lokitz, B. S.; Vasilieva, Y. A.; Myrick, L. J.; Scales, C. W.; Lowe, A. B.; McCormick, C. L. *Macromolecules* **2006**, *5*, 1724.
- (142) Edmondson, S.; Osborne, V. L.; Huck, W. T. S. *Chem. Soc. Rev.* **2004**, *33*, 14.
- (143) Tsujii, Y.; Ejaz, M.; Sato, K.; Goto, A.; Fukuda, T. *Macromolecules* **2001**, *34*, 8872.
- (144) Fu, G. D.; Zong, B. Y.; Kang, E. T.; Neoh, K. G. *Ind. Eng. Chem. Res.* **2004**, *43*, 6723.
- (145) Yu, W. H.; Kang, E. T.; Neoh, K. G. *Langmuir* **2005**, *21*, 450.
- (146) Perrier, S.; Takolpuckdee, P.; Westwood, J.; Lewis, D. M. *Macromolecules* **1987**, *20*, 675.
- (147) Takolpuckdee, P.; Westwood, J.; Lewis, D. M.; Perrier, S. *Macromol. Symp.* **2004**, *216*, 23.
- (148) Skaff, H.; Emrick, T. *Angew. Chem. Int. Ed.* **2004**, *43*, 5383.
- (149) Bae, W. S.; Convertine, A.; McCormick, C. L.; Urban, M. W. *Langmuir* **2007**, *23*, 667.
- (150) Sumerlin, B. S.; Lowe, A. B.; Stroud, P. A.; Zhang, P.; Urban, M. W.; McCormick, C. L. *Langmuir* **2003**, *19*, 5559.
- (151) Matsumoto, K.; Tsuji, R.; Yonemushi, Y.; Yoshida, T. *Chem. Lett.* **2004**, *33*, 4526.
- (152) Shan, J.; Nuopponen, M.; Jiang, H.; Kauppinen, E.; Tenhu, H. *Macromolecules* **2003**, *36*, 4526.
- (153) Tornøe, C. W.; Christensen, C.; Meldal, M. *J. Org. Chem.* **2002**, *67*, 3057.

- 
- (154) Ranjan, R.; Brittain, W. J. *Macromolecules* **2007**, *40*, 6217.
- (155) Ranjan, R.; Brittain, W. J. *Macromol. Rapid. Commun.* **2008**, *29*, 1104.
- (156) Coessens, V.; Pintauer, T.; Matyjaszewski, K. *Prog. Polym. Sci.* **2001**, *26*, 337.
- (157) Schulz, D. N.; Patil, A. O. *Acs Symp. Ser.* **1998**, *704*, 1.
- (158) Mantovani, G.; Ladmiral, V.; Tao, L.; Haddleton, D. M. *Chem. Commun.* **2005**, 2089.
- (159) Bontempo, D.; Li, R. C.; Ly, T.; Brubaker, C. E.; Maynard, H. D. *Chem. Commun.* **2005**, 2089.
- (160) Lowe, A. B.; Summerlin, B. S.; Donovan, M. S.; McCormick, C. L. *J. Am. Chem. Soc.* **2002**, *124*, 11562.
- (161) York, A. W.; Scales, W. C.; Huang, F.; McCormick, C. L. *Biomacromolecules* **2007**, *8*, 2337.
- (162) Kolb, H. C.; Finn, M. G.; Sharpless, K. B. *Angew. Chem. Int. Ed.* **2004**, *40*, 2004.
- (163) Wang, Q.; Chittaboina, S.; Barnhill, H. N. *Lett. Org. Chem.* **2005**, *2*, 293.
- (164) Kolb, H. C.; Sharpless, K. B. *Drug Discovery Today*. **2003**, *24*, 1128.
- (165) Tornøe, C. W.; Christensen, C.; Meldal, M. *J. Org. Chem.* **2002**, *67*, 3057.
- (166) Rostovtsev, V. V.; Green, L. G.; Fokin, V. V.; Sharpless, K. B. *Angew. Chem. Int. Ed.* **2002**, *41*, 2596.
- (167) Wu, P.; Feldman, A. K.; Nungent, A. K.; Hawker, C. J.; Scheel, A.; Voit, B.; Pyun, J.; Frechet, J. M. J.; Sharpless, K. B.; Fokin, V. V. *Angew. Chem. Int. Ed.* **2004**, *116*, 4018.
- (168) Jorelemon, M. J.; O'Reilly, R. K.; Hawker, C. J.; Wooley, K. L. *J. Am. Chem. Soc.* **2005**, *127*, 16892.

- 
- (169) O'Reilly, R. K.; Joralemon, M. J.; Wooley, K. L.; Hawker, C. J. *Chem. Mater.* **2005**, *17*, 5976.
- (170) Wu, P.; Malkoch, M.; Hunt, J. N.; Vestberg, R.; Kaltgrad, E.; Finn, M. G.; Fokin, V.; Sharpless, K. B.; Hawker, C. J. *Chem. Commun.* **2005**, 5775.
- (171) Riva, R.; Schmeits, S.; Stoffelbach, F.; Jerome, C.; Jerome, R.; Lecomte, P. *Chem. Commun.* **2005**, 5334.
- (172) van Steenis, D. J. V. C.; David, O. R. P.; van Strijdonck, G. P. F.; van Maarseveen, J. H.; Reek, J. N. H. *Chem. Commun.* **2005**, 4333.
- (173) Parrish, B.; Breitenkamp, R. B.; Emrick, T. *J. Am. Chem. Soc.* **2005**, *127*, 7404.
- (174) Diaz, D. D.; Punna, S.; Holzer, P.; McPherson, A. K.; Sharpless, K. B.; Fokin, V. V.; Finn, M. G. *J. Polym. Sci., Part A: Polym. Chem.* **2004**, *42*, 4392.
- (175) Tsarevsky, N. V.; Bernaerts, K. V.; Dufour, B.; Du, Prez, F. E.; Matyjaszewski, K. *Macromolecules* **2004**, *37*, 9308.
- (176) Opsteen, J. A.; van Hest, J. C. M. *Chem. Commun.* **2005**, 57, 1.
- (177) Tsarevsky, N. V.; Sumerlin, B. S.; Matyjaszewski, K. *Macromolecules* **2005**, *38*, 3558.
- (178) Sumerlin, B. S.; Tsarevsky, N. V.; Louche, G.; Lee, R. Y.; Matyjaszewski, K. *Macromolecules* **2005**, *38*, 7540.
- (179) Gao, H.; Louche, G.; Sumerlin, B. S.; Jahed, N.; Golas, P.; Matyjaszewski, K. *Macromolecules* **2005**, *38*, 8979.
- (180) Laurent, B. A.; Grayson, S. M. *J. Am. Chem. Soc.* **2006**, *128*, 4238.
- (181) Johnson, J. A.; Lewis, D. R.; Diaz, D. D.; Finn, M. G.; Koberstein, J. T.; Turro, N. *J. Am. Chem. Soc.* **2006**, *128*, 6564.

- 
- (182) Ladmiral, V.; Mantovani, G.; Clarkson, G. J.; Cauet, S.; Irwin, J. L.; Haddleton, D. *M. J. Am. Chem. Soc.* **2006**, *128*, 4823.
- (183) Agut, W.; Taton, D.; Lecommandoux, S. *Macromolecules* **2007**, *40*, 5653.
- (184) Lutz, J. F.; Borner, H. G.; Weichenhan, K. *Macromol. Rapid Commun.* **2005**, *26*, 514.
- (185) Vogt, A. P.; Sumerlin, B. S. *Macromolecules* **2006**, *39*, 5286.
- (186) O'Reilly, R. K.; Joralemon, M. J.; Lui, W.; Hawker, C. J.; Wooley, K. L. *J. Polym. Sci., Part A: Polym. Chem.* **2006**, *44*, 5203.
- (187) Gondi, S. R.; Vogt, A. P.; Sumerlin, B. S. *Macromolecules* **2007**, *40*, 474.
- (188) Ostaci, R. V.; Damiron, D.; Capponi, S.; Vignaud, G.; Leger, L.; Grohens, Y.; Drockenmuller, E. *Langmuir* **2008**, *24*, 2732.
- (189) Clowes, A. W.; Karnovsky, M. J. *Nature* **1977**, *265*, 625.
- (190) Jackson, R. L.; Busch, S. J.; Cardin, A. L. *Physiol. Rev.* **1991**, *71*, 481.
- (191) Linhardt, R. J.; Kerns, R. J.; Vlahov, I. R. In *Biomedical Functions and Biotechnology of Natural and Artificial Polymers*; ATL Press:1996; p 45.
- (192) Akashi, M.; Sakamoto, N.; Suzuki, K.; Kishida, A. *Bioconjugate Chem.* **1996**, *7*, 393.
- (193) Lutz, J. F.; Borner, H. G. *Prog Polym Sci* **2008**, *33*, 1.
- (194) Sun, X. L.; Grande, D.; Baskaran, S.; Hanson, S. R.; Chaikof, E. L. *Biomacromolecules* **2002**, *3*, 1065.
- (195) Miura, Y.; Yasuda, K.; Yamamoto, K.; Koike, M.; Nishida, Y.; Kobayashi, M. *Biomacromolecules* **2007**, *8*, 2129.

- 
- (196) Spain, S. G.; Gibson, M. I.; Cameron, N. R. *J. Polym. Sci. Part A: Polym. Chem.* **2007**, *45*, 2059.
- (197) Yoshida, T. *Prog. Polym. Sci.* **2001**, *26*, 379.
- (198) Chandra, R.; Rustgi, R. *Prog. Polym. Sci.* **1998**, *23*, 1273.
- (199) Gruner, S. A. W.; Locardi, E.; Lohof, E.; Kessler, H. *Chem. Rev.* **2002**, *102*, 491.
- (200) Ladmiraal, V.; Melia, E.; Haddleton, D. M. *Eur. Polym. J.* **2004**, *40*, 431.
- (201) Dwek, R. A. *Chem. Rev.* **1996**, *96*, 683.
- (202) Varki, A. *Glycobiology* **1993**, *3*, 97.
- (203) Duncan, R. *Nature Rev. Drug Discov.* **2003**, *2*, 347.
- (204) Langer, R.; Tirrell, D. A. *Nature* **2004**, *428*, 487.
- (205) Whitesides, G. M. *Small* **2005**, *1*, 172.
- (206) Zhang, S. *Nature Biotech.* **2003**, *21*, 1171.
- (207) Lee, Y. C.; Lee, R. T. *Acc. Chem. Res.* **1995**, *28*, 321.
- (208) Yoshida, T.; Akasaka, T.; Choi, Y.; Hattori, K.; Yu, B.; Mimura, T. *J. Polym. Sci. Part A: Polym. Chem.* **1999**, *3*, 789.
- (209) Morra, M. *Biomacromolecules* **2005**, *6*, 1205.
- (210) Yusa, S. I.; Shimada, Y.; Mitsukami, Y.; Yamamoto, T.; Morishima, Y. *Macromolecules* **2003**, *36*, 4208.
- (211) Vasilieva, Y. A.; Thomas, D. B.; Scales, C. W.; McCormick, C. L. *Macromolecules* **2004**, *37*, 2728.
- (212) Donovan, M. S.; Lowe, A. B.; Summerlin, B. S.; McCormick, C. L. *Macromolecules* **2002**, *35*, 4123.

- 
- (213) Donovan, M. S.; Stanford, T. A.; Lowe, A. B.; Summerlin, B. S.; Mitsukami, Y.; McCormick, C. L. *Macromolecules* **2002**, *35*, 4570.
- (214) Lai, J. T.; Filla, D.; Shea, R. *Macromolecules* **2002**, *35*, 6754.
- (215) Favier, A.; Charreyre, M. T.; Chaumant, P.; Pichot, C. *Macromolecules* **2002**, *35*, 8271.
- (216) Scales, C. W.; Vaselieva, Y. A.; Convertine, A. J.; Lowe, A. B.; McCormick, C. L. *Biomacromolecules* **2005**, *6*, 1846.
- (217) Lowe, A. B.; Summerlin, B. S.; McCormick, C. L. *Polymer* **2003**, *44*, 6761.
- (218) Ganacaud, F.; Monteiro, M. J.; Gilbert, R. G.; Dourges, M. A.; Thang, S. H.; Rizzardo, E. *Macromolecules* **2000**, *33*, 6738.
- (219) Strohalm, J.; Kopecek, J. *Angew. Makromol. Chem* **1978**, 109.
- (220) Feldermann, A.; Coote, M. L.; Stenzel, M. H.; Davis, T. P. and Barner-Kowollik, C. J. *Am. Chem. Soc.* **2004**, *126*, 15915.
- (221) Yang, J.; Xu, C.; Wang, C.; Kopecek, J. *Biomacromolecules* **2006**, *7*, 1187.
- (222) Yang, J.; Xu, C.; Konak, C.; Kopecek, J. *Biomacromolecules* **2008**, *9*, 510.
- (223) Nori, A.; Jensen, K. D.; Tijeria, M.; Kopeckova, P.; Kopecek, J. *Bioconjugate Chem.* **2003**, *14*, 44.
- (224) Ding, H.; Proding, W. M.; Kopecek, J. *Bioconjugate Chem.* **2006**, *17*, 514.
- (225) McCormick, C. L.; Kirkland, S. E.; York, A. W. *Polymer Reviews* **2006**, *46*, 421.
- (226) York, A. W.; Kirkland, S. E.; McCormick, C. L. *Advanced Drug Delivery Reviews* **2008**, *60*, 1018.
- (227) McCormick, C. L.; Summerlin, B. S.; Lokitz, B. S.; Stempka, J. E. *Soft Matter* **2008**, *4*, 1760.

- 
- (228) Alidedeoglu, A. H.; York, A. W.; McCormick, C. L.; Morgan, S. E.  
*Macromolecules* **2008**, submitted.
- (229) Crescenzi, V.; Francescangeli, A.; Taglienti, A.; Capitani, D.; Mannina, L.  
*Biomacromolecules* **2003**, *4*, 1045.
- (230) Ambrosi, M.; Cameron, N. R.; Davis, B. G.; Stolnik, S. *Org Biomol Chem* **2005**, *3*,  
1476.
- (231) Li, Y.; Benicewicz, B. C. *Polymer Preprint* **2007**, *48(1)*, 524.
- (232) Urban, M. W. *Attenuated Total Reflectance Spectroscopy of Polymers-Theory and  
Practice*; American Chemical Society: Washington, DC, **1996**.
- (233) Moad, G.; Chong, Y. K.; Postma, A.; Rizzardo, E. *Polymer* **2005**, *46*, 8458.
- (234) Patton L. D.; Advincula, R. C. *Macromolecules* **2006**, *39*, 8674.
- (235) Fadeev, A. Y.; McCarthy, T. J. *Langmuir* **2000**, *16*, 7268.
- (236) Fadeev, Y. A.; McCarthy, T. J. *Langmuir* **1999**, *15*, 7238.
- (237) Huisgen, R. In *1,3-Dipolar Cycloadditional Chemistry*; Padwa, A., Ed.; Wiley: New  
York, **1984**.
- (238) Bartlett, P. D.; Altschul, R. *J Am Chem Soc* **1945**, *67*, 812.
- (239) Bartlett, P. D.; Tate F. A. *J Am Chem Soc* **1953**, *75*, 91.
- (240) Litt, M.; Eirich, F. R. *J Polym Sci* **1960**, *45*, 379.
- (241) Odian, G. In *Principles of Polymerization*; Wiley-Interscience: New York, **1991**.
- (242) Laible, R. S. *Chem Rev* **1958**, *58*, 807.
- (243) Sakurada I.; Takashi, G. *Chem High Polym Jpn* **1954**, *11*, 266.
- (244) Hill, D. J. T.; O'Donnell, J. H.; Perera, M. C. S.; Pomery, P. *J Eur Polym Mater*  
**1997**, *33*, 1353.

- 
- (245) Ranby, B. *Appl Polym Symp* **1975**, 26, 327.
- (246) Gaylord, N. G.; Eirich, F. R. *J Am Chem Soc* **1952**, 74, 334.
- (247) Gaylord, N. G.; Eirich, F. R. *J Am Chem Soc* **1952**, 74, 337.
- (248) Schildknecht, C. E. In *Encyclopedia of Polymer Science and Engineering*; Marks, H. F.; Bikales, N. M.; Overberger, C. G.; Willey-Interscience: New York, **1986**.
- (249) Dyball, C. J. (Pennwalt Co.), US Pat 4,263,417; April 21, 1981.
- (250) Hofmann, G. H. (E. I. Du Pont de Nemours and Co.), US Pat 4,139,692; December 25, 1979.
- (251) Sugiyama, H.; Sugimachi, M.; Yoshikawa, M.; Ishiharada, M.; Tanuma, I.; Naito, K.; Hotta, A. (Bridgestone Co.), US Pat 5,684,913; November 4, 1997.
- (252) Ceska, G. W. *J Appl Polym Sci* **1974**, 18, 427.
- (257) Lock, M. R.; El-Aesser, M. S.; Klein, A.; Vanderhoff, J. W. *J Appl Polym Sci* **1991**, 42, 1065.
- (254) Tanaka, K.; Takahashi, K.; Kanada, M.; Kato, Y.; Ichihara, M. (Toyo Contact Lens Co. Ltd), US Pat 4,139,692; February 19, 1979.
- (255) Mol'Kova L. V.; Kulikova, A. Y.; Mil'Chenko, N.; Kuvirina, M.; Nozrina, F. D. *Vysokomoleculyarnye Soedineniya* **1986**, 28, 293.
- (260) Sigetomi, Y.; Kojima, T.; Ono, N. *J Polym Sci Part A: Polym Chem* **1990**, 28, 3317.
- (257) Heatley, F.; Lovell, P. A.; McDonald J. *Eur Polym Mater* **1993**, 29, 255.
- (258) Hendrana, S.; Hill, D. J. T.; Perera, M. C. S.; Pomery, P. *J Polym Int* **2001**, 50, 597.
- (259) Hendrana, S.; Hill, D. J. T.; Perera, M. C. S.; Pomery, P. *J Polym Int* **2001**, 50, 700.



- 
- (260) Asua, J. M. In *Polymeric Dispersions: Principles and Applications*; Kluwer Academic: Dordrecht, **1997**.
- (261) Lovell, P. A.; El-Aesser, M. S. In *Emulsion Polymerization and Emulsion Polymers*; Wiley: Chichester, England, **1997**.
- (262) Urban, D.; Takamura, K. In *Polymer Dispersions and their Industrial Applications*; Wiley-VHC: Weinheim, Germany, **2002**.
- (263) Warson, H.; Finch, C. In *Applications of Synthetic Resins and Latices*; Wiley: Chichester, England, **2001**.
- (264) Asua, J. M. *J Polym Sci: Part A Polym Chem* **2004**, *42*, 1025.
- (265) Sajjadi, S.; Brooks, B. W. *Chem Eng Sci* **2000**, *55*, 4757.
- (266) Naga, N. J. *J Polym Sci Part A: Polym Chem* **2006**, *44*, 6083.
- (267) Hermanson, K. D.; Liu, S.; Kaler, E. W. *J Polym Sci Part A: Polym Chem* **2006**, *44*, 6055.
- (268) Nicolas, J.; Charleux, B.; Magnet, S. *J Polym Sci Part A: Polym Chem* **2006**, *44*, 4142.
- (269) Wu, J.; Tomba, P.; Oh, J. K.; Winnik, M. A.; Farwaha, R.; Rademacher, J. *J Polym Sci Part A: Polym Chem* **2005**, *22*, 5581.
- (270) Bouvier-Fontes, L.; Pirri, R.; Asua, J. M.; Leiza, J. R. *J Polym Sci Part A: Polym Chem* **2005**, *43*, 4684.
- (271) Ray, W. H.; Gall, C. E. *Macromolecules* **1969**, *2*, 425.
- (272) Chujo, K.; Harada, Y.; Tokuhara, S.; Tanaka, K. *J Polym Sci* **1969**, *27*, 321.
- (273) Gerrens, H. *J Polym Sci Part C* **1969**, *15*, 77.
- (274) Snuparek, J. *Angew Makromol Chem* **1972**, *25*, 113.

- 
- (275) Snuparek J. *Makromol Chem Suppl* **1985**, 10/11, 129.
- (276) El-Aasser, M. S.; Makgawinita, T.; Vanderhoff, J. W. *J Polym Sci Polym Chem Ed* **1983**, 21, 2363.
- (277) Noel, L. F. J.; Van Zon, J. M. A. M.; German, A. L. *J Appl Polym Sci* **1994**, 51, 2073.
- (278) Gracey, B. P.; Kamp, W. J.; Anson, W. P. H. (BP International Limited) WO 00/26175, May 11, 2000.
- (279) Gaylord, N. G.; Kujawa, F. M. *J Polym Sci* **1959**, 41, 495.
- (280) Gaylord, N. G.; Kujawa, F. M. *J Polym Sci* **1956**, 21, 327.
- (281) Young, W. G.; Webb, I. D. *J Am Chem Soc* **1951**, 73, 780.
- (282) [http://www.fitzchem.com/pdf/CYOT75\\_DS1.pdf](http://www.fitzchem.com/pdf/CYOT75_DS1.pdf).
- (283) Araujo, P. H. H.; Sayer, C.; Poco, J. G. R.; Guidici, R. *Polym Eng Sci* **2002**, 42, 1442.
- (284) Daniels, E. S.; Sudol, D. E.; El-Aasser, M. S. In *Polymer Latexes*; Comstock, M. J., Eds.; American Chem Society: Atlanta, 1991; p 117. ACS Symposium Series 492.
- (285) Yilinkou, R. G.; Kaliszan, R. *Chromatographia* **1990**, 30, 277.
- (286) Wells, M. J.; Clark, J. R. *Anal Chem* **1981**, 53, 1341.
- (287) Cardenas, J. N.; O'Driscoll, K. F. *J Polym Sci Polym Ed* **1977**, 15, 1883.
- (288) Titirici, M.-M.; Sellergren, B. *Chem. Mater.* **2006**, 18, 1773.
- (289) Baum, M.; Brittain, W. J. *Macromolecules* **2002**, 35, 610.
- (290) Li, C. Z.; Benicewicz, B. C. *Macromolecules* **2005**, 38, 5929.
- (291) Li, C. Z.; Han, J.; Ryu, C. Y.; Benicewicz, B. C. *Macromolecules* **2006**, 39, 3175.
- (292) Liu, C. H.; Pan, C. Y. *Polymer* **2007**, 48, 3679.

- 
- (293) Nguyen, D. H.; Vana, P. *Polym. Adv. Technol.* **2006**, *17*, 625.
- (294) Perrier, S.; Takolpuckdee, P.; Mars, C. A. *Macromolecules* **2005**, *38*, 6770.
- (295) Zhao, Y. L.; Perrier, S. *PMSE Preprints* **2007**, *96*, 619.
- (296) Ranjan, R.; Brittain, W. J. *Polym. Prepr.* **2007**, *48*, 797.
- (297) Zhang, Y. F.; Luo, S. Z.; Liu, S. Y. *Macromolecules* **2005**, *38*, 9813.
- (298) Zhang, K.; Gao, L.; Chen, Y. M. *Macromolecules* **2007**, *40*, 5916.
- (299) Matyjaszewski, K.; Miller, P. J.; Shukla, N.; Immaraporn, B.; Gelman, A.; Luokala, B. B.; Siclovan, Tiberiu M. G.; Vallant, K. T.; Hoffmann, H.; Pakula, T. *Macromolecules* **1999**, *32*, 8716.